

# Signaling Design in Ultra-Wideband Wireless Communication Systems

A Dissertation  
in  
Information Science and Engineering  
Submitted to Graduate School of Science and Technology  
Niigata University  
in  
Partial Fulfillment of the Requirements  
for the Degree of  
Doctor of Philosophy in Engineering

Sum Chin Sean

March 2007



# Abstract

In this research, the study of signaling design in ultra wideband (UWB) system is conducted. UWB signaling design can be effectively manipulated for the purposes of performance improvement and interference mitigation. Timing jitter, as a critical issue in UWB signaling design, is also investigated to assess its impact to system performance.

Chapter 1 describes the research background, and the motivation that becomes the catalyst to the completion of this study. Then the objectives are listed to provide a clear direction for the study. Finally the overview of the thesis is to define the areas in which the research has covered.

Chapter 2 provides an overall introduction to UWB systems, with specific emphasis on direct sequence (DS) and DS multiband (MB). System models including signal model, received signal and receiver model are presented and discussed in detail. The UWB system is designed to propagate over multipath and multi-user channel. The considered multipath environment is defined by the IEEE 802.15.3a channel models (CM). The characteristics of the CM's are also introduced and elaborated with suggested further references. Multi-user environment in this study assumes that asynchronous simultaneous users share the same propagation channel with similar transmitted power. Next, applying the system model developed, performance of UWB system corresponding to different parameters and propagation environments are presented and analyzed.

Chapter 3 deals with signaling design in varying low chip duty factor (DF), a unique parameter in UWB system. Firstly, three methods of designing low DF UWB signal are introduced. Each method manipulates different parameters, requires different system resources and is capable of offering respective advantages. Then, the systems are simulated over multipath and multi-user environment in the presence of a coexisting narrowband signal. In multipath and multi-user environment, the interactions between low DF UWB signaling design to channel fading, self interference and multi-user interference are analyzed, and the related system performance are evaluated. Additionally, assuming the presence of a coexisting narrowband signal, the advantage of low DF UWB signaling over narrowband interference is also presented and discussed. System performance is evaluated from both the perspectives of energy capture and bit error rate. In this chapter, besides DS

and DS-MB spreading techniques, time hopping (TH) and DS-TH spreading techniques are also coupled to low DF UWB signal to provide more thorough investigations.

Chapter 4 proposes two interference mitigation techniques developed by manipulating signaling design in DS and DS-MB UWB system. UWB system occupies a wide bandwidth, thus easily receives interference from co-existing narrowband systems, and simultaneously generates UWB interference to these narrowband systems. Techniques which are able to mitigate this mutual interference by: (a) suppressing sub-band power in a multiband UWB system and (b) employing signaling design with low DF, are developed and presented. Firstly, DS-MB-UWB system with sub-band power suppression is proposed and the ability to mitigate mutual interference is discussed. Next, DS and DS-MB-UWB systems employing low DF signaling design are proposed with analysis of their interference mitigation capabilities. Then, by combining the mitigation techniques to respective UWB systems, performance in coexistence with a narrowband system over different propagation environments is investigated. Additionally, the effects of applying different parameters in system design are also presented and commented.

Chapter 5 highlights and mitigates the impact of timing jitter in UWB signaling design. Timing jitter exists in all digital communication systems, and is particularly pronounced in UWB signal with nano-second order pulses. Firstly, the introduction on timing jitter existing in UWB receiver is presented. Then, the relationship between timing jitter and the degradation of correlator output in the receiver is discussed. Next, the statistical properties of timing jitter are characterized and modeled. Applying the system model and timing jitter model, the performance of UWB system over multipath and multi-user environment in the presence of timing jitter is evaluated. The compromised performance improvement achievable by adding different system resources are investigated and commented corresponding to varying timing jitter. Lastly, a mitigation technique to timing jitter is developed by employing DS-MB-UWB signaling design, and the results are shown.

Chapter 6 sums up the study with concluding remarks. The prospects of signaling design in UWB performance improvement and interference mitigation are commented with potential future works.

# Acknowledgments

I would like to take this opportunity to convey my highest appreciation to all those who have contributed directly and indirectly in the completion of this research and the writing of this thesis. First and foremost, I would like to thank my academic advisers Assoc. Prof. Shigenobu Sasaki and Prof. Hisakazu Kikuchi for their guidance throughout the course. Dr. Sasaki, in particular, has not only offered unlimited support to this research, but has also enlightened me with new perspectives of linking academic research to practical applications. I would also like to express my gratitude to Dr. Shogo Muramatsu, Niigata University and Dr. Jie Zhou, Nanjing Institute of Technology for their inspiring guidance. Thanks to the review committee members of this thesis, Prof. Masakazu Sengoku and Prof. Kenichi Mase who have given invaluable comments. The Communication Laboratory is the place I spend most of my time in during research, and is like a second home to me. Thanks to my fellow laboratory members for making it a homely and harmonious working environment. Also, sincere thanks to Mr. Mohammad Azizur Rahman for the fruitful discussions throughout the research. Studying in Japan had always been a dream to me, special thanks to the Monbukagakusho Scholarship for making this dream come true. I would also like to thank all the individuals in the Department of Electrical and Electronic Engineering, Graduate School of Science and Technology and the International Exchange Support Center, Niigata University for supporting this research from all aspects. The support and encouragement of my family is what kept me motivated against all obstacles and challenges throughout the entire duration of this research, sincere thanks to them. Last but not least, to Ms. Loke Eng Hui, thank you for standing by me all these years. You are all my reasons.

Sum Chin Sean

*Niigata University*  
*March 2007*



# Contents

<b>Abstract</b>	<b>3</b>
<b>Acknowledgments</b>	<b>5</b>
<b>1 Introduction</b>	<b>15</b>
1.1 Research Background and Motivation . . . . .	15
1.2 Research Objective . . . . .	17
1.3 Research Overview . . . . .	17
<b>2 Introduction to UWB System</b>	<b>19</b>
2.1 System Models . . . . .	20
2.1.1 Signal Model . . . . .	20
2.1.2 Received Signal . . . . .	22
2.1.3 Receiver Model . . . . .	23
2.2 Energy Capture and System Performance . . . . .	24
2.3 Multipath Channel Model . . . . .	25
2.4 Simulation Setup and Parameters . . . . .	26
2.5 Performance in Multipath Channel . . . . .	27
2.6 Performance in Multi-user Channel . . . . .	34
2.7 Concluding Remarks . . . . .	35
<b>3 Impact of Chip Duty Factor</b>	<b>37</b>
3.1 Chip Duty Factor in Signaling Design . . . . .	38
3.1.1 Signal Models . . . . .	38
3.1.2 Varying Chip Duty Factor . . . . .	39
3.2 Performance in Multipath Channel . . . . .	41
3.2.1 DS-UWB Signaling Design with Low DF . . . . .	41
3.2.2 Comparison with Other UWB Modulations . . . . .	47
3.3 Performance in the Presence of Narrowband Interference . . . . .	53
3.4 DS-MB-UWB System with Overlapped Sub-bands . . . . .	55
3.5 Concluding Remarks . . . . .	57

<b>4</b>	<b>Interference Mitigation</b>	<b>59</b>
4.1	Sub-band Power Suppression . . . . .	60
4.2	Low Chip Duty Factor Mitigation . . . . .	62
4.3	Performance with Interference Mitigation . . . . .	63
4.3.1	Performance with Sub-band Suppression Mitigation . . . . .	64
4.3.2	Performance with Low DF Mitigation . . . . .	69
4.4	Concluding Remarks . . . . .	74
<b>5</b>	<b>Timing Jitter in UWB System</b>	<b>75</b>
5.1	Timing Jitter . . . . .	76
5.2	Simulation Model and Parameters . . . . .	77
5.2.1	System Parameters . . . . .	78
5.2.2	Timing Jitter Model . . . . .	78
5.3	Performance in the Presence of Timing Jitter . . . . .	79
5.3.1	Performance in Multipath Channel . . . . .	80
5.3.2	Performance in Multi-user Channel . . . . .	88
5.4	Timing Jitter Mitigation Technique . . . . .	92
5.5	Concluding Remarks . . . . .	95
<b>6</b>	<b>Conclusion</b>	<b>97</b>
6.1	Summary . . . . .	97
6.2	Future Works . . . . .	98
	<b>Bibliography</b>	<b>99</b>
	<b>Publication List</b>	<b>107</b>

# List of Figures

2.1	Top level block diagram of UWB system. . . . .	20
2.2	DS-MB-UWB (a)Signaling and (b)Spectral Diagram. . . . .	21
2.3	Illustration of Received Signal Channel Response and Place- ment of Template Signals in the Rake Receiver. . . . .	24
2.4	BER Performance vs. SNR over Different Multipath Chan- nels for DS-UWB System. $T_p=1\text{ns}$ , $N_s=15$ , $L_c=8$ , $f_c=5\text{GHz}$ . . . . .	28
2.5	BER Performance vs. SNR for Different Rake Receivers for DS-UWB System. $T_p=1\text{ns}$ , $N_s=15$ , $f_c=5\text{GHz}$ , CM1. . . . .	29
2.6	BER Performance vs. Selected and Combined Paths for Dif- ferent Rake Receivers for DS-UWB System. $T_p=1\text{ns}$ , $N_s=15$ , $f_c=5\text{GHz}$ , SNR=20dB. . . . .	30
2.7	BER Performance vs. Chip Length over Different Multipath Channels for DS-UWB System, $T_p=1\text{ns}$ . $L_c=8$ , $f_c=5\text{GHz}$ , SNR=22dB. . . . .	31
2.8	BER Performance vs. Pulse Duration over Different Mul- tipath Channels for DS-UWB System. $L_c=8$ , $f_c=6.75\text{GHz}$ , SNR=22dB. . . . .	32
2.9	BER Performance vs. SNR over Different Multipath Chan- nels for DS-MB-UWB System. $L_c=8$ , PG=20. . . . .	33
2.10	BER Performance vs. Rake Fingers over Different Multipath Channels for DS-MB-UWB System. SNR=24dB, PG=20. . . . .	34
2.11	BER Performance vs. Number of Users for DS-UWB System. $T_p=1\text{ns}$ , $L_c=8$ , $N_s=15$ , $f_c=5\text{GHz}$ , SNR=24dB. . . . .	35
3.1	Illustrations for (a) DS-TH-UWB, (b) DS-UWB and (c) TH- UWB Signal. In this example, $N_s=4$ and $N_c=5$ . . . . .	39
3.2	Signaling Design with lower DF by Employing lower $N_s$ . (a) $\delta=0.5$ , $N_s=12$ , (b) $\delta=0.125$ , $N_s=3$ , (c) $\delta=0.04$ , $N_s=1$ . . . . .	40
3.3	Signaling Design with lower DF by Employing lower $T_p$ . (a) $\delta=0.5$ , (b) $\delta=0.25$ , (c) $\delta=0.125$ . . . . .	41
3.4	Signaling Design with lower DF by Employing lower PRF. (a) $\delta=0.5$ , (b) $\delta=0.25$ , (c) $\delta=0.125$ . . . . .	42

3.5	BER Performance vs. Chip Duty Factor Manipulating Varying Chip Length for DS-UWB System. PG=24, SNR=20dB, $L_c=8$ , $f_c=4$ GHz. . . . .	43
3.6	BER Performance vs. Chip Duty Factor Manipulating Varying Spreading Bandwidth for DS-UWB System. SNR=20dB, $L_c=8$ , $f_c=4$ GHz. . . . .	45
3.7	BER Performance vs. Chip Duty Factor Manipulating Varying PRF for DS-UWB System. SNR=20dB, $L_c=8$ , $f_c=4$ GHz. . . . .	46
3.8	Energy Capture vs. Chip Duty Factor for DS, TH and DS-TH UWB Systems. $W_t=2$ GHz, $L_c=8$ , $f_c=6$ GHz. . . . .	48
3.9	Energy Capture vs. Selected and Combined Paths for DS, TH and DS-TH UWB Systems. $W_t=2$ GHz, $f_c=6$ GHz. . . . .	49
3.10	BER Performance vs. Chip Duty Factor for DS, TH and DS-TH UWB Systems. SNR=20dB, $L_c=8$ , $W_t=2$ GHz, $f_c=6$ GHz. . . . .	50
3.11	BER Performance vs. SRake Selected and Combined Paths for DS, TH and DS-TH UWB Systems. SNR=20dB, $f_c=6$ GHz, $W_t=2$ GHz. . . . .	51
3.12	BER Performance vs. Number of Users for DS, TH and DS-TH UWB Systems. (a)CM1 and (b)CM2. $K=6$ , SNR=20dB, $W_t=2$ GHz, $f_c=6$ GHz. . . . .	52
3.13	BER Performance vs. SIR for DS, TH and DS-TH UWB Systems. (a)CM1 and (b)CM2. SNR=20dB, $W_t=2$ GHz, $L_c=8$ , $f_c=6$ GHz, $f_{nrb}=6$ GHz, $W_j=10$ MHz. . . . .	54
3.14	BER Performance vs. Chip Duty Factor and Chip Length for DS-UWB System in the Presence of Narrowband Interference. SIR=10dB, $L_c=8$ , $f_c=6$ GHz, $f_{nrb}=6$ GHz, $W_j=10$ MHz. . . . .	55
3.15	BER Performance vs. Overlap Percentage of Sub-bands for DS-UWB System Manipulating Low DF Design. SNR=18dB, $L_c=8$ , $W_t=4$ GHz. . . . .	56
4.1	Spectral Diagram of Sub-band with Power Suppression. (1) $\Delta b' = 0$ (no power suppression), (2) $\Delta b' = 0.2$ , (3) $\Delta b' = 0.5$ , (4) $\Delta b' = 0.8$ , (5) $\Delta b' = 0.9$ and (6) $\Delta b' = 1$ (full power suppression). . . . .	61
4.2	Impact of UWB Signals with Varying DF Design on Coexisting Narrowband Signal. (a) Coexisting Narrowband Signal, UWB Signals with (b) $\delta=1$ and $N_s=24$ , (c) $\delta=0.5$ and $N_s=12$ , and (d) $\delta=0.04$ and $N_s=1$ . . . . .	62
4.3	BER Performance vs. Level of Sub-band Power Suppression for DS-MB-UWB System. SNR=25dB, SIR=-5dB. (Power suppression is applied on sub-band with $f_{ma=4}=6.5$ GHz.) . . . . .	65
4.4	BER Performance vs. SIR for DS-MB-UWB System. $B=4$ , SNR=20dB, $L_c=8$ , CM1. . . . .	67

4.5	BER Performance vs. SNR for DS-MB-UWB System. SIR=-5dB, $L_c=8$ , $B=4$ , CM1. . . . .	68
4.6	BER Performance vs. Selected and Combined Paths for DS-MB-UWB System. SNR=25dB, SIR=-5dB, $B=4$ , CM1. . . .	69
4.7	BER Performance vs. Chip Duty Factor for DS-MB-UWB System. SNR=25dB, SIR=-5dB, $B=4$ . . . . .	70
4.8	BER Performance vs. SIR for DS-UWB System. SNR=16dB, $L_c=8$ , $f_c=6$ GHz, $f_{nrp}=6$ GHz, $W_j=10$ MHz, CM1. . . . .	71
4.9	BER Performance vs. Data Rate for DS-UWB System. CM1, PG=48, SNR=16dB, SIR=10dB, $L_c=8$ , $f_c=6$ GHz, $f_{nrp}=6$ GHz, $W_j=10$ MHz. . . . .	72
4.10	BER Performance vs. Number of Users for DS-UWB System. SNR=16dB, SIR=10dB, $L_c=8$ , $f_c=6$ GHz, $f_{nrp}=6$ GHz, $W_j=10$ MHz, CM1. Signal to Multi-user Interference Ratio is set to unity. . . . .	73
5.1	Placement of Template Signals by Correlators in the Rake Receiver. Solid line arrows: ideal positions of the template, Dashed line arrows: positions of the template with timing jitter $\nu$ . . . . .	77
5.2	Received Modulated Gaussian Pulse and its Normalized Autocorrelation Function. $T_p=2$ ns, $t_m=0.39T_p$ , $f_c=4$ GHz. . . . .	78
5.3	BER Performance vs. Root Mean Square Jitter over Different Multipath Channels for DS-UWB System. SNR=20dB, $T_p=2$ ns, $f_c=4$ GHz, $L_c=8$ , $\delta=1$ , CM1-4. . . . .	80
5.4	Simplified Relationship between the Average Value of Normalized Correlator Output and Timing Jitter (AWGN and channel fading neglected). $T_p=2$ ns and $f_c=4$ GHz. . . . .	81
5.5	BER Performance vs. Chip Length for DS-UWB System. SNR=25dB, $T_p=2$ ns, $f_c=4$ GHz, $L_c=8$ , $\delta=1$ , CM1. . . . .	82
5.6	BER Performance vs. SNR for DS-UWB System. $N_s=31$ , $T_p=2$ ns, $\delta=1$ , $f_c=4$ GHz, $L_c=8$ , CM1. . . . .	83
5.7	BER Performance vs. Pulse Duration for DS-UWB System. SNR=25dB, $N_s=15$ , $\delta=1$ , $f_c=4$ GHz, $L_c=8$ , CM1. . . . .	84
5.8	Truncated Noiseless Channel Response over CM1 for Transmitted Unit Energy Pulse Duration 0.267ns (top) and 3ns (bottom). . . . .	85
5.9	BER Performance vs. Chip Duty Factor for DS-UWB System. SNR=25dB, $N_s=15$ , $T_c=4$ ns, $f_c=4$ GHz, $L_c=8$ , CM1. . . .	86
5.10	BER Performance vs. Combined and Selected Paths for DS-UWB System. SNR=25dB, $N_s=31$ , $T_p=2$ ns, $\delta=1$ , $f_c=4$ GHz, CM1. . . . .	87
5.11	BER Performance vs. Center Frequency for DS-UWB System. SNR=25dB, $N_s=31$ , $T_p=2$ ns, $\delta=1$ , $L_c=8$ , CM1. . . . .	88

5.12	BER Performance vs. Number of Interfering Users for DS-UWB System. SNR=30dB, $N_s=31$ , $T_p=2\text{ns}$ , $\delta=1$ , $L_c = 8$ , $f_c=4\text{GHz}$ , CM1. . . . .	89
5.13	BER Performance vs. RMSJ in Multi-user and Multipath Channels for DS-UWB System. SNR=30dB, $T_p=2\text{ns}$ , $\delta=1$ , $f_c=4\text{GHz}$ , $L_c=8$ , CM1-4. . . . .	90
5.14	BER Performance vs. SNR in Multi-user Environment for DS-UWB System. $N_s=31$ , $T_p=2\text{ns}$ , $\delta=1$ , $L_c = 8$ , $f_c=4\text{GHz}$ , CM1. . . . .	91
5.15	Multipath Channel with Exponentially Decaying PDP. . . . .	92
5.16	BER Performance vs. SNR for Different UWB Signaling Design. $L_c = 4$ , $W_t=6\text{GHz}$ , NRMSJ=0.01%, $T_d=200\text{ns}$ , Exponential Decaying PDP, $C=10$ . . . . .	94
5.17	Energy Capture vs. Normalized RMSJ for Different UWB Signaling Design. $L_c = 4$ , $W_t=6\text{GHz}$ , $T_d=200\text{ns}$ , Exponential Decaying PDP, $C=10$ . . . . .	95

# List of Tables

2.1	IEEE 802.15.3a Multipath Channel Models. . . . .	26
2.2	Simulation Parameters for DS-UWB and DS-MB-UWB Systems. . . . .	27
3.1	Pairs of DF and $N_s$ for DS-UWB Signaling Design. . . . .	42
3.2	Pairs of DF and $N_s$ for DS, TH and DS-TH UWB Signaling Design. . . . .	47
3.3	Pairs of DF and $N_s$ for DS-UWB Signaling Design in the Presence of Narrowband Interference. . . . .	54
3.4	DF and Overlap Percentage (OP) of Sub-bands. . . . .	57
4.1	Simulation Parameters for DS-MB-UWB System with Interference Mitigation . . . . .	64
4.2	Pairs of DF and $N_s$ for DS-MB-UWB System with Sub-band Suppression Mitigation. . . . .	64
4.3	Relationship Between Level of Sub-band Power Suppression, Multiband DF and Average DF for DS-MB-UWB System. . .	65
5.1	Simulation Parameters for DS-UWB System in the Presence of Timing Jitter. . . . .	79



# Chapter 1

## Introduction

### 1.1 Research Background and Motivation

For the past few decades, wireless communication systems have been evolving rapidly, from initially as an alternative technology, to eventually shadowing the superiority of the conventional wired communication systems. Today, replacing crisscrossing cables with wireless connectivity has become a major trend for recent communication applications.

The transition from the second to the third and fourth generation mobile radio, the rise of wireless connections of Wi-Fi and Bluetooth that enable information exchange anywhere anytime, are among the many examples proving the fact that wireless technology is growing continuously to meet consumer demands for higher capacity, faster service and better security. One immediate effect of this overwhelming growth is the overcrowding of the already scarce radio frequency (RF) spectrum. As a result, the availability of the RF spectrum has becoming more limited with the introduction of more new radio services.

Ultra wideband (UWB) technology offers a timely solution to this deadlock by allowing new services to coexist with current radio systems with minimal or no interference. UWB is a ‘new engineering technology’ focusing particularly on new perspectives of application with no new physical properties [1]. The early applications of UWB can be traced back to high resolution radar systems [2]. After that, the technology has been given new direction on military, collision avoidance and positioning applications following the publication of [3]. Not until late 1990’s that the commercialization of UWB devices and systems took place, initiated by companies [4, 5].

The intensified hype gathering around UWB technology owes a great deal to its capability of supporting high data rates, from the already demonstrated 100Mbps, to the potentials in order of Gbps over short distance. This feature enables consumer applications ranging from wireless home networks with multiple streaming of large multimedia files, to remote sensing

and tracking devices with high accuracy. These applications would not have been possible with the conventional wireless systems. Besides, the modulation of pulses directly into the transmitting antenna also provides encouraging benefits of less complex transceiver designs. This feature captures specially manufacturers aiming to produce inexpensive high-tech consumer products. Furthermore, the employment of short and low duty cycle pulses improves immunity towards multipath propagation, and meanwhile requires low power consumption, which directly translates to longer battery lifespan. Moreover, the precise ranging characteristic of UWB technology also enables applications such as automotive collision avoidance, effective traffic control and so on.

All these technical advantages and potential applications have directed a huge amount of attention on UWB technology. The key players are none other than the multi national corporations in the telecommunication business and research-based communication institutions. The momentum is accumulated so rapidly that the participation of regulators are becoming more aggressive. Up to date, several specifications and guidelines have been drawn to assist its direction of research, development and implementation [6–8].

Despite the inviting advantages offered, there are still numerous challenges to be overcome before UWB technology can become a popular and ubiquitous technology. One significant challenge to date is the regulatory problems. In order to ‘submerge’ under and coexist with other wireless systems, especially licensed wireless services, UWB technology has to convince service providers that the potential interference is not harmful to their existing services. Also, although the promise of simple and low cost system is delivered, several technical and implementation issues remain.

Among other technical challenges urgently in need of attention, is the issue on combating interference and fading channels. Multipath propagation, multiple access and coexisting narrowband signal have been major sources of interference compromising UWB performance. These interference have to be addressed and mitigated. In this thesis, one of the main objectives is to deal with interference due to various propagation environments by employing signaling design. Besides, timing error caused by circuitry imperfection has also severely degraded signal reception in the UWB receiver. Therefore, another objective of this thesis is to assess the impact of timing error on system performance and relevant methods to mitigate it. Detailed background for each of the challenges is given specific discussion and treatment in the introduction section of respective chapters.

Realizing the ‘unfinished business’ in UWB technology, this study is conducted to tackle these main issues from the perspective of signaling in the physical layer design. The next section lists out clearly the objectives and goals of this study.

## 1.2 Research Objective

The objectives of this research are:

1. To study and understand UWB system from the perspective of signaling design.
2. To identify the potential advantages offered by UWB signaling with low chip duty factor.
3. To develop interference mitigation techniques for UWB system through signaling design.
4. To assess and mitigate the impact of timing jitter in UWB signaling.

## 1.3 Research Overview

The remaining chapters of the thesis are organized as below:

Chapter 2 intends to give a brief introduction on UWB system, by attempting to provide answers to typical questions regarding signaling design, such as:

- How does designing different signaling schemes affect system performance in general?
- What is the relationship between system performance to different system parameters and propagation environment?

In this chapter, spreading techniques direct sequence (DS) and DS multi-band (MB) methods are introduced. Signal models and receiver models are presented with emphasis from the energy capture perspective. Then, system performance corresponding to parameters such as signal to noise ratio (SNR), chip length, number of bands, operating frequency are also investigated. The different system response in various propagation channels such as multipath channel and multi-user channel are shown and analyzed. Additionally, in multipath environment, Rake receiver is essential and is thus investigated in detail.

Chapter 3 intends to investigate the impact of employing low chip duty factor (DF) in UWB signaling design on system performance, by answering questions such as:

- How to design a low DF UWB signal?
- What are the advantages and tradeoff parameters of the low duty UWB signal?

This chapter shows the fundamental difference between UWB signal and the conventional spread spectrum signal. Parameters involved in designing a low DF UWB signal are listed and discussed. Next, system performance of low DF UWB systems corresponding to these parameters are presented and analyzed. Analysis is also conducted by employing different UWB spreading methods such as time hopping (TH) and DS-TH techniques. Additionally, performance in the presence of narrowband interference is also commented.

Chapter 4 intends to develop mitigation techniques for UWB system against interference. It is interesting to understand that:

- Can interference be mitigated by simply applying different signaling designs?
- How can these mitigation techniques be designed?

In this chapter, a narrowband interference is considered to spectrally coexist with the UWB signal. Two interference mitigation techniques are developed through signaling design to reduce mutual interference between UWB system to and from the coexisting narrowband systems. The proposed mitigation methods are the sub-band power suppression mitigation method and the low DF mitigation method. In this chapter, both methods are given detailed treatment, highlighting corresponding design issues, advantages and tradeoff requirements.

Chapter 5 intends to understand the impact of timing jitter in UWB signaling design. Some typical questions about timing jitter are:

- How significant is the impact of timing jitter in UWB system?
- How to mitigate the impact of timing jitter?

This chapter shows the performance degradation due to timing jitter in correspondence to different parameters such as root mean square jitter, SNR and pulse duration. The impact of timing jitter is also shown in varying propagation channels such as multipath channel and multi-user channel. Then, a jitter-mitigation technique employing multiband signaling method is introduced and the results are discussed.

Chapter 6 concludes with comments on the prospects of signaling design in UWB systems. Potential future works are also given.

## Chapter 2

# Introduction to UWB System

Conventional UWB system transmits and receives very short pulses and is commonly known as impulse radio (IR) [9]. And by modulating pulses to different time slots in a relatively long pulse repetition interval, multiple access can be supported in a common propagation environment. This is known as the time hopping (TH) UWB system [10,11].

As UWB technology receives more attention from the wireless community, other modulation methods are also proposed to be coupled with the technology [12]. Among others widely applied, is the popular direct sequence (DS) method. DS spreading is an established method in the spread spectrum (SS) technology [13], and can be conveniently employed in the UWB system. This spreading method is well known in the digital cellular industry to possess useful properties such as low peak to average power ratio [14] and robustness to multi-user interference [15]. Work in [16] draws some differences between UWB and DS-SS. A general overview on DS-UWB system performance is being investigated in [17]. However, there are still numerous unexplored aspects in its performance in various propagation environment. Therefore, the first purpose of this chapter is to investigate these unexplored areas of DS signaling in UWB system.

Next, the idea of DS spreading in UWB can be extended to multiband (MB) system to become DS-MB-UWB system. This is a novel hybrid system that occupies several narrower sub-bands instead of a wider single band. The advantage of occupying more than a single band can be given in [18]. However, despite the advantages able to be offered by DS-MB-UWB system, not much attention has been given in current literatures. Therefore, another purpose of this chapter is to explore the potentials of DS-MB signaling for UWB system in different propagation environments.

The outline of this chapter is given as below. Firstly, the system models of both DS-UWB and DS-MB-UWB system over various channels are intro-

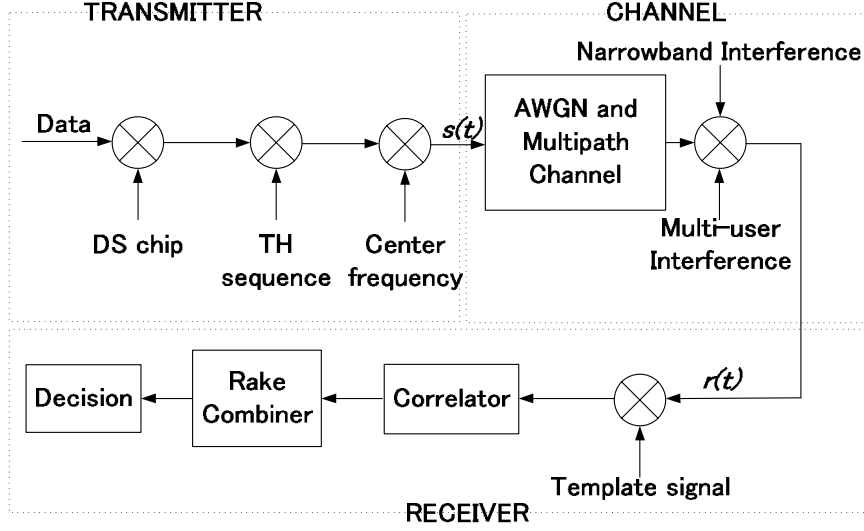


Figure 2.1: Top level block diagram of UWB system.

duced. Then the multipath channel model is presented. Finally the system performance in these propagation channels are investigated and analyzed.

## 2.1 System Models

In this section, a detailed description on the DS-UWB and DS-MB-UWB system model is presented. The top level block diagram of a general UWB system in fig.2.1 consists of three main parts: transmitter, channel and receiver.

### 2.1.1 Signal Model

By assuming the binary phase shift keying (BPSK) as data modulation, the transmitted DS-MB-UWB signal of the  $k$ -th user can be given by:

$$s^{(k)}(t) = \sqrt{E_p} \sum_{i=-\infty}^{\infty} \sum_{j=0}^{N_s-1} d_i c_j^{(k)} p(t - iT_s - j\frac{T_p}{\delta}) \cos(2\pi f_m^{(k)}(t - j\frac{T_p}{\delta}))$$

$$m = 1, 2, \dots, B \quad (2.1)$$

where  $d_i$  is the  $i$ -th BPSK data bit uniform over  $\{+1, -1\}$ , each with bit energy  $E_b$ ,  $c_j$  is the  $j$ -th user-dependent DS code of random sequence over  $\{+1, -1\}$ ,  $N_s$  is the number of chips per bit,  $T_s$  is the bit duration,  $T_p$  is the transmitted pulse duration,  $\delta$  is the chip duty factor (DF),  $\delta = T_p/T_c$  where  $T_c$  is the chip duration,  $E_p$  is the energy per pulse,  $p(t)$  is the unit

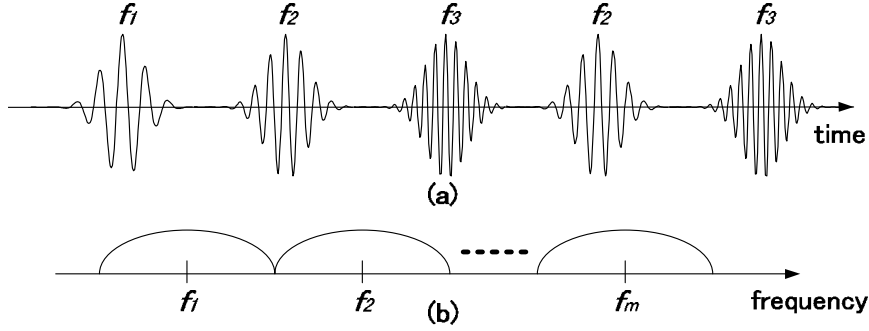


Figure 2.2: DS-MB-UWB (a) Signaling and (b) Spectral Diagram.

energy pulse waveform,  $f_m$  is the multiband frequency selected randomly from a total of  $B$  number of sub-bands to form a user-dependent frequency hopping sequence, with probability of each  $f_m$ , as  $P(f_m) = 1/B$ . Also note that system data rate  $R_b$  and processing gain (PG) are given by  $1/T_s$  and  $N_s B/\delta$  respectively.

In (2.1), the BPSK data is spread by  $N_s$  chips each with center frequency  $f_m$ . The center frequency is constantly hopping from one sub-band to another, chosen from the total  $B$  sub-bands. The sub-bands are spectrally orthogonal towards each other. The signaling diagram can be shown in fig.2.2(a) and the spectral diagram in fig.2.2(b). The multiband frequency hopping rate  $S_r$ , or how frequent the changing of  $f_m$  is, can be expressed by  $1/T_c$ . This means that the hopping of multiple sub-bands is synchronized with the transition of the DS chips. One DS chip is modulated with one center frequency, then the next chip with a different center frequency, and so on. The sub-band bandwidth  $W_{sub}$  and system total bandwidth  $W_t$  can be defined as  $2/T_p$  and  $2B/T_p$  respectively. Energy per sub-band  $E_{sub}$  can be defined as  $E_b P(f_m) = E_b/B$ .

Next, we can easily generate a single band DS-UWB signal by modifying the multiple hopping bands of the DS-MB-UWB signal in (2.1) to a fixed center frequency  $f_c$ , as:

$$s^{(k)}(t) = \sqrt{E_p} \sum_{i=-\infty}^{\infty} \sum_{j=0}^{N_s-1} d_i c_j^{(k)} p(t - iT_s - j\frac{T_p}{\delta}) \cos(2\pi f_c t) \quad (2.2)$$

Here, PG and  $W_t$  can be defined as  $N_s/\delta$  and  $2/T_p$  respectively. Properties of the DS-UWB signal can be viewed as similar to the DS-MB-UWB signal except for the constant center frequency.

At the receiver side, DS chips with the same polarities and center frequency (or frequencies) as the corresponding transmitted signal are used as the template signal for correlation process. In other words, it is assumed that

the receiver has knowledge of the DS chip sequence and frequency hopping pattern of the transmitter.

### 2.1.2 Received Signal

The received signal over an AWGN and multipath channel in the presence of narrowband interference for the  $k$ -th user can be given by:

$$r^{(k)}(t) = s^{(k)}(t) * h(t) + \eta(t) + \epsilon(t) \quad (2.3)$$

where  $h(t)$  is the channel impulse response,  $*$  represents the convolution process,  $\eta(t)$  is the white Gaussian noise and  $\epsilon(t)$  is the interference from the coexisting narrowband signal.

For DS-MB-UWB signal, (2.3) can be described as:

$$r^{(k)}(t) = \sqrt{E_p} \sum_{i=-\infty}^{\infty} \sum_{j=0}^{N_s-1} d_i c_j^{(k)} m(t - iT_s - j\frac{T_p}{\delta}) \cos(2\pi f_m^{(k)}(t - j\frac{T_p}{\delta})) + \eta(t) + \epsilon(t) \quad m = 1, 2, \dots, B \quad (2.4)$$

And for DS-UWB signal, (2.3) can be described as:

$$r^{(k)}(t) = \sqrt{E_p} \sum_{i=-\infty}^{\infty} \sum_{j=0}^{N_s-1} d_i c_j^{(k)} m(t - iT_s - j\frac{T_p}{\delta}) \cos(2\pi f_c t) + \eta(t) + \epsilon(t) \quad (2.5)$$

where  $m(t) = p(t) * h(t)$  is the channel response of the signal.

We assume that the channel remains constant for the entire bit duration. Note that the transmitted pulse  $p(t)$  has unit energy, channel response  $m(t)$  has energy  $E_d = \int_0^{T_d} m^2(t) dt$ , and  $E_d \leq N_s E_p$  due to fading. Here,  $T_d$  is the maximum delay spread with respect to the first arriving path. The total number of resolvable multipath is therefore given by  $L = T_d/T_p$ .

As described by (2.3), a spectrally coexisting narrowband signal is assumed to be present in the channel. The narrowband signal can be further given as:

$$\epsilon(t) = \sqrt{2P_j} \sum_{x=-\infty}^{\infty} v_x g(t - xT_j) \cos(2\pi f_{nr} t) \quad (2.6)$$

where  $v_x$  represents the  $x$ -th BPSK phase randomly uniform on  $\{+1, -1\}$ ,  $T_j$  is the data duration,  $f_{nr}$  is the center frequency,  $g(t)$  is the signal waveform with signal power  $P_j$  and bandwidth  $W_j = 2/T_j$ .

Here, we also define the signal to noise ratio (SNR) and signal to interference ratio (SIR) to be  $E_b/N_0$  and  $E_b T_s / 2P_j$ , where  $N_0$  is the one-sided AWGN PSD.

Then, considering signal from multi users sharing the same channel, the total received signal can be given by:

$$r(t) = \sum_{k=0}^{K-1} r^{(k)}(t - \phi_k) \quad (2.7)$$

where  $K$  is the total number of simultaneous users sharing the same channel,  $\phi_k$  represents the time delays of the interfering signals from other asynchronous users received by the  $k$ -th user and  $0 \leq \phi_k < T_s$ .

### 2.1.3 Receiver Model

By employing a Rake receiver, a template signal is generated to perform correlation process with the received signal.

For DS-MB-UWB signal, the template signal can be described as:

$$\psi^{(k)}(t) = \frac{1}{\sqrt{N_s}} \sum_{j=0}^{N_s-1} c_j^{(k)} p(t - j\frac{T_p}{\delta}) \cos(2\pi f_m^{(k)}(t - j\frac{T_p}{\delta})) \quad (2.8)$$

And for DS-UWB signal, as:

$$\psi^{(k)}(t) = \frac{1}{\sqrt{N_s}} \sum_{j=0}^{N_s-1} c_j^{(k)} p(t - j\frac{T_p}{\delta}) \cos(2\pi f_c t) \quad (2.9)$$

Note that the receiver is assumed to obtain knowledge of the sequence and spreading codes of the transmitted signal. Here  $\psi^{(k)}(t)$  is used to correlate with  $r(t)$  at delays of multiple  $T_p$  [19]. This is where multipath resolvability can be increased as low DF signal in the multiples of  $T_c$  being resolved in multiples of  $T_p$ . Since it is well understood that we are modeling the receiver of the  $k$ -th user, here on the superscript  $k$  will be left out from the template signal  $\psi^{(k)}(t)$ .

The correlation between  $\psi(t)$  and  $r(t)$  at the  $l$ -th Rake finger with delay  $\tau_l$  can be described as:

$$Z_l = \int_0^{T_b} r(t)\psi(t - \tau_l)dt = \sqrt{E_p N_s E_d} \chi_l \alpha(\tau_l) + \eta_l + \epsilon_l \quad l = 0, 1, \dots, L - 1 \quad (2.10)$$

where  $\alpha(\tau_l) = \int_{-\infty}^{\infty} m(t)p(t - \tau_l)dt$  is the correlation between channel response  $m(t)$  and unit energy pulse  $p(t)$  at delay  $\tau_l$ ,  $\chi_l$  is the signal amplitude at delay  $\tau_l$ ,  $\eta_l = \int_0^{T_s} \eta(t)\psi(t)dt$  is the Gaussian noise at delay  $\tau_l$ , and  $\epsilon_l = \int_0^{T_s} \epsilon(t)\psi(t)dt$  is the interference energy at delay  $\tau_l$ .

Note that  $\alpha(\tau) = 0$  if  $\tau \leq 0$  or  $\tau \geq T_d$ . We employ Rake receivers with maximal ratio combining (MRC) method [19] for energy capture, assuming

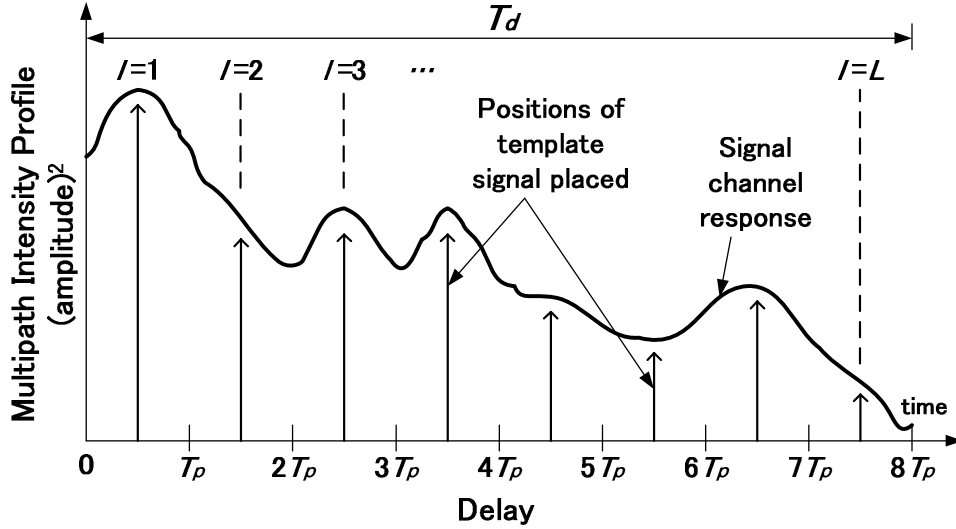


Figure 2.3: Illustration of Received Signal Channel Response and Placement of Template Signals in the Rake Receiver.

both magnitude and phase of the channel response are known, and also equal gain combining (EGC) method [19], assuming only the phase of the channel response is known. The placement of template signals by Rake receiver in multiples of  $T_p$  in the channel response with maximum delay spread  $T_d$  can be illustrated in fig.2.3.

Next, the Rake combiner combines the resolvable paths to form the decision statistics. If all  $L$  paths are combined, the receiver is known as an all Rake (ARake) receiver, whereas if only the best  $L_c < L$  paths are combined, the receiver is known as a selective Rake (SRake) receiver. An SRake receiver has a compromised energy capture capability, with lower system complexity [19].

## 2.2 Energy Capture and System Performance

The idea of energy capture (EC) for impulse radio is initially proposed in [20] and is later applied to characterize system performance in multipath environment [21]. In this section, EC is extended into the analysis of DS-UWB and DS-MB-UWB system performance corresponding to different parameters.

The energy able to be captured by the Rake receiver in a total number of  $L_c$  paths are given as:

$$E_{cap} = E_p N_s E_d \sum_{l=0}^{L_c-1} |\chi_l \alpha(\tau_l)|^2 \quad (2.11)$$

It is important to note that  $E_{cap}$  is the energy captured by matching the template signal to the channel response, and  $E_{cap} < E_d$  due to fading, self interference and Rake fingers. From (2.11), we can also express the normalized captured energy as:

$$E'_{cap} = \frac{E_{cap}}{E_d} * 100\% \quad (2.12)$$

Here, we can define  $E'_{cap}$  (in %) as the ratio between the captured energy  $E_{cap}$  and the ideal total energy in received signal  $E_d$ .

Next, applying the captured energy, the combined resolvable paths are used to form the decision statistics. The decision statistic for MRC method can be described as:

$$Z = \sqrt{E_p N_s E_d} \sum_{l=0}^{L_c-1} \chi_l \alpha(\tau_l) Z_l = E_p N_s E_d \sum_{l=0}^{L_c-1} \chi_l^2 \alpha(\tau_l) \alpha(\tau_l) + \eta + \epsilon \quad (2.13)$$

where  $\eta = \sum_{l=0}^{L_c-1} \sqrt{E_p N_s E_d} \chi_l \alpha(\tau_l) \eta_l$  is the Gaussian noise in all  $L_c$  paths and  $\epsilon = \sum_{l=0}^{L_c-1} \sqrt{E_p N_s E_d} \chi_l \alpha(\tau_l) \epsilon_l$  is the interference energy existing in all  $L_c$  paths.

And for MRC method, as:

$$Z = \sum_{l=0}^{L_c-1} \beta_l Z_l = \sqrt{E_p N_s E_d} \sum_{l=0}^{L_c-1} \beta_l \chi_l \alpha(\tau_l) + \eta + \epsilon \quad (2.14)$$

where  $\beta_l = \{+1, -1\}$ ,  $\eta = \sum_{l=0}^{L_c-1} \beta_l \eta_l$  is the Gaussian noise in all  $L_c$  paths and  $\epsilon = \sum_{l=0}^{L_c-1} \beta_l \epsilon_l$  is the interference energy existing in all  $L_c$  paths.

Finally, system performance is quantified as bit error rate (BER) which can be described as:

$$\text{BER} = P(d_i = +1)P(Z_i < 0|d_i = +1) + P(d_i = -1)P(Z_i > 0|d_i = -1) \quad (2.15)$$

where  $P(\cdot)$  denotes probability and  $Z_i$  is the decision statistic of the  $i$ -th data  $d_i$ .

## 2.3 Multipath Channel Model

The multipath channel model [22, 23] proposed by IEEE P802.15 working group for wireless personal area network (WPAN) is applied in this research.

Table 2.1: IEEE 802.15.3a Multipath Channel Models.

Model	LOS/NLOS	Distance	RMS Delay
CM1	LOS	0-4m	5.28ns
CM2	NLOS	0-4m	8.03ns
CM3	NLOS	4-10m	14.28ns
CM4	Extreme NLOS	–	25ns

This realistic indoor multipath channel models for UWB communications are proposed with reference to the classical work in [24], with slight modification on the multipath gain magnitude as lognormal distributed instead of Rayleigh distributed.

The impulse response of the  $i$ -th realization can be given by [22]:

$$h_x(t) = X_x \sum_{l=0}^{\lambda_{cl}} \sum_{l=0}^{\lambda_{ray}} a_{y,l}^x \zeta_D(t - T_l^x - \tau_{y,l}^x) \quad (2.16)$$

where  $\zeta_D$  is the Dirac delta function,  $\{a_{x,l}^x\}$  are the multipath gain coefficients,  $\{T_l^x\}$  is the delay of the  $l$ -th cluster,  $\{\tau_{y,l}^x\}$  is the delay of the  $y$ -th multipath component (ray) relative to the  $l$ -th cluster arrival time  $\{T_l^x\}$ ,  $\{X_x\}$  is the log-normal shadowing term,  $\lambda_{cl}$  is the total number of clusters and  $\lambda_{ray}$  is the number of rays in each cluster.

Eq.(2.16) can be different for different physical condition of the indoor multipath channel. Note that [22, 23] have not included path loss model. Brief descriptions for these channel models are shown in tab.2.1<sup>1</sup>.

## 2.4 Simulation Setup and Parameters

The system and channel model developed in the previous sections are employed to investigate the system performance of DS and DS-MB-UWB systems through computer simulations.

DS-UWB and DS-MB-UWB signals are transmitted over multipath, multi-user channels in the presence of a coexisting narrowband signal. This section discusses the performance in multipath and multi-user environment, while the impact of narrowband interference will be discussed in later chapters. Multipath channel models in [22] are applied. Also, modulated Gaussian pulse with center frequency  $f_c$  (in the case of DS-MB-UWB, multiple center frequencies  $f_m$  with  $m=1,2,3,\dots,B$ ) are assumed. The pulse can be described as:

$$p(t) = \cos(2\pi ft) \exp\left(-2\pi \left(\frac{t}{t_m}\right)\right) \quad (2.17)$$

<sup>1</sup>LOS: line of sight. NLOS: Non LOS. CM: Channel Model, RMS: root mean square.

Table 2.2: Simulation Parameters for DS-UWB and DS-MB-UWB Systems.

Parameters	
pulse duration $T_p$	0.267ns to 4ns
chip length $N_s$	1 to 40
SNR	0dB to 24dB
Rake fingers $L_c$	1 to $L$
Rake combining method	MRC, EGC
Multipath Channel Model	IEEE 802.15.3a CM1, CM2, CM3, CM4
number of simultaneous users	1 to 8
data modulation	BPSK
pulse waveform	modulated Gaussian

where  $t_m = 0.39T_p$  is the pulse width constant,  $T_p$  is the pulse duration and  $f$  is the pulse center frequency. The summary of simulation parameters can be shown in tab.2.2.

## 2.5 Performance in Multipath Channel

### DS-UWB Performance vs. SNR

Fig.2.4 presents the DS-UWB system performance vs. SNR in various multipath channel models. System parameters such as  $T_p$ ,  $L_c$ ,  $N_s$  are set to be 1ns, 8 and 15 respectively. The system operates at  $f_c=5\text{GHz}$  and the receiver employs Rake with MRC. Also, single user environment is assumed.

It is found that as SNR increases, BER performance can be improved. SNR is an input resource that measures the strength of signal over AWGN noise. Therefore, with higher SNR, stronger signal is generated and error in the decision statistic can be reduced. In other words, more energy can be captured at higher SNR. Here, it is shown that BER for CM1 is better than CM2, CM2 than CM3 and CM3 than CM4. BER performance in CM1 outperforms CM2 due to a stronger direct path and shorter delay spread in the LOS propagation, whereas CM2 and CM3 outlines the degradation of fading due to transceiver distance. CM4 highlights the degradation due to fading in an extreme NLOS channel. Fading in a dense multipath environment is one of the major factor determining performance for UWB communications.

### DS-UWB Performance vs. Different Rake Receptions

Next, the DS-UWB performance corresponding to different Rake receivers are presented and discussed in fig.2.5. Here, Rake receivers employing MRC and EGC methods with varying number of Rake fingers are considered. It is observed that Rake with MRC generally outperforms its EGC counterpart.

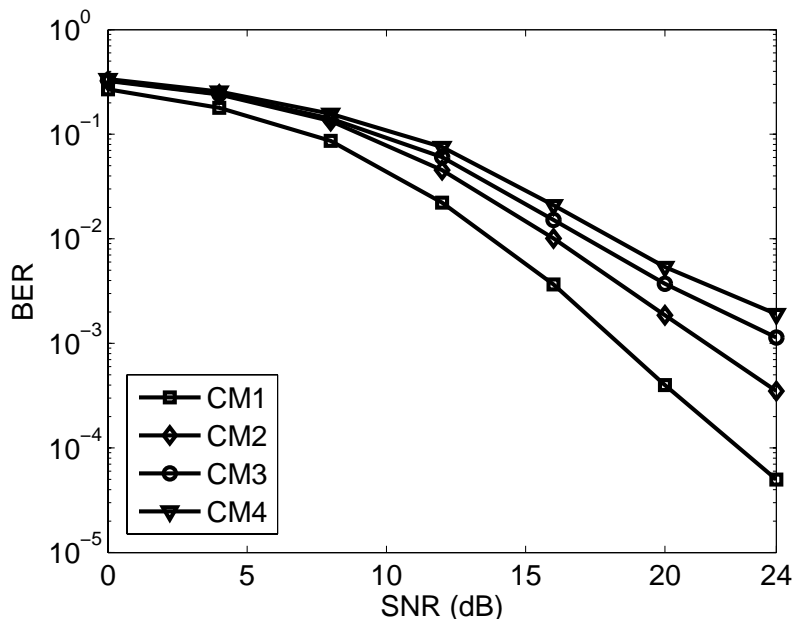


Figure 2.4: BER Performance vs. SNR over Different Multipath Channels for DS-UWB System.  $T_p=1\text{ns}$ ,  $N_s=15$ ,  $L_c=8$ ,  $f_c=5\text{GHz}$ .

An MRC ARake combining a total of  $L$  paths is found to perform relatively the best, followed by MRC SRake with  $L_c < L$  combined paths. In MRC Rake, less employed Rake fingers means less complex receiver structure but also compromised performance. As for EGC Rake receivers, when  $L_c$  increases from 1, BER performance improves until an optimum point, where after, despite more  $L_c$  is employed, BER performance on the other hand, degrades. This suggests that there are optimum  $L_c$  values for EGC Rake receivers. It is also worth noting that performance becomes the worst as  $L_c$  approaching ARake for EGC method. This is due to lacking of signal magnitude estimation and dominance of AWGN as  $L_c$  approaches  $L$ .

Determining the combination of receiver type and  $L_c$  depends on respective demands on the tradeoff between system complexity and system performance.

### DS-UWB Performance vs. Rake Fingers

Fig.2.6 furthers the analysis on performance of Rake reception corresponding to varying selected and combined paths in multipath channel for DS-UWB system.

For MRC Rake reception, as more  $L_c$  is being employed, better BER performance can be achieved. This observation is valid for all CM1 to CM4,

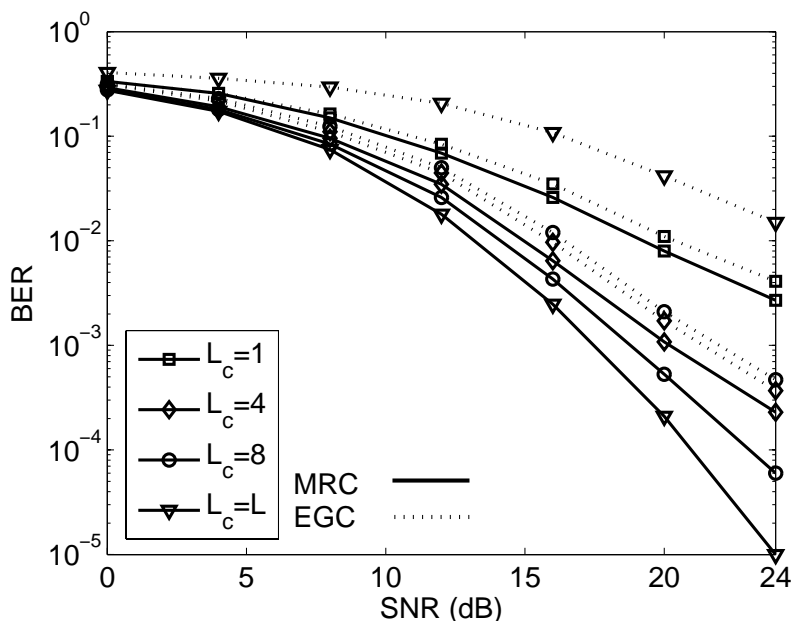


Figure 2.5: BER Performance vs. SNR for Different Rake Receivers for DS-UWB System.  $T_p=1\text{ns}$ ,  $N_s=15$ ,  $f_c=5\text{GHz}$ , CM1.

with CM1 having the best performance and CM4, the worst. Additionally, it is found that increasing  $L_c$  does not always improve BER performance. There is a point where after BER ‘saturates’ and does not further improve despite continuously increasing  $L_c$ . This  $L_c$  can be referred as the ‘saturated  $L_c$ ’. For all CM, the ‘saturated  $L_c$ ’ take place at around  $L_c=18$ . This can be explained that EC is effective at the first several paths where most of the signal energy is gathered in, and slowly declines in following resolvable paths. This observation suggests that there exists a limit of employing SRake with more  $L_c$  to enhance BER performance, since higher  $L_c$  means more complex receiver structure.

On the other hand, for EGC Rake reception, when  $L_c$  increases from 1, performance improvement can be observed. However, there is a point where continuously increasing  $L_c$  will on the contrary, degrades system performance. These ‘optimum  $L_c$ ’ have different values for respective channel models,  $L_c=5$  for CM1,  $L_c=12$  for CM2,  $L_c=15$  for CM3 and  $L_c=25$  for CM4. This ‘optimum  $L_c$ ’ exists because EGC Rake receiver combines the resolvable paths regardless of the amount of signal energy present in each path. Thus, as  $L_c$  increases from 1, more energy can be captured, and BER performance improves. But as  $L_c$  further increases, more noise is captured in paths with very little amount of fractional signal energy, and AWGN

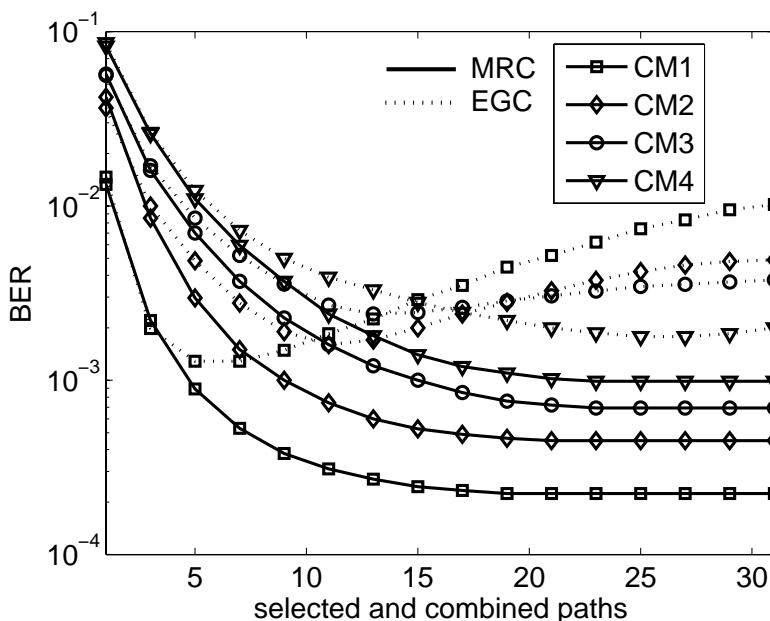


Figure 2.6: BER Performance vs. Selected and Combined Paths for Different Rake Receivers for DS-UWB System.  $T_p=1\text{ns}$ ,  $N_s=15$ ,  $f_c=5\text{GHz}$ ,  $\text{SNR}=20\text{dB}$ .

becomes more dominant.

Unlike EGC, degradation is not observed in Rake MRC because it places weight in every resolvable path in accordance to the amount of signal energy present, thus reducing the possibility of noise being captured.

Another comment in EGC Rake receiver is that at higher range of  $L_c$ , CM2, CM3 and CM4 perform better than CM1. Note that CM2, CM3 and CM4 are NLOS channels, with a weak direct path, but more fractional energy in the following paths. As in CM1 with LOS channel, a larger amount energy is present in the first few paths. Therefore, at lower  $L_c$ , better performance is observed in CM1, but the opposite is observed for CM2, CM3 and CM4.

This section presents different characteristics for different types of Rake receiver in multipath environment. The different performance of each type Rake receiver enables more flexible design options meeting various demands for performance-receiver complexity tradeoff.

### DS-UWB Performance vs. Chip Length

In DS-UWB signaling, another essential parameter is the DS chip length. The relationship between chip length  $N_s$  and BER performance can be

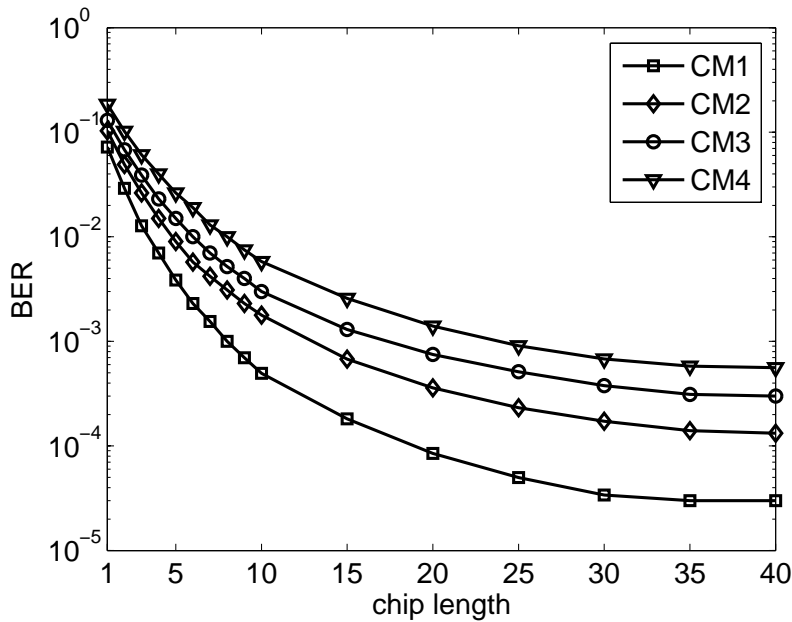


Figure 2.7: BER Performance vs. Chip Length over Different Multipath Channels for DS-UWB System,  $T_p=1\text{ns}$ ,  $L_c=8$ ,  $f_c=5\text{GHz}$ ,  $\text{SNR}=22\text{dB}$ .

shown in fig.2.7. Here the SNR is 22dB and multipath model CM1 to CM4 are considered. Also, single user environment is assumed.

It can be observed in fig.2.7 that in all channel models CM1 to CM, as  $N_s$  increases, BER performance improves. As more  $N_s$  is used to spread one data symbol, polarity randomization of the chips can be increased. This divides the same bit energy  $E_b$  into more fractional pulse energy  $E_p$ , thus enhances EC and reduces probability of wrong detection in the receiver. In DS signaling, chip length is a direct system resource that can be used to obtain better performance, with the tradeoff of processing gain (PG) and data rate.

Additionally, it is also noted that increasing  $N_s$  to improve BER performance is only effective up to a level, where ‘saturation’ takes place. After the ‘saturation’ point, no significant enhancement can be observed despite further increasing  $N_s$ . It is found that the saturation in fig.2.7 takes place at approximately  $N_c=35$ .

### DS-UWB Performance vs. Pulse Duration

Up to this section, analysis are conducted at system spreading bandwidth  $W_t=2\text{GHz}$  ( $T_p=1\text{ns}$ ). This section provides discussion on performance corresponding to system with varying  $W_t$ . Spreading bandwidth is also an

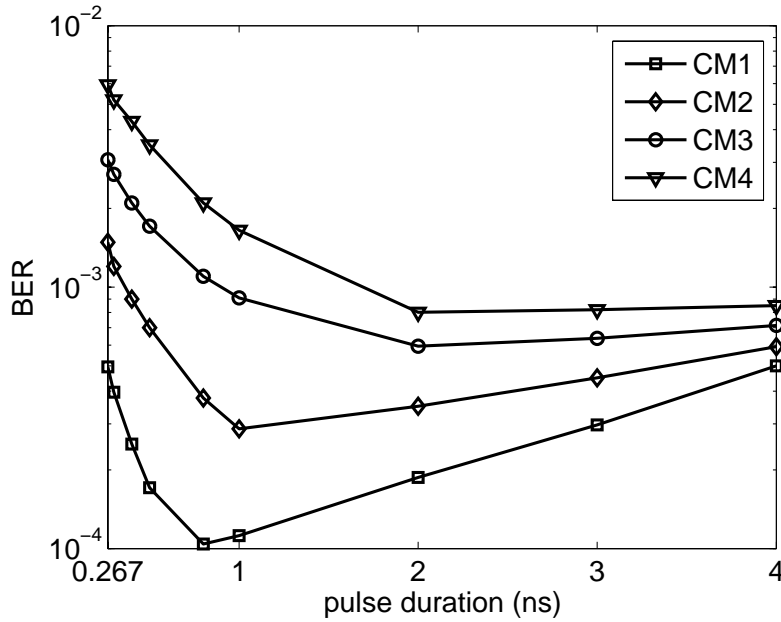


Figure 2.8: BER Performance vs. Pulse Duration over Different Multipath Channels for DS-UWB System.  $L_c=8$ ,  $f_c=6.75\text{GHz}$ ,  $\text{SNR}=22\text{dB}$ .

essential parameter in UWB signaling, allowing more energy to be transmitted at a fixed PSD.

Fig.2.8 shows the relationship between DS-UWB system performance and  $T_p$ . The center frequency  $f_c$  is constantly set to 6.75GHz with varying  $W_t$ .

As  $T_p$  decreases from 4ns to approximately 1ns, BER performance in all CM1 to CM4 generally improves. The reason is that as  $T_p$  decreases, less channel fading is experienced by the signal. In other words, at shorter  $T_p$ , the match filter is able to match the template signal in (2.9) to the received signal in (2.7) more effectively. This explains the enhancement of BER due to shorter  $T_p$ .

However, as  $T_p$  continues to decrease, BER performance on the other hand, degrades. As  $T_p$  becomes even shorter, the total number of resolvable paths  $L = T_d/T_p$  becomes considerably larger. By employing SRake with constant  $L_c=8$ , EC becomes less efficient in the increasing  $L$ . Furthermore, at very short  $T_p$ , AWGN takes over to become the more dominant factor compared to the captured energy, therefore causing BER to degrade significantly, as shown in the range of  $0.267\text{ns} \leq T_p \leq 1\text{ns}$  for CM1 and CM2,  $0.267\text{ns} \leq T_p \leq 2\text{ns}$  for CM3 and CM4, as shown in fig.2.8.

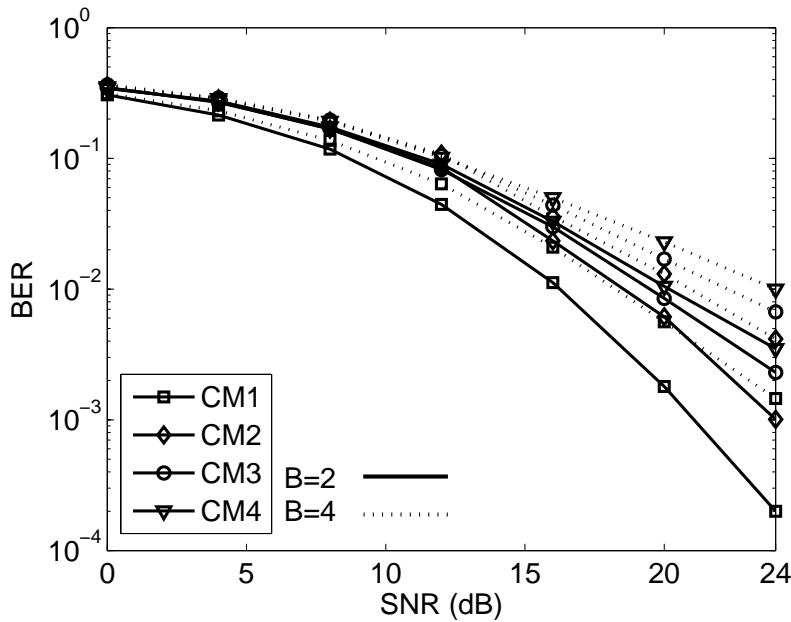


Figure 2.9: BER Performance vs. SNR over Different Multipath Channels for DS-MB-UWB System.  $L_c=8$ ,  $PG=20$ .

### DS-MB-UWB Performance vs. SNR

This section extends the analysis of DS-UWB signaling to multiband system, namely the DS-MB-UWB system. Fig.2.9 presents the relationship between DS-MB-UWB system performance and SNR. Number of bands  $B$  considered for DS-MB-UWB signaling are 2 and 4 bands. Total bandwidth  $W_t$  and  $PG$  for both systems are designed to be similar for fair comparison. For  $B=2$ ,  $T_p=2\text{ns}$ ,  $N_s=10$ , with center frequencies  $f_1=3.5\text{GHz}$  and  $f_2=4.5\text{GHz}$ , whereas for  $B=4$ ,  $T_p=4\text{ns}$ ,  $N_s=5$ , with center frequencies  $f_1=3.25\text{GHz}$ ,  $f_2=3.75\text{GHz}$ ,  $f_3=4.25\text{GHz}$  and  $f_4=4.75\text{GHz}$ .

Fig.2.9 shows that system with  $B=2$  generally outperforms system with  $B=4$  in all CM1 to CM4. The reason is that in order to keep the  $PG$  constant, shorter pulse and longer chip length are employed for system with lower  $B$ , thus result in superiority over system with higher  $B$ . Besides, relative performance among different multipath channels for DS-MB-UWB system are not different from that of the DS-UWB system.

### DS-MB-UWB Performance vs. Rake Fingers

Fig.2.10 presents the performance results for different Rake fingers for DS-MB-UWB system. Here, SNR and  $PG$  are designed to be 24dB and 20

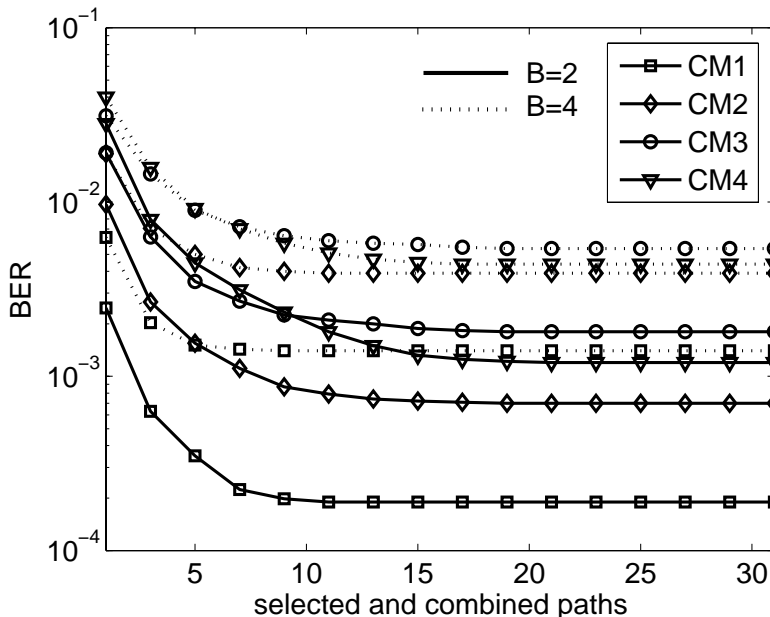


Figure 2.10: BER Performance vs. Rake Fingers over Different Multipath Channels for DS-MB-UWB System. SNR=24dB, PG=20.

respectively. Systems with  $B=2$  and 4 are considered. Also, Rake receiver with MRC method is used.

It is observed that in multiband systems, the behavior of MRC Rake receiver performs alike to that in DS-UWB signaling system. BER performance improves as  $L_c$  increases until the 'saturation  $L_c$ '. System with  $B=4$  collectively have worse performance than  $B=2$ .

One notable point in DS-MB-UWB signaling is on performance in CM3 and CM4. At lower  $L_c$ , system performs better in CM3 but as  $L_c$  increases, the opposite is observed. And at the 'saturated  $L_c$ ', BER performance for CM4 outperforms CM3. This can be explained that DS-MB-UWB signal is subject to more degradation due to distance than extreme NLOS condition.

## 2.6 Performance in Multi-user Channel

So far, only the scenario of a single user is considered in performance evaluation for UWB systems in various multipath channels. This section investigates the impact on system performance when more users are sharing the same channel.

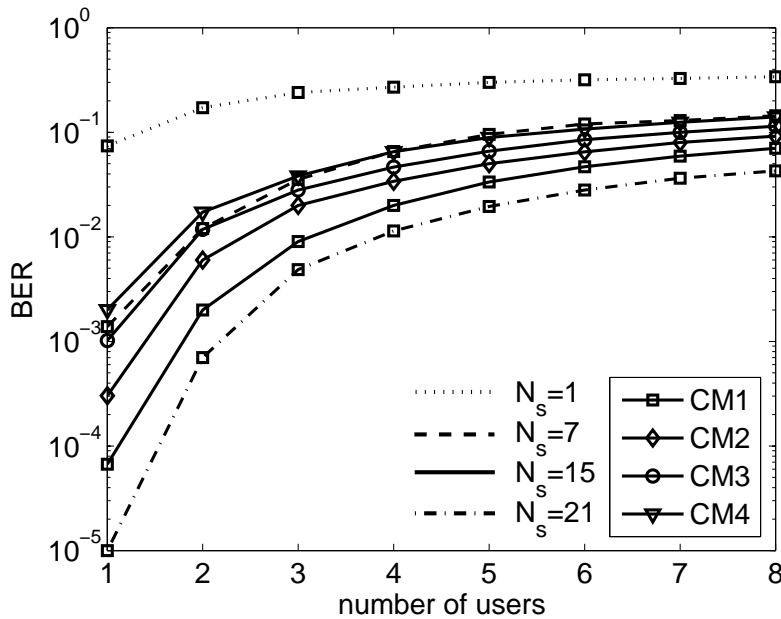


Figure 2.11: BER Performance vs. Number of Users for DS-UWB System.  $T_p=1\text{ns}$ ,  $L_c=8$ ,  $N_s=15$ ,  $f_c=5\text{GHz}$ ,  $\text{SNR}=24\text{dB}$ .

### DS-UWB Performance vs. Number of Users

Fig.2.11 presents the results for BER performance corresponding to number of simultaneous users in the multi-user channel. System parameters such as  $T_p$ ,  $L_c$  and  $\text{SNR}$  are set to  $1\text{ns}$ ,  $8$  and  $24\text{dB}$  respectively. The system is operating at  $5\text{GHz}$  with a  $W_t=2\text{GHz}$ . Transmit power of all users, including the desired user, are assumed to be similar. Here, asynchronous multiple access is considered.

As more users are present in the channel, BER performance degrades. Different multipath channels are found to have different impact on the system performance. System is CM1 outperforms the other NLOS channels, while CM4 is relatively the worst. Besides that, to improve BER performance, higher  $N_s$  can be employed to increase polarity randomization among users. From fig.2.11, system with higher  $N_s$  outperforms those with lower.

## 2.7 Concluding Remarks

In this chapter, introductions on DS-UWB and DS-MB-UWB systems are presented. System model including signaling model, channel model and receiver model are developed. Then by using computer simulations, the

performance of the systems are investigated over multipath and multi-user environments. Different Rake receivers with varying Rake fingers are employed to evaluate the system performance in multipath channels. Additionally, the effects of other system resources such as chip length, spreading bandwidth and SNR are also investigated.

Future works include the hybrid of TH signals in multiband UWB system to further utilize the potentials.

The next chapter will further discuss the details manipulating chip duty factor in signal design to achieve purposes such as fading channel mitigation and narrowband interference mitigation.

## Chapter 3

# Impact of Chip Duty Factor

Unlike conventional spread spectrum (SS) system which intends to decrease PSD by increasing spreading bandwidth at a fixed data rate, UWB system attempts to increase data rate by increasing spreading bandwidth at a fixed PSD [25]. This is a fundamental difference distinguishing UWB from SS system, although both share certain similarities in characteristics. Particularly in signal design, the manipulation of chip duty factor (DF) for bandwidth spreading is a unique characteristic for UWB system. This chapter introduces UWB system with low DF and discusses the signaling design with relevant advantages.

The early UWB radio known as IR [9] employs signal with low DF to increase robustness [26] in dense multipath environments [27] and to support multiple access through TH modulation [10]. The great potentials displayed by UWB radio has invited a huge amount of attention attempting to fully utilize its technical advantage. Eventually, the DS method, previously applied for SS system, is proposed [14, 17] and became another popular option for UWB spreading.

IR is able to effectively combat multipath fading and support multiple access channel due to the employment of low DF signaling. Similarly, it should also be beneficial if the proposed DS-UWB system can be coupled with low DF signal designs to further accelerates its capability. However, up to date, most DS-UWB systems in current literatures design signals with unity DF, which does not display much difference from the conventional DS-SS system. Furthermore, the impact of varying DF on performance of both IR and DS-UWB systems also remains unclarified. Works such as [28] has proposed a general low DF UWB system, without detailed investigation on the DF signaling characteristics. In other words, the effects of applying low DF signal is still a less understood topic in UWB system.

Therefore, the main purpose of this chapter is to clarify the relationship between UWB system and low DF signaling over multipath and multi-user environment. Investigation is conducted on system performance correspond-

ing to various system designs such as Rake receptions, spreading techniques and so on. The focus of this chapter should be of timely interest to the UWB community, especially after the initiative shown towards the application of low duty cycle (LDC) mitigation [8].

Additionally, the hybrid of DS and TH modulation is also found to be another encouraging modulation option [29] for UWB signal. DS and TH UWB systems are found to offer respective advantages under different circumstances [30,31], merging the two should be a good idea to simultaneously obtain strength of both. Currently, there are still many unexplored regions in the DS-TH-UWB system, especially in the issue of varying low DF signaling.

The outline of this chapter is given as below. Firstly, the design of low DF is described for DS, TH and DS-TH UWB signaling. Then system performance in fading channel is discussed. The analysis can also be found in the author's publications [32,33]. Next, the effects of using low DF signals in the presence of a coexisting narrowband signal is analyzed. Finally, low DF DS-MB-UWB signal with overlapping multiple sub-bands is introduced and discussed.

## 3.1 Chip Duty Factor in Signaling Design

### 3.1.1 Signal Models

A BPSK DS-TH-UWB transmitted signal of the  $k$ -th user can be described as:

$$s^{(k)}(t) = \sqrt{E_p} \sum_{i=-\infty}^{\infty} \sum_{j=0}^{N_s-1} d_i c_j^{(k)} p(t - iT_s - j\frac{T_p}{\delta} - q_j^{(k)}T_p) \cos(2\pi f_c t) \quad (3.1)$$

where  $d_i$  and  $c_j$ , both with random uniform values of  $\{+1,-1\}$ , are the  $i$ -th BPSK data and  $j$ -th user-dependent DS spreading code respectively,  $N_s$  is the number of chips (each with duration  $T_c$ ) per bit,  $T_p$  is the pulse duration with pulse energy  $E_p$ ,  $\delta = T_p/T_c$  is the chip duty factor DF and  $0 < \delta \leq 1$ ,  $T_s$  is the bit duration with bit energy  $E_b = N_s E_p$ ,  $q_j = \{0, 1, 2, \dots, N_c\}$  is the user-dependent TH sequence that provides an additional time shift of  $q_j T_p$  to the  $j$ -th pulse,  $N_c = T_c/T_p = 1/\delta$  is the total number of time slots available for the time hopping pulse,  $f_c$  is the pulse center frequency and  $p(t)$  is the transmitted pulse waveform. Note that spreading bandwidth  $W_t$  can be approximated by  $2/T_p$ . The system data rate  $R_b$  and processing gain PG are defined as  $1/T_s$  and  $N_s/\delta = N_s N_c$ , respectively. Signaling diagram for DS-TH-UWB can be referred to fig.3.1(a), where pulses with different polarities are placed in different time slots in every  $T_c$ .

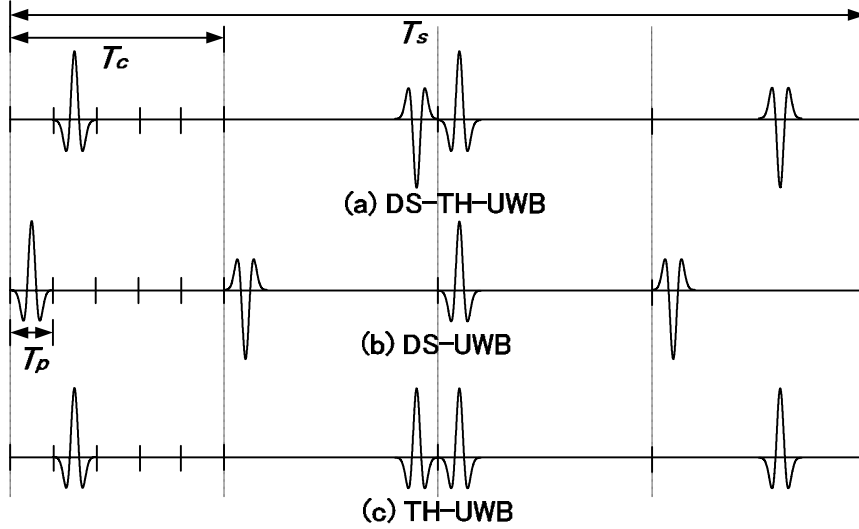


Figure 3.1: Illustrations for (a) DS-TH-UWB, (b) DS-UWB and (c) TH-UWB Signal. In this example,  $N_s=4$  and  $N_c=5$ .

Next, (3.1) can be modified easily to obtain the DS-UWB signal of the  $k$ -th user, by simply setting the TH sequence  $q_j$  to constant 0, as below:

$$s^{(k)}(t) = \sqrt{E_p} \sum_{i=-\infty}^{\infty} \sum_{j=0}^{N_s-1} d_i c_j^{(k)} p(t - iT_s - j\frac{T_p}{\delta}) \cos(2\pi f_c t) \quad (3.2)$$

Here, the PG is defined as  $N_s/\delta$ . Signaling diagram for DS-UWB is shown in fig.3.1(b), where pulses with different polarities are placed in the first time slot in every  $T_c$ .

Likewise, modifying (3.1), the TH-UWB signal of the  $k$ -th user can be obtained by setting DS code  $c_j$  to constant 1, as below:

$$s^{(k)}(t) = \sqrt{E_p} \sum_{i=-\infty}^{\infty} \sum_{j=0}^{N_s-1} d_i p(t - iT_s - j\frac{T_p}{\delta} - q_j^{(k)} T_p) \cos(2\pi f_c t) \quad (3.3)$$

where the PG is defined as  $N_s N_c$ . Here, signaling diagram for TH-UWB is shown in fig.3.1(c), where pulses with similar polarity are placed in different time slots in every  $T_c$ .

### 3.1.2 Varying Chip Duty Factor

As mentioned in earlier sections, DF can be described as:

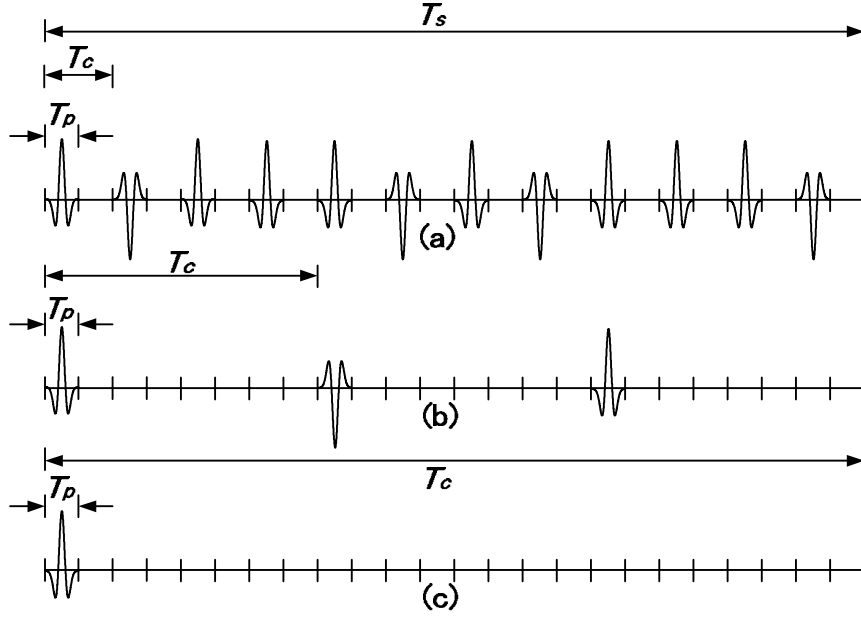


Figure 3.2: Signaling Design with lower DF by Employing lower  $N_s$ . (a)  $\delta=0.5$ ,  $N_s=12$ , (b)  $\delta=0.125$ ,  $N_s=3$ , (c)  $\delta=0.04$ ,  $N_s=1$ .

$$\delta = T_p/T_c = T_p N_s/T_s \quad (3.4)$$

By using (3.4), the signal models are applied to design signals with varying DF. The design of DF can be achieved through 3 methods, each manipulating different system parameters, namely chip length, pulse duration and pulse repetition frequency. Each method offers different advantages and requires respective system resources. These methods are described in the following sections.

### Low DF Signaling Design with Varying Chip Length

This method manipulates the number of chips per bit  $N_s$  to design signal with lower DF. By setting  $T_p$  and  $T_s$  constant, decreasing  $N_s$  decreases DF while maintaining  $W_t$ , PG and  $R_b$ . The illustration of such signal design with specific numerical examples can be shown in fig.3.2.

### Low DF Signaling Design with Varying Pulse Duration

Next, pulse duration  $T_p$  can also be manipulated to design signal with lower DF. By decreasing  $T_p$  while setting  $T_c$ ,  $T_s$  and  $N_s$  constant, DF can be decreased at the expense of wider spreading bandwidth  $W_t$  and higher PG, while  $R_b$  is constant. The illustration can be shown in fig.3.3.

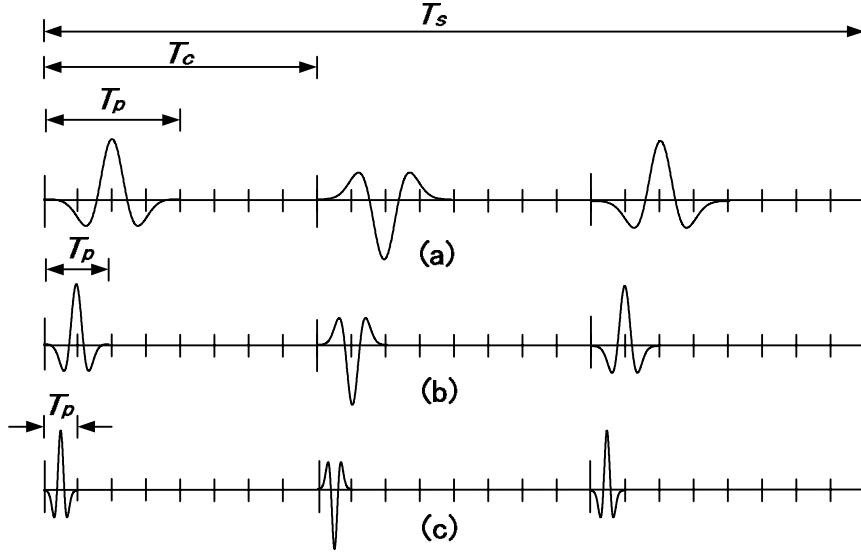


Figure 3.3: Signaling Design with lower DF by Employing lower  $T_p$ . (a)  $\delta=0.5$ , (b)  $\delta=0.25$ , (c)  $\delta=0.125$ .

### Low DF Signaling Design with Varying Pulse Repetition Frequency

Pulse repetition frequency PRF can be described as:

$$PRF = 1/T_c \quad (3.5)$$

PRF can be reduced to lengthen the interval from one pulse to the following pulse. In other words,  $T_c$  is increased as PRF decreases, as shown in (3.5). As a result, DF can be decreased by reducing PRF. In this design,  $T_p$  and  $N_s$  remain constant, while  $T_c$  and  $T_s$  increases, with data rate  $R_b$  as the tradeoff parameter. The illustration of the signaling diagram can be shown in fig.3.4.

The rest of the system models can be assumed to be similar to those described in the previous section. Received signal can be described by (2.7), the decision statistic by (2.13), normalized EC by (2.12), and the BER performance by (2.15).

## 3.2 Performance in Multipath Channel

### 3.2.1 DS-UWB Signaling Design with Low DF

The DS-UWB signal with low DF design described in (3.2) is transmitted over multipath and multi-user channel. Multipath channel models in [22]

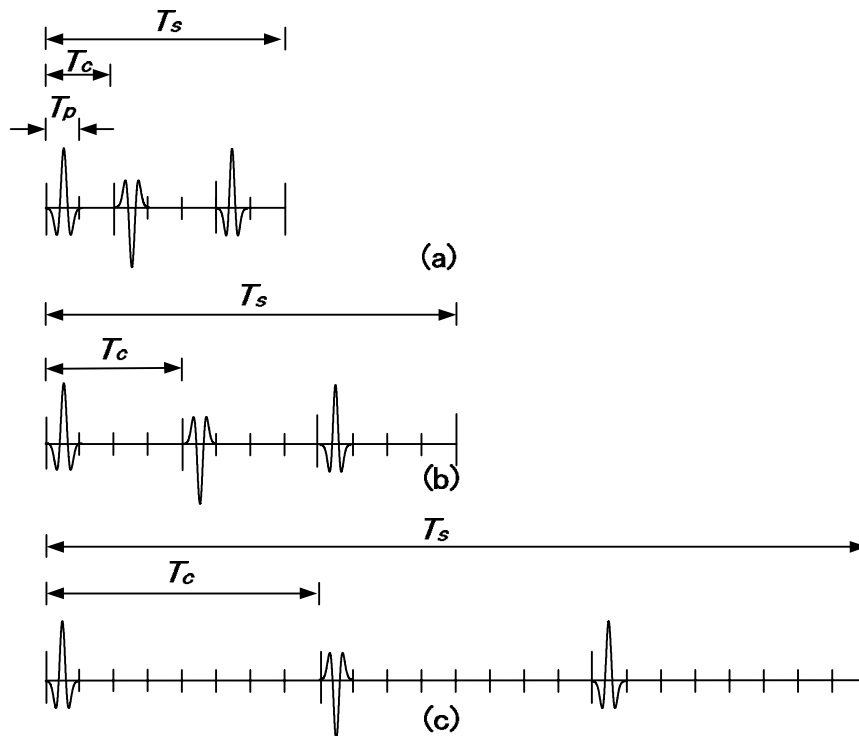


Figure 3.4: Signaling Design with lower DF by Employing lower PRF. (a)  $\delta=0.5$ , (b)  $\delta=0.25$ , (c)  $\delta=0.125$ .

are applied. Modulated Gaussian pulse with center frequency  $f_c$  described in (2.17) is used.

### Manipulating Chip Length

For signaling design illustrated in fig.3.2, the pairs of DF and  $N_s$  are listed in tab.3.1<sup>1</sup>. In this system, PG=24 remain constant despite changing of DF and  $N_s$ . The  $W_t$  considered are 2, 4 and 8GHz, with  $T_p=1, 0.5$  and  $0.25$ ns respectively. Parameters such as SNR,  $L_c$  and  $f_c$  are set to be 20dB, 8 and 4GHz respectively.

Fig.3.5 presents the impact of employing different DF (right ordinate)

<sup>1</sup>Figures are rounded up for simplicity.

Table 3.1: Pairs of DF and  $N_s$  for DS-UWB Signaling Design.

DF	0.04	0.08	0.13	0.17	0.25	0.5	1
$N_s$	1	2	3	4	6	12	24

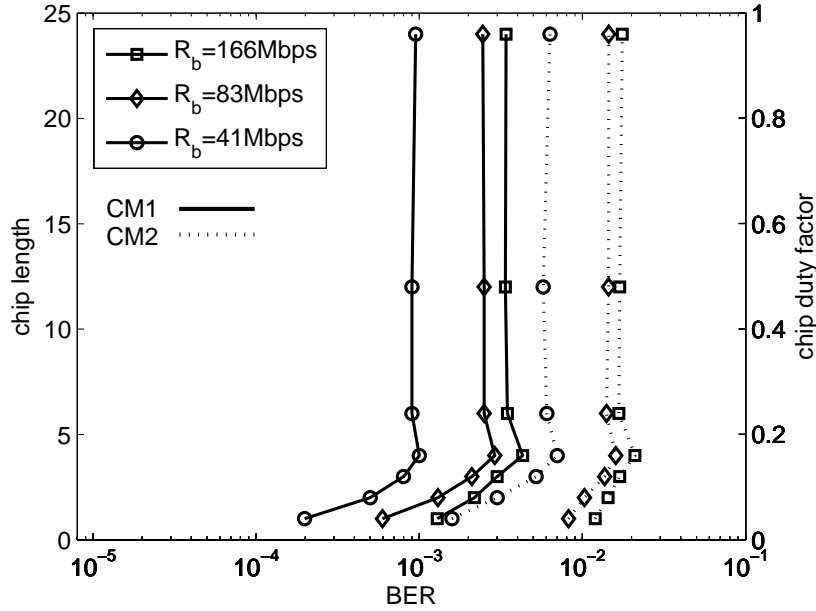


Figure 3.5: BER Performance vs. Chip Duty Factor Manipulating Varying Chip Length for DS-UWB System. PG=24, SNR=20dB,  $L_c=8$ ,  $f_c=4$ GHz.

paired up with the respective  $N_s$  (left ordinate) in systems with different  $R_b$ . As a general observation, system with lower  $R_b$  outperforms that of higher  $R_b$ . It is found that as DF decreases from  $\delta=1$  to 0.17, the BER performance does not display significant degradation until  $\delta=0.25$ . At  $\delta=0.17$ , slight performance degradation can be observed as compared to  $\delta=0.25$ . This can be explained that as DF decreases, inter-chip interference (ICI) is reduced because the distance between adjacent chips becomes farther apart. On the other hand, simultaneously as DF decreases, shorter  $N_s$  is employed (refer to tab.3.1) in order to maintain PG. Shorter  $N_s$  indicates that less number of chips are used to spread one data bit. In other words, the same amount of bit energy is distributed to less number of chips. This increases the energy per pulse and therefore also increases the amount of ‘ICI per pulse’. Lower DF paired up with shorter  $N_s$  causes two opposing factors: (1) decreasing DF decreases ICI thus improves BER performance and, (2) decreasing  $N_s$  increases energy per pulse and ‘ICI per pulse’, thus degrades BER performance. The combination of these two factors decides the improvement or degradation of performance, depending which is more dominant. If the positive factor of decreasing DF is more dominant, BER performance improves. On the other hand, if the negative factor of shorter  $N_s$  is more dominant, BER performance degrades.

By changing DF and  $N_s$ , the number of selected and combined paths  $L_c$  and total resolvable paths  $L$  can be manipulated and thus determine the BER performance. At  $0.25 \leq \delta \leq 1$ , both factors are equally strong, causing the BER performance to remain constant. However, as DF decreases from  $\delta=0.25$  to 0.17, BER performance becomes noticeably worse due to the factor of shorter  $N_s$  (increasing ICI per pulse) becoming more dominant over the factor of decreasing DF (decreasing ICI). Next, as DF continues to decrease below  $\delta=0.17$ , BER performance is found to improve significantly. This is because the lower DF becomes, the more ICI can be mitigated. In this range, the decreasing DF is dominant over the factor of shorter  $N_s$ . This indicates that the mitigation of ICI becomes effective at lower range of DF (DF less than 0.17) despite increasing ‘ICI per pulse’.

For BER performance corresponding to different multipath channel models, it is observed that performance in CM1 is better than in CM2. This is due to a strong direct path for the LOS CM1. Additionally, CM2 has longer delay spread, causing not only ICI but also inter-symbol interference (ISI), thus further degrading BER performance.

The discussions above conclude that the advantage of BER improvement in DS-UWB system by employing lower DF can only be achieved in  $\delta \leq 0.17$ . Additionally, by manipulating DF and  $N_s$ , a worst case for BER performance can be observed, where decreasing DF results in degraded BER. The avoidance of this ‘worst case’ value is essential in system designs with different demands and tradeoff.

### Manipulating Pulse Duration

In this section, the impact of varying DF on BER performance with spreading bandwidth  $W_t$  as a tradeoff parameter is investigated. To design  $\delta$  from 0.01 to 1,  $T_c$  is set to constant 4ns and  $T_p$  is varied from 0.04ns to 4ns, as illustrated in fig.3.3. By reducing  $T_p$ ,  $W_t$  becomes wider. Here, it is notable that  $R_b$  remains constant.

Fig.3.6 presents the results for BER performance according to varying DF, with DF placed at the left ordinate and  $W_t$  at the right. Firstly, it is observed that BER performance in multipath channel CM1 outperforms that in CM2. This is due to the greater degradation of signal over non-LOS environment, and also the ISI caused by longer delay spread in CM2. Furthermore, as  $\delta$  falls below 0.4, more BER improvement is observed in CM1 as compared to CM2. This suggests that the use of lower DF signal is more effective in CM1.

Next, the observation can be divided into two parts for discussion. Firstly, for  $0.85 \leq \delta \leq 1$ , system performance degrades. Secondly, for  $\delta < 0.85$ , system performance improves considerably. At  $0.85 \leq \delta \leq 1$ ,  $T_p$  is decreased to the range of  $0.85T_c \leq T_p \leq T_c$ . Note that Rake receivers increase multipath resolvability by placing template signals in multiples of  $T_p$  to capture

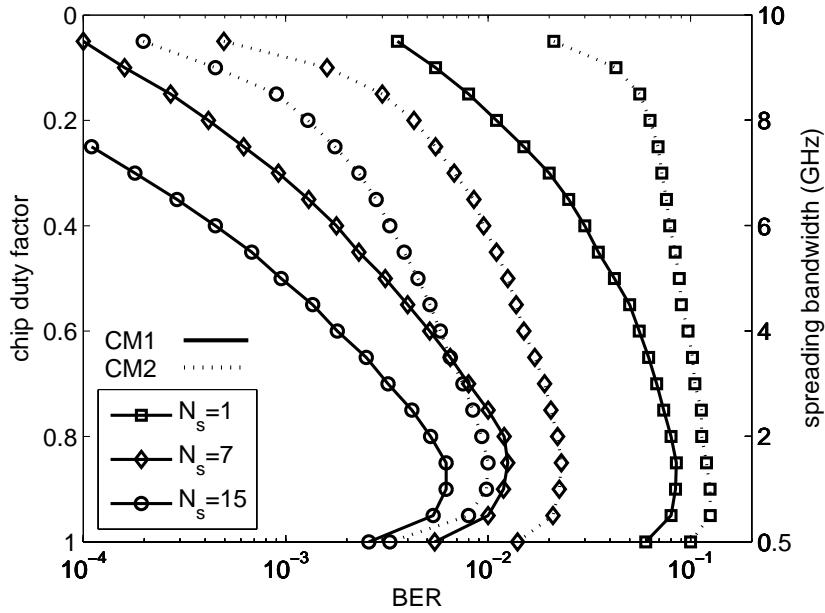


Figure 3.6: BER Performance vs. Chip Duty Factor Manipulating Varying Spreading Bandwidth for DS-UWB System. SNR=20dB,  $L_c=8$ ,  $f_c=4$ GHz.

energy from receiving signal in multiples of  $T_c$ . However, in the range of  $0.85T_c \leq T_p \leq T_c$ , the template signals are constantly placed between two adjacent multipaths, and are therefore subjected to partial correlation from these adjacent multipaths. This degrades the amount of energy able to be captured by the template signals, especially when the adjacent multipaths consist of opposing polarities. This factor contributes mainly to the BER degradation taking place in the region  $0.85 \leq \delta \leq 1$ .

Secondly, as DF continues to decrease below 0.85, performance improvement is observed. This is because at  $\delta < 0.85$ ,  $T_p$  becomes notably shorter and thus the possibility of the template signal being placed between two adjacent multipaths becomes lower. This results in the effect of partial correlation to become less significant. Besides, decreasing DF reduces ICI and ISI by separating the adjacent pulses farther apart. Furthermore, with shorter  $T_p$ , more paths  $L$  can be resolved and less channel fading is experienced, thus increasing the EC of Rake receivers. All these factors contribute to the improvement of BER performance at  $\delta < 0.85$  when  $L_c$  paths is selected and combined.

The discussions above conclude that in order to obtain significant performance improvement from employing lower DF, the signal has to be designed to have DF lower than 0.85.

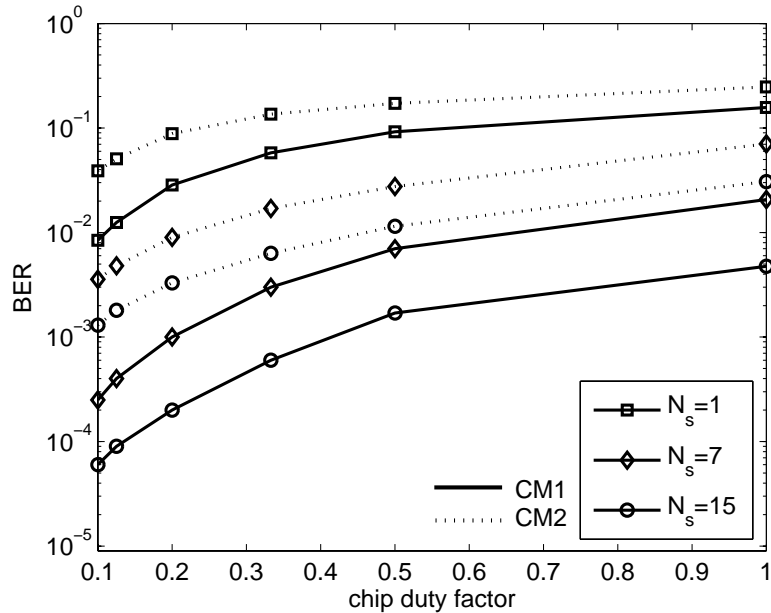


Figure 3.7: BER Performance vs. Chip Duty Factor Manipulating Varying PRF for DS-UWB System. SNR=20dB,  $L_c=8$ ,  $f_c=4$ GHz.

The discussion of  $W_t$  as a tradeoff parameter as DF decreases can also be referred to the right ordinate in fig.3.6. At  $0.6\text{GHz} \leq W_t \leq 9\text{GHz}$ , BER performance can be improved by increasing  $W_t$ . This is reasonable because wider  $W_t$  enables system to experience less channel fading. However, at  $W_t \leq 0.6\text{GHz}$ , the contrary is observed, where increasing  $W_t$  from 0.5 to 0.6GHz on the other hand, degrades BER performance. This suggests that there exist a ‘worst case’ for DS-UWB system employing wider  $W_t$ . This ‘worst case’ normally takes place in lower range of  $W_t$ , with  $\delta$  in the range of 0.9 to 1.

### Manipulating Pulse Repetition Frequency

In this section, the impact of  $\delta$  from 0.1 to 1 is investigated by setting  $T_p$  to constant 4ns and  $T_c$  from 4ns to 40ns, thus reducing the system PRF from 250MHz to 25MHz. The illustration of the signaling design can be given in fig.3.4.

From fig.3.7 we found that as  $\delta$  decreases, BER performance improves. This is because as  $\delta$  decreases,  $T_c$  becomes longer, and thus separating adjacent pulses farther apart. As a result, ICI and ISI can be reduced. The BER degradation within  $0.5 \leq \delta \leq 1$  is not observed here because  $T_c$  is extended in multiples of  $T_p$ , thus avoiding the range where partial correlation from

two multipaths occur.

However in this design, as a tradeoff parameter for BER improvement, data rate  $R_b$  becomes lower.

### 3.2.2 Comparison with Other UWB Modulations

Besides DS-UWB signaling, TH and hybrid DS-TH modulations can also be applied as options for UWB spreading. This section presents and discusses the impact of DF on performance of these UWB systems from the perspective of EC. Low DF UWB signaling is designed by manipulating  $N_s$ , while setting  $T_p$  and  $T_s$  constant, as shown in fig.3.2. Parameters such as SNR,  $W_t$ ,  $L_c$  and  $f_c$  are set to be 20dB, 2GHz, 8 and 6GHz. Also, PG is constantly set to be 48 in this system. Multipath channel models CM1 and CM2 are considered, with the scenario of a single user occupying the propagation channel. The DF and  $N_s$  pairs can be shown in tab.3.2<sup>2</sup>.

#### Energy Capture

The EC mechanism can be described by amount of energy captured  $E_{cap}$  in (2.11) and percentage of normalized captured energy  $E'_{cap}$  in (2.12). Fig.3.8 shows the comparison of EC for DS, TH and DS-TH UWB systems corresponding to various DF.

Firstly, the results for DS and DS-TH UWB systems in CM1 is discussed. An interesting finding is that DS-UWB actually outperforms DS-TH-UWB system. The only difference between the two is the additional time shift due to TH sequence in DS-TH signal. This TH sequence is identified as one of the main factor contributing to the inferior EC capability in DS-TH system. In DS signal, the pulse-to-pulse distance is constant, resulting only the last portion of ICI of an instantaneous pulse to have effect on the following pulse. However, In DS-TH signal, the time shift causes the pulses to be placed at random time slots, resulting the pulse-to-pulse distance to vary considerably. Therefore, ICI of an instantaneous pulse may become strong (at short pulse-to-pulse distance) at times and weaker (at long pulse-to-pulse distance) at other. And from fig.3.8 it is found that the average ICI in DS-TH signal is

---

<sup>2</sup>Since TH modulation is involved, 0.5 is chosen to be the highest DF. Figures are rounded up for simplicity.

Table 3.2: Pairs of DF and  $N_s$  for DS, TH and DS-TH UWB Signaling Design.

DF	0.02	0.04	0.08	0.13	0.17	0.25	0.5
$N_s$	1	2	4	6	8	12	24

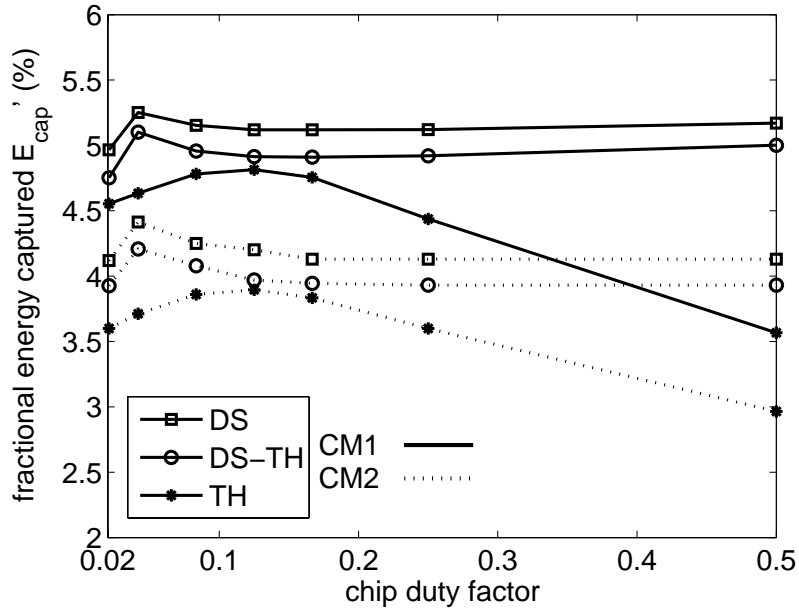


Figure 3.8: Energy Capture vs. Chip Duty Factor for DS, TH and DS-TH UWB Systems.  $W_t=2\text{GHz}$ ,  $L_c=8$ ,  $f_c=6\text{GHz}$ .

stronger than the ICI in DS signal. The stronger ICI in DS-TH system has caused its EC to be less effective than DS system.

Next, for DS and DS-TH system in CM1, as DF decreases, both systems display similar EC behavior :  $E'_{cap}$  constant initially, followed by improvement, and then degradation takes place. The amount of energy able to be captured in the Rake receiver is determined by the interactions of ICI corresponding to varying DF. The occurrence of two simultaneous but opposing factors due to decreasing DF : (a) decreasing total ICI and (b) increasing energy per pulse thus ICI per pulse, are the main reasons of such system behavior. This analysis have been given in the previous section.

Secondly, the results of TH-UWB system in CM1 are discussed. It is found that TH system performs relatively the worst as compared to DS and DS-TH systems. The previous discussion suggested that the time shift due to TH sequence causes stronger ICI to the system and therefore degrades EC considerably. In TH system, apart from the time shift, EC capability is subjected to even worse degradation due to the lack of polarity randomization for different pulses. It is observed that TH system has the worst EC performance at high DF,  $\delta=0.5$ . This is reasonable because at  $\delta=0.5$ , only 2 time slots are available for hopping. As  $\delta$  decreases from 0.5 to 0.13, better EC can be achieved. This can be explained that as DF decreases, more time

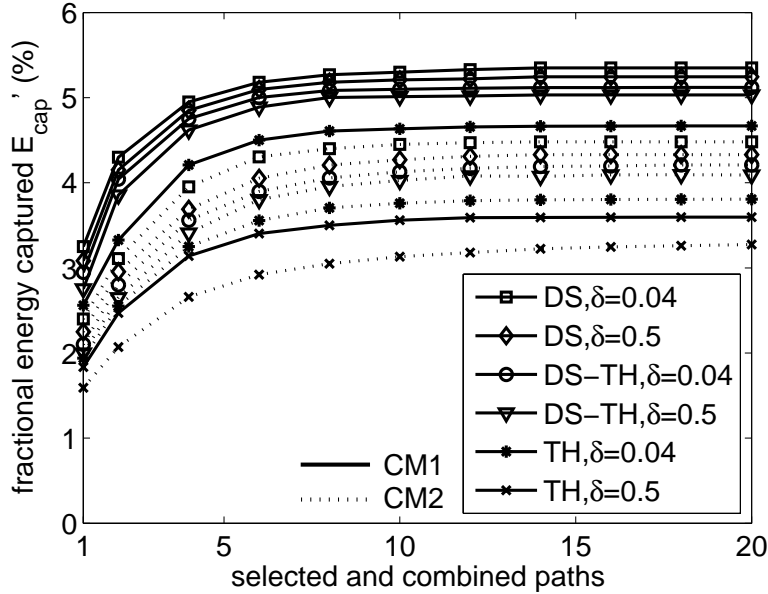


Figure 3.9: Energy Capture vs. Selected and Combined Paths for DS, TH and DS-TH UWB Systems.  $W_t=2\text{GHz}$ ,  $f_c=6\text{GHz}$ .

slots are available for hopping. And besides, decreasing DF also reduces the total amount of ICI. On the contrary, at  $\delta < 0.13$ , the negative factor of decreasing  $N_s$  becomes more dominant, thus causes the EC capability to be degraded to  $E'_{cap}=4.5\%$  at  $\delta=0.02$ .

Thirdly, the effects of different multipath channels on the EC capability in DS, TH and DS-TH systems are analyzed. As shown in fig.3.8, all systems are able to achieve higher EC in CM1 as compared to CM2, with the exception of  $\delta=0.5$  for TH system. In LOS propagation of CM1, a strong direct path, with relatively large amount of fractional signal energy is present, resulting the EC to be more effective. For non-LOS in CM2, the absence of the direct path causes the lost of reasonably large amount of signal energy able to be captured, thus resulting in EC to be less effective. Besides, the channel delay spread due to CM2 is considerably longer than CM1, therefore generating not only ICI but also stronger ISI. On top of the effects of ICI, ISI causes further degradation to adjacent bits and compromises the EC capability in the receiver more severely.

Discussion so far focused on SRake receivers with  $L_c=8$ . Here, fig.3.9 shows the performance comparison of Rake reception with varying  $L_c$  for DS, TH and DS-TH systems.

In fig.3.9, it is observed that as  $L_c$  increases, EC generally increases

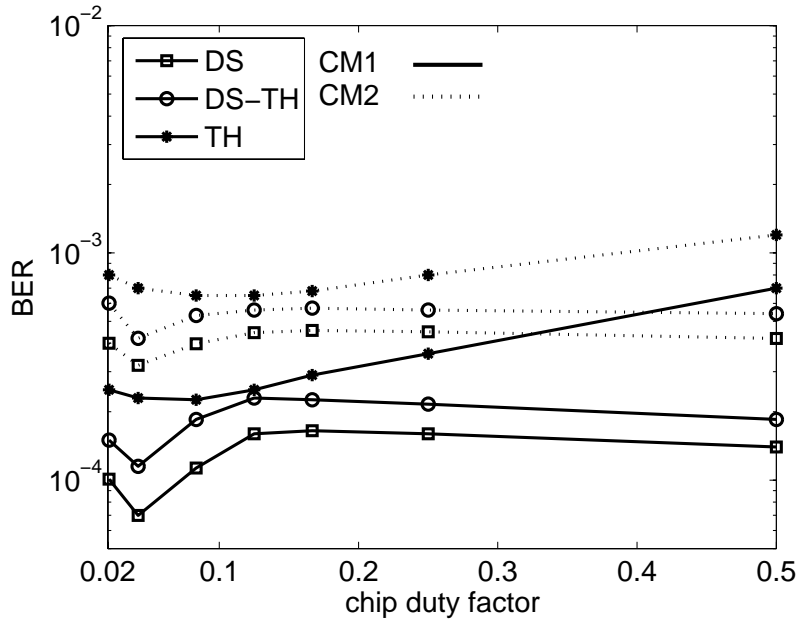


Figure 3.10: BER Performance vs. Chip Duty Factor for DS, TH and DS-TH UWB Systems. SNR=20dB,  $L_c=8$ ,  $W_t=2$ GHz,  $f_c=6$ GHz.

regardless of spreading schemes. This is reasonable because more fractional energy in the received signal can be captured by combining more number of best selected multipaths by the SRake receiver. The highest achievable EC is approximately  $E'_{cap}=5\%$ . This suggests that the fractional EC is severely saturated by ICI with reference to [34] reporting that SRake EC reaches as high as approximately 20% without the presence of ICI.

The ‘saturation  $L_c$ ’ is observed in all UWB signaling, mostly below  $L_c < 10$ . Additionally, CM2 is found to degrade EC capability more severely due to longer delay spread and the absence of direct path.

### BER Performance vs. Chip Duty Factor

Fig.3.10 and fig.3.11 present the comparison for BER performance of UWB systems with DS, TH and DS-TH signaling, corresponding to different DF and  $L_c$ . System BER performance is determined by EC capability of the Rake receivers as described in (2.13) and (2.15).

Fig.3.10 verifies the idea that the BER performance is dependent on EC in the Rake receivers. DF values showing lower EC in fig.3.8 have inferior BER performance in fig.3.10. In other words, results for EC in fig.3.8 can be used to explain the observations in every DF value in fig.3.10.

DS signaling is found to have the best performance among the three in

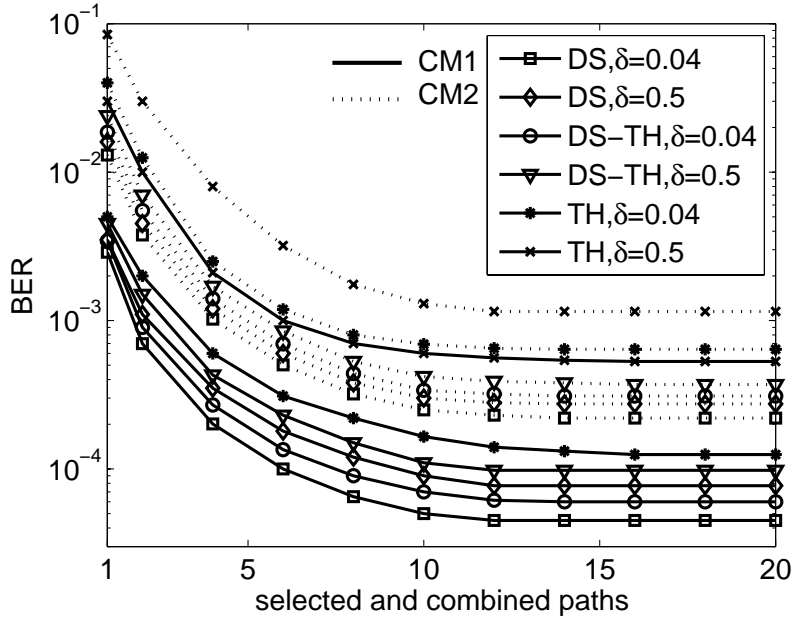


Figure 3.11: BER Performance vs. SRake Selected and Combined Paths for DS, TH and DS-TH UWB Systems. SNR=20dB,  $f_c=6$ GHz,  $W_t=2$ GHz.

single user environment, followed by DS-TH signaling. On the other hand, TH signaling has the relative worst performance. Also, optimum DF values are observed to exist for all systems, suggesting that careful signaling design is necessary to achieve optimized performance. In multipath channel CM1, the systems collectively performing better than in CM2, with the exception of TH system at high  $\delta=0.5$ .

### BER Performance vs. Rake Fingers

Next, in fig.3.11 also shows that BER performance is dependent on EC capability. For all three systems, BER performance for  $\delta=0.04$  outperform those with  $\delta=0.5$ . This statement is valid in all range of  $L_c$ . Among all, DS system has the best BER performance, and TH relatively the worst. The ‘saturation  $L_c$ ’, after which no BER improvement can be observed despite further increasing  $L_c$ , is noted at  $L_c=10$ .

### BER Performance vs. Number of Users

Discussion so far has been focused on the assumption of single user environment. Next, BER performance of DS, TH and DS-TH UWB systems are reviewed considering more than one user sharing the propagation channel.

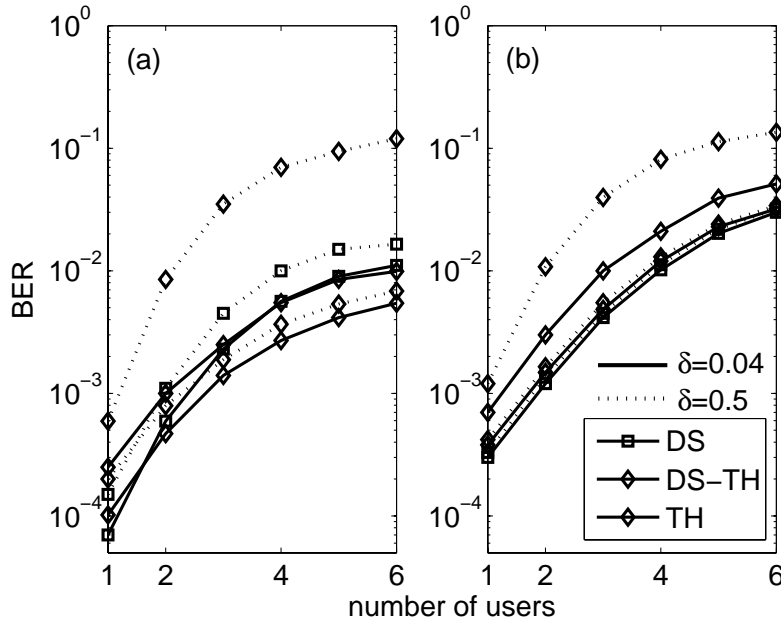


Figure 3.12: BER Performance vs. Number of Users for DS, TH and DS-TH UWB Systems. (a)CM1 and (b)CM2.  $K=6$ ,  $\text{SNR}=20\text{dB}$ ,  $W_t=2\text{GHz}$ ,  $f_c=6\text{GHz}$ .

System parameters such as SNR,  $L_c$  and  $f_c$  are set to be 20dB, 8 and 6GHz. Here, transmission of multiple users are assumed to be asynchronous in time and all users transmit signal with similar power. The total number of users,  $K$  is set to 6. Fig.3.12 is divided into (a) CM1 and (b) CM2.

In previous discussions, it is found that in single user environment, DS system outperforms DS-TH system. In fig.3.12(a) for CM1 communication, at number of users  $U=1$ , DS system with  $\delta=0.04$  performs the best, followed by DS-TH systems with  $\delta=0.04$ . However, as  $U$  increases, it is worth noting that DS-TH system outperforms DS system starting from  $U=2$ , and beyond  $U > 3$ , the superior performance of DS-TH system becomes more noticeable. In DS systems, all pulses are placed at the first time slot in every  $T_c$ , therefore the possibility for catastrophic collision [10] (where large number of pulses from two or more signals are received simultaneously) to occur is high. Catastrophic collision severely degrades the system performance. This is the reason of DS systems becoming inferior as  $U$  increases beyond 1. And as DF increases, the possibility of catastrophic collision also increases correspondingly, degrading performance even more seriously.

On the other hand, for DS-TH and TH systems, although suffering the cause of increasing ICI due to the time hopping feature in single user environ-

ment, here in multi-user environment, catastrophic collision can be avoided effectively. The non-uniform spacing of the pulses results in less collision among signals from different users. This explains why BER performance for TH system with  $\delta=0.04$  is almost similar to that of the DS system with  $\delta=0.04$  at  $U=3$  and beyond. Moreover, with the random polarity pulses in DS-TH system, BER performance in propagation channel with higher  $U$  becomes even more superior.

It is noted that TH system with  $\delta=0.5$  has severely degraded BER performance. This is due to the high DF that compromises the ability to avoid catastrophic collision.

Referring to fig.3.12(b), TH system performance in CM2 is not very different from that in CM1. As for DS and DS-TH systems in CM2, the difference in respective BER performance is also found to be less distinguishable. This can be explained that with stronger ICI and furthermore ISI in CM2 propagation, the EC capability of the receivers degrades collectively regardless of DF and modulation methods, thus compromising system performance in an overall manner.

### 3.3 Performance in the Presence of Narrowband Interference

Since UWB system occupies a large bandwidth and is likely to coexist with other existing narrowband systems, it is also of practical interest to investigate the impact of DF on BER performance for DS, TH and DS-TH UWB systems in the presence of narrowband interference. Here, The narrowband interference described in (2.6) is assumed to have center frequency  $f_{nrb}=6\text{GHz}$  and bandwidth  $W_j=10\text{MHz}$ . Also, single user environment is assumed. In this section, we also divide fig.3.13 into (a) CM1 and (b) CM2 for more comprehensible discussion.

Fig.3.13(a) presents the relationship between SIR and BER performance for DS, TH and DS-TH UWB systems in different DF for CM1. Generally, as SIR increases, BER performance for all systems improves. Particularly, BER performance improvement is observed to be more rapid in the range of  $-20\text{dB}\leq\text{SIR}\leq 0\text{dB}$  for DS and DS-TH systems, and in the range of  $-10\text{dB}\leq\text{SIR}\leq 10\text{dB}$  for TH system. In these ranges, increasing SIR to improve system performance is found to be the most effective.

For DS and DS-TH systems employing different DF, slight performance advantages can be observed at lower  $\delta$ . Among all, TH system performs relatively the worst in all range of SIR regardless of DF value.

Also, for non LOS channel CM2, the achievable BER improvement due to increasing SIR is less significant. This can be observed in fig.3.13(b) that as SIR increases to 20dB, BER values reaches below  $10^{-3}$ , whereas for CM1 at SIR approaching 20dB, BER values as low as around  $10^{-4}$  can be

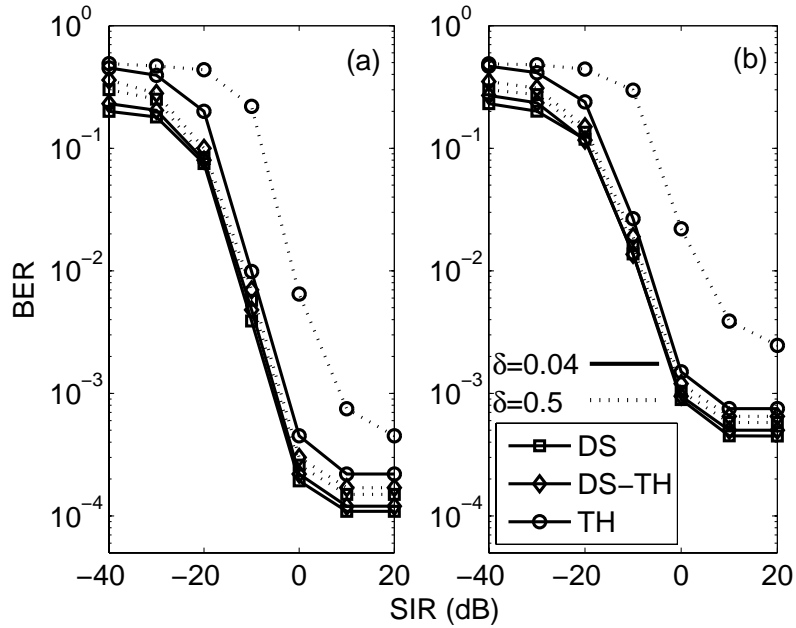


Figure 3.13: BER Performance vs. SIR for DS, TH and DS-TH UWB Systems. (a)CM1 and (b)CM2. SNR=20dB,  $W_t=2\text{GHz}$ ,  $L_c=8$ ,  $f_c=6\text{GHz}$ ,  $f_{nrb}=6\text{GHz}$ ,  $W_j=10\text{MHz}$ .

Table 3.3: Pairs of DF and  $N_s$  for DS-UWB Signaling Design in the Presence of Narrowband Interference.

DF	0.02	0.04	0.08	0.13	0.17	0.25	0.5	1.0
$N_s$	1	2	4	6	8	12	24	48

achieved. Apart from that, the patterns of BER graphical curvature as SIR increases are similar for both CM1 and CM2.

Next, DS-UWB performance in varying DF in the presence of a coexisting narrowband signal is evaluated. The design for lower DF can be achieved by manipulating  $N_s$ , as illustrated in fig.3.2. This signaling design is chosen because system resources such as  $W_t$ , PG and  $R_b$  can be set constant for fair comparison. Tab.3.3 shows the pairs of  $N_s$  and DF, with total PG=48. Here,  $W_t$  considered are 2, 4 and 7.5GHz respectively. The narrowband interference has  $f_{nrb}=6\text{GHz}$  and  $W_j=10\text{MHz}$ .

Fig.3.14 presents the relationship between DF  $\delta$  (right ordinate) with respective  $N_s$  pair (left ordinate) and BER performance. We found that as  $0.2 \leq \delta \leq 1$ , BER performance remain constant. Performance improvement is only observed at  $\delta < 0.2$ .

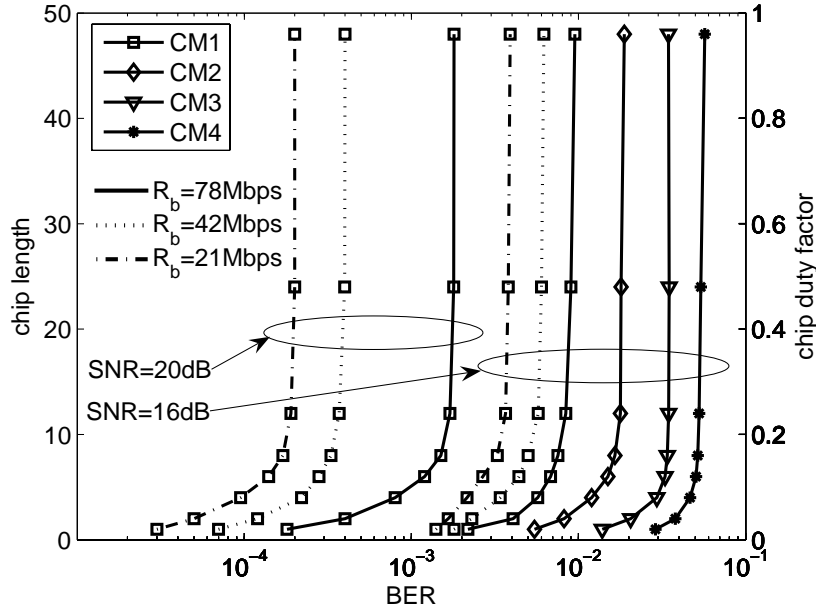


Figure 3.14: BER Performance vs. Chip Duty Factor and Chip Length for DS-UWB System in the Presence of Narrowband Interference. SIR=10dB,  $L_c=8$ ,  $f_c=6\text{GHz}$ ,  $f_{nrp}=6\text{GHz}$ ,  $W_j=10\text{MHz}$ .

As compared to propagation environment without narrowband interference shown in fig.3.10, the presence of narrowband interference in the channel as shown in fig.3.14 results in no significant optimum DF value. Here, as DF decreases from  $\delta=1$ , BER performance initially remains constant and at  $\delta \leq 0.2$ , performance improvement takes place.

### 3.4 DS-MB-UWB System with Overlapped Sub-bands

In this section, by employing DS-MB-UWB signal described in (2.1), pulsed multiband UWB system with sub-bands overlapping with each other is designed by manipulating lower DF.

The overlap percentage (OP) of the sub-bands can be described as:

$$OP = \frac{W_{sub}B - W_t}{W_t} * 100\% \tag{3.6}$$

Here, OP (in %) is the quantification of the percentage of overlapped area between sub-bands. In order to overlap the sub-bands, sub-band bandwidth  $W_{sub}$  is increased while total bandwidth  $W_t$  remains constant. Therefore, as

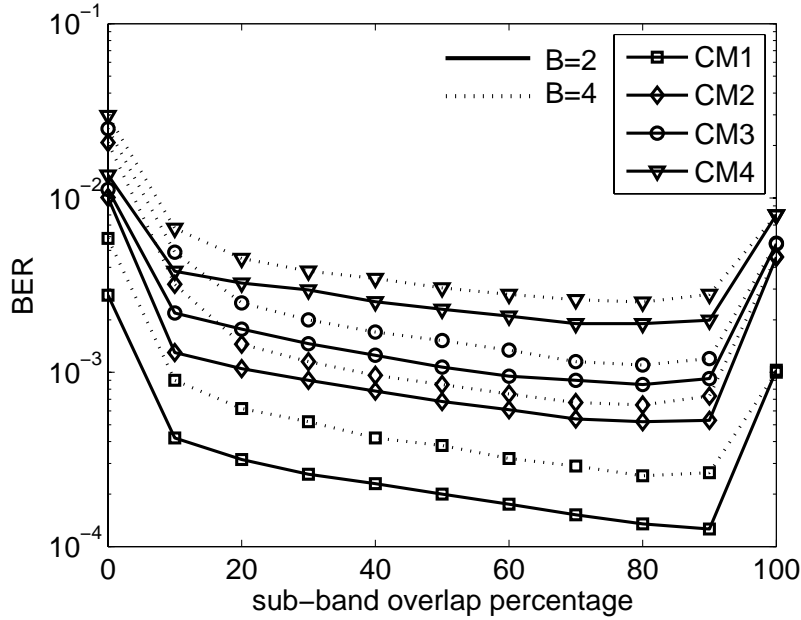


Figure 3.15: BER Performance vs. Overlap Percentage of Sub-bands for DS-UWB System Manipulating Low DF Design. SNR=18dB,  $L_c=8$ ,  $W_t=4$ GHz.

$W_{sub}$  becomes wider, OP become higher. The  $W_{sub}$  is increased by decreasing  $T_p$  while maintaining  $T_c$ , thus resulting signal to have lower DF as  $W_{sub}$  and OP increase.

With  $W_{sub}$  becoming wider and  $W_t$  constant, center frequency  $f_m$  of each sub-band has to be changed as OP increases. The center frequencies can be described as:

$$f'_m = f_1 + (m - 1) \frac{W_t - W_{sub}}{B - 1} \quad m = 1, 2, \dots, B \quad (3.7)$$

where  $f_1$  is the first DS-MB-UWB sub-band.

Summary of OP and corresponding DF can be shown in tab.3.4. In this system, SNR, and  $L_c$  are set to be 18dB and 8 respectively. Number of employed sub-bands  $B$  assumed in this section is 2 and 4. In order to conduct a fair comparison, system with  $B=2$  has  $N_s=16$ , whereas system with  $B=4$  has  $N_s=8$ .

Fig.3.15 presents the BER performance of DS-MB-UWB system with overlap sub-bands manipulating lower DF signaling design. As OP increases from 0% to 90% (signal with lower DF is employed), BER performance is found to improve. Improvement is found to be particularly significant at  $0\% \leq OP \leq 10\%$ . Then as OP increases from 10% to 90%, BER performance improves gradually.

Table 3.4: DF and Overlap Percentage (OP) of Sub-bands.

$B=2$										
DF	1.00	0.90	0.77	0.71	0.67	0.63	0.59	0.56	0.53	0.50
OP(%)	0	10	30	40	50	60	70	80	90	100
$B=4$										
DF	1.00	0.77	0.53	0.46	0.40	0.36	0.33	0.30	0.27	0.25
OP(%)	0	10	30	40	50	60	70	80	90	100

The reason is that by employing signal with lower DF, less channel fading is experienced, thus improving EC capability of the Rake receiver, and BER performance. Furthermore, lower DF also means reduction of ICI and ISI due to adjacent pulses becoming farther apart. Note that although the sub-bands overlap in frequency domain, the pulses are orthogonal in time domain. However, as OP approaches 100%, the multiband system can be viewed as becoming a single band system, since all the sub-bands are merging into one. Therefore, the advantage of frequency diversity becomes less significant, and degradation of performance occurs.

For propagation in multipath channel CM1 to CM4, it can be seen that system in CM1 constantly perform better than CM2, CM2 than CM3 and CM3 than CM4, especially in the range of  $10\% \leq OP \leq 90\%$ . At both ends ( $OP=0\%$  and  $100\%$ ), the difference among BER performance in CM2 to CM4 are not obvious. BER performance in CM1 still remains the best among all. Additionally, systems with  $B=2$  outperforms that with  $B=4$ , since the former has twice  $N_s$  as compared to the latter. At  $OP=100\%$ , BER performance becomes similar since both systems are approaching to become single band systems.

### 3.5 Concluding Remarks

In this chapter, UWB signaling design with low chip duty factor is presented. Firstly, the three design methods of low DF signaling by manipulating different system parameters are introduced and discussed in detail. Then by using computer simulations, the impact of employing these different low DF signaling on system energy capture capability and BER performance is presented and analyzed. Performance of UWB systems with DS, TH and hybrid DS-TH spreading techniques are evaluated in multipath environments. The effects of propagation in multi-user channel is also included. Besides, narrowband interference is also considered to exist by assuming the presence of a spectrally coexisting narrowband signal. The corresponding system performance is discussed. Finally, by manipulating low DF, sub-bands in a DS-MB-UWB system is designed to overlap with each other. The system

performance due to the overlap sub-bands is evaluated and commented.

Future works include the investigation of peak to average power of low DF UWB signals and the corresponding PSD changes. The relationship between UWB system performance, multiple access and coexistence capability to peak power should also be an interesting topic.

The next chapter will discuss interference mitigation technologies of UWB system, for the purpose of reducing interference generated to and from other coexisting narrowband systems.

## Chapter 4

# Interference Mitigation

Due to the characteristic of UWB system occupying ultra wide bandwidth, spectral coexistence with other narrowband systems becomes unavoidable. Thus, UWB system is subjected to potential interference from active wireless services in the same or nearby bands [35], and at the same time, may also cause interference to these services [36]. Besides, there are reports on mutual interference taking place on each other [37,38]. The issue on interference is currently one of the major challenges to the deployment of UWB system.

Hence, there has been a surge in demands for development of interference mitigation techniques in the UWB community. Among the ones proposed in current literatures, the detect and avoid (DAA) technology [8,39] and the low duty cycle (LDC) technology [8,40] are widely discussed and recommended.

For the purpose of mitigating mutual interference, an effective way is to reduce transmitted power in the UWB frequency band. However, most conventional UWB systems, such as DS-UWB and TH-UWB, are designed in single band. With single band system, reducing transmitted power may severely compromise system performance and achievable range, thus limiting design options for interference mitigation. As a solution, instead of reducing transmitted power, DAA technology changes the system operating frequency when narrowband signal is detected within the UWB bandwidth.

In this chapter, in order to provide more flexible design options, the mitigation mechanism is designed by employing DS-MB-UWB signaling. With multiple sub-bands in DS-MB-UWB system, transmitted power in the particular sub-band coexisting with the narrowband signal can be suppressed, while other ‘clean’ sub-bands remain unchanged. This will effectively reduce the UWB interference to other narrowband systems, and simultaneously reduce narrowband interference generated to UWB system. This chapter proposes and discusses the sub-band suppression mitigation technique for DS-MB-UWB system.

Additionally, signaling design with different DF can also be an effective approach to mitigate mutual interference. Both single and multiband UWB

systems are able to manipulate DF for interference mitigation purposes. Employing signal with low DF in single band system has been discussed in the LDC technology. Therefore, in this chapter, besides single band system, the use of low DF in multiband UWB system is also proposed to further increase the mitigation capabilities. Besides, low DF signaling design also enables self interference (SI) [41, 42] and multi-user interference (MUI) [43, 44] to be mitigated at the same time. This topic is commented in the previous chapter and will be discussed in this chapter together with the mitigation of narrowband interference.

The outline of this chapter is given as below. Firstly the interference mitigation mechanism by suppressing sub-band power in DS-MB-UWB signaling is described. Then, the manipulation of DF in UWB signal to mitigate interference is described. Also, low DF UWB signaling in mitigating SI and MUI is also commented. Finally, the results are presented and analyzed.

## 4.1 Sub-band Power Suppression

The BPSK modulated DS-MB-UWB signal of the  $k$ -th user as given in (2.1) is as below:

$$s^{(k)}(t) = \sqrt{E_p} \sum_{i=-\infty}^{\infty} \sum_{j=0}^{N_s-1} d_i c_j^{(k)} p(t - iT_s - j\frac{T_p}{\delta}) \cos(2\pi f_m^{(k)}(t - j\frac{T_p}{\delta}))$$

$$m = 1, 2, \dots, B \quad (4.1)$$

The denotations for (4.1) can be found following (2.1). In this section, it is worth to note that  $f_m$  is the multiband frequency selected randomly from a total of  $B$  number of sub-bands to form a user-dependent frequency hopping sequence, with probability of each  $f_m$ , as  $P(f_m) = 1/B$ . Each sub-band has an equal chance to be selected.

If the narrowband signal  $\epsilon(t)$  described in (2.6) is detected within any sub-band with center frequency  $f_m = f_{ma}$  (assuming  $f_{ma}$  represents the center frequency of the sub-band coexisting with the narrowband signal) of the signal, power can be reduced in that particular sub-band during transmission, for the purpose of mitigating the UWB interference towards the narrowband signal, and at the same time reducing narrowband interference towards UWB system.

From (4.1), the multiband hopping sequence controls the amount of energy in each sub-band by assigning how frequent a particular sub-band appears in the hopping sequence. If narrowband signal is detected within a particular sub-band, imbalanced weights in frequency hopping sequence can be assigned by repeating other unaffected sub-bands more frequently as compared to the affected sub-band. As a result, the fractional energy in

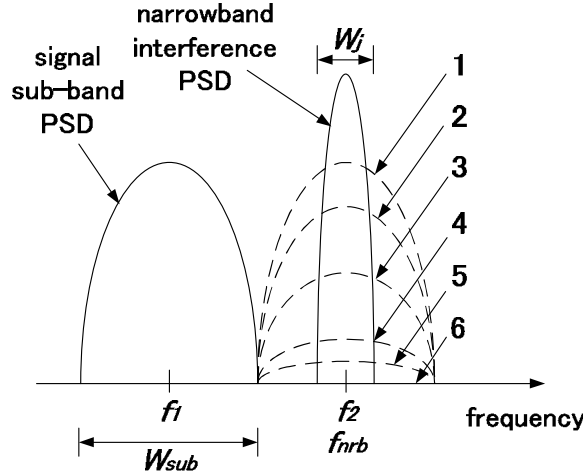


Figure 4.1: Spectral Diagram of Sub-band with Power Suppression. (1)  $\Delta b' = 0$  (no power suppression), (2)  $\Delta b' = 0.2$ , (3)  $\Delta b' = 0.5$ , (4)  $\Delta b' = 0.8$ , (5)  $\Delta b' = 0.9$  and (6)  $\Delta b' = 1$  (full power suppression).

the affected sub-band with center frequency  $f_{ma}$  decreases. The probability of  $f_{ma}$  being selected in the multiband hopping sequence with imbalanced weight can be shown as:

$$P(f_{ma}) = P(f_m) - \Delta b = \frac{1}{B} - \Delta b, \quad ma = \{1|2|3|\dots|B\} \quad (4.2)$$

where  $\Delta b$  is the suppression level assigned to reduce the occurrence of  $f_{ma}$  and  $0 \leq \Delta b \leq 1/B$ . The normalized suppression level can therefore be described as:

$$\Delta b' = \frac{\Delta b}{P(f_m)} \quad ma = \{1|2|3|\dots|B\} \quad (4.3)$$

where  $0 \leq \Delta b' \leq 1$ . As  $\Delta b'$  increases, more sub-band energy is suppressed. The illustration of the spectral diagram of the suppressed sub-band corresponding to  $\Delta b'$  can be shown in fig.4.1.

Then, the fractional energy in the affected sub-band after power suppression becomes:

$$E'_{sub} = E_b P(f_{ma}) \quad ma = \{1|2|3|\dots|B\} \quad (4.4)$$

where the unsuppressed sub-band energy  $E_{sub} = E_b P(f_m)$ ,  $P(f_{ma}) \leq P(f_m)$  and  $E'_{sub} \leq E_{sub}$ .

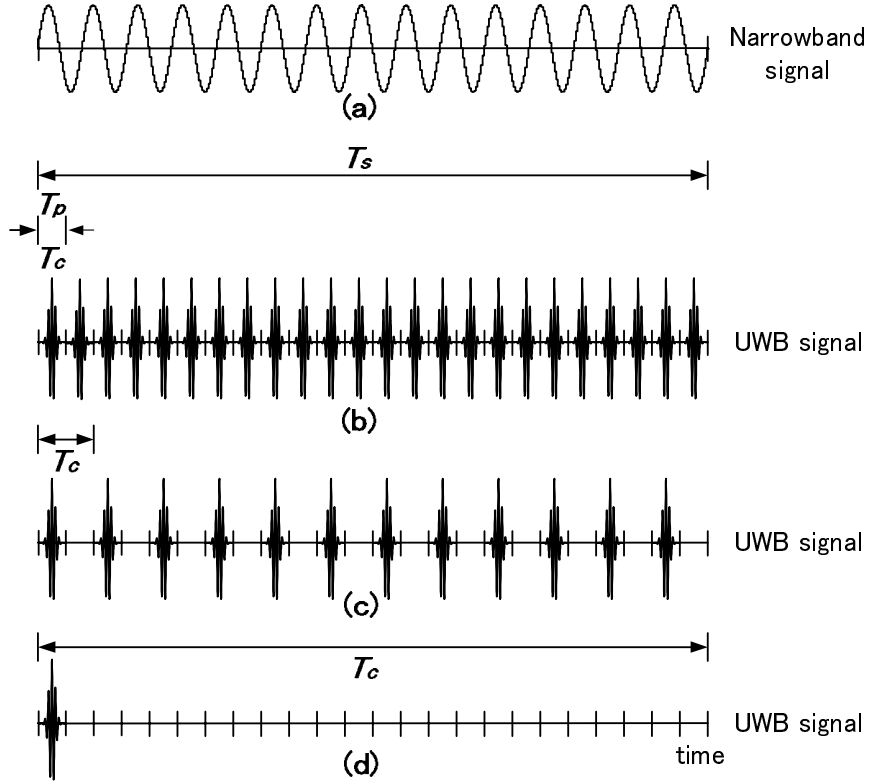


Figure 4.2: Impact of UWB Signals with Varying DF Design on Coexisting Narrowband Signal. (a) Coexisting Narrowband Signal, UWB Signals with (b)  $\delta=1$  and  $N_s=24$ , (c)  $\delta=0.5$  and  $N_s=12$ , and (d)  $\delta=0.04$  and  $N_s=1$ .

By suppressing power in the affected sub-band, potential interference from the DS-MB-UWB system to other narrowband systems can be mitigated, and vice versa.

## 4.2 Low Chip Duty Factor Mitigation

Previous chapter presents and explains impact of employing different DF in UWB signaling. In this section, low DF signaling design is used as a mitigation technique to mutual interference between UWB system and coexisting narrowband systems. Low DF signaling is designed by manipulating  $N_s$  while maintaining  $W_t$ ,  $R_b$  and PG. Employing signaling with lower DF simply means that less number of chips are assigned to spread the same symbol, as described in fig.3.2.

From the viewpoint of interference mitigation, signal with lower DF has less chips per bit, and thus generating less ‘collision’ with the coexisting

narrowband signal in time domain. Referring to fig.4.2, UWB signal in fig.4.2(b) with  $\delta=1$  ‘collides’ with the narrowband signal for 24 times per symbol, while in fig.4.2(c) with  $\delta=0.5$ , only 12 ‘collisions’ take place. Then as DF decreases to  $\delta=0.04$  in fig.4.2(d), number of ‘collision’ reduces to 1 time per symbol. The higher the ‘collision’ rate in the same symbol duration, the stronger the mutual interference becomes. Additionally, it is also worth to take note that as DF decreases, energy per bit increases considerably, resulting in higher pulse peak power.

Up to this section, for single band system as well as multiband system with completely random sub-band assignment in frequency hopping sequence, the term ‘DF’ in the discussions are assumed to be the average DF. However, in multiband systems, if imbalanced weight is applied on the frequency hopping sequence, the sub-band DF  $\delta_{ma}$  of the suppressed sub-band changes correspondingly and can be described as:

$$\delta_{ma} = BP(f_{ma})\delta \quad ma = \{1|2|3|\dots|B\} \quad (4.5)$$

where  $f_{ma}$  is the center frequency of the suppressed sub-band,  $P(f_{ma})$  is the probability of  $f_{ma}$  to be selected in the frequency hopping sequence, and  $\delta$  is the average DF (or simply referred as DF up to this section).

From (4.5), it can be shown that in UWB system with single band,  $\delta_{ma}=\delta$  because there is no sub-band power suppression. And in multiband system with random frequency hopping sequence,  $\delta_{ma}=\delta$  because  $P(f_{ma})=P(f_m)$ , and  $BP(f_m)=1$ . On the other hand, when power suppression on a sub-band is performed,  $P(f_{ma}) < P(f_m)$  and  $BP(f_{ma}) < 1$ , thus resulting in  $\delta_{ma} < \delta$ . In other words, when higher sub-band suppression level  $\Delta b'$  is applied, the average DF  $\delta$  remains constant but DF the for suppressed sub-band  $\delta_{ma}$  decreases correspondingly.

Besides, by designing the UWB signal to lower DF, SI and MUI can also be mitigated simultaneously on top of mutual interference from narrowband signal. Therefore, it not only reduces UWB interference to wireless systems in the nearby bands, but also further improves the performance of UWB system.

### 4.3 Performance with Interference Mitigation

The mitigation techniques discussed in this chapter are applied in the both DS-UWB and DS-MB-UWB systems developed in the previous chapters. The system performance are evaluated and presented in the following sections.

Table 4.1: Simulation Parameters for DS-MB-UWB System with Interference Mitigation

Parameters	
total bandwidth $W_t$	4GHz
sub-band bandwidth $W_{sub}$	1GHz
number of sub-bands $B$	4
sub-band frequencies $f_1, f_2, f_3, f_4$	3.5, 4.5, 5.5, 6.5GHz
combined paths $L_c$	8
narrowband signal frequency $f_{nrb}$	6.5GHz
narrowband signal bandwidth $W_j$	10MHz

Table 4.2: Pairs of DF and  $N_s$  for DS-MB-UWB System with Sub-band Suppression Mitigation.

DF	0.04	0.08	0.13	0.17	0.25	0.33	0.50	1.00
$N_s$	1	2	3	4	6	8	12	24

### 4.3.1 Performance with Sub-band Suppression Mitigation

Based on the system model described in the previous sections, the performance of DS-MB-UWB system applying sub-band power suppression over multipath channel in the presence of a coexisting narrowband signal is investigated using computer simulations.

The DS-MB-UWB system is designed to occupy  $B=4$  sub-bands. The system transmits modulated Gaussian pulse over two types of IEEE 802.15.3a UWB indoor multipath channel models [22], both LOS and NLOS channels. The coexisting narrowband signal is a cosine waveform BPSK modulated, with  $f_{nrb} = f_{m=4}$  and  $W_j=10\text{MHz}$ . In other words, the 10MHz narrowband signal is constantly placed at the center frequency of the fourth sub-band of the DS-MB-UWB system. The summary for the simulation parameters are listed in tab.4.1.

To ensure fair comparison, the system is designed with constant  $PG=24$ . Each DF value is paired up with respective  $N_s$ , as shown in tab.4.2. As DF becomes lower, less  $N_s$  is employed to maintain the PG. The signaling diagram of the signal with different combinations of DF and  $N_s$  can be shown in fig.3.2. Note that  $R_b$ ,  $W_t$  and  $W_{sub}$  are constant.

Here on, unless specified otherwise, the term ‘DF’ refers to the average chip duty factor  $\delta$ .

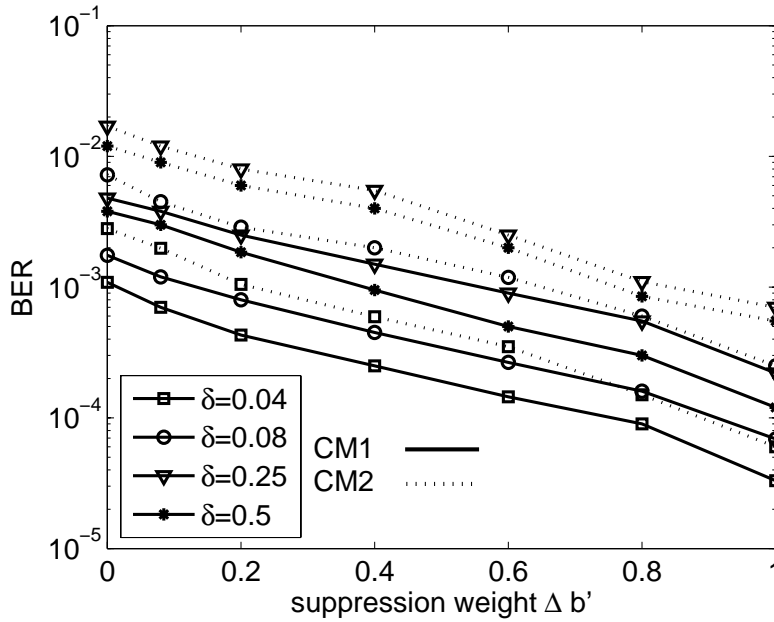


Figure 4.3: BER Performance vs. Level of Sub-band Power Suppression for DS-MB-UWB System. SNR=25dB, SIR=-5dB. (Power suppression is applied on sub-band with  $f_{ma=4}=6.5\text{GHz}$ .)

Table 4.3: Relationship Between Level of Sub-band Power Suppression, Multiband DF and Average DF for DS-MB-UWB System.

Power Suppression Level $\Delta b'$	1	0.8	0.6	0.4	0.2	0
Multiband DF $\delta_{ma}$	0	$0.2\delta$	$0.4\delta$	$0.6\delta$	$0.8\delta$	$\delta$

### DS-MB-UWB Performance vs. Level of Sub-band Power Suppression

Fig.4.3 presents the interference mitigation capability by suppressing the power of the sub-band coexisting with a narrowband signal. By increasing  $\Delta b'$ , we are able to suppress and reduce the power in the affected sub-band, as illustrated in fig.4.1. At the same time, by increasing  $\Delta b'$ , the sub-band chip duty  $\delta_{ma}$  in the suppressed sub-band (in this case, sub-band with  $f_{ma=4}=6.5\text{GHz}$ ) also changes accordingly as described in (4.5). The relationship between  $\Delta b'$ ,  $\delta_{ma}$  and  $\delta$  can be shown in tab.4.3.

From fig.4.3, it is found that BER performance can be improved by increasing  $\Delta b'$ . When a narrowband signal coexists with a DS-MB-UWB sub-band, the DS-MB-UWB system is subjected to narrowband interfer-

ence every time the system occupies that particular sub-band assigned by the frequency hopping sequence. Therefore, in order to reduce the impact of mutual interference to and from the narrowband signal, the power in the affected sub-band can be reduced by simply decreasing its probability of being selected in the frequency hopping sequence. On the other hand, other unaffected sub-bands can be repeated more frequently. In other words imbalanced frequency hopping weight is applied to the system so that the affected sub-band has less power as compared to other 'clean' sub-bands. According to (4.4), by allocating higher  $\Delta b'$  to the affected sub-band, the probability of that particular sub-band to be selected can be reduced, thus achieving the purpose of sub-band power suppression and interference mitigation.

From another perspective, BER performance can also be improved by reducing the sub-band DF  $\delta_{ma}$  of the affected sub-band, while the average DF is maintained. As  $\delta_{ma}$  is decreased from  $\delta$  to fractions of  $\delta$ , BER performance shows improvement.

Note that system performance is strongly dependent on the strength of the narrowband signal. The next section discusses the topic from the perspective of signal to interference ratio.

### DS-MB-UWB Performance vs. SIR

Narrowband signals with different strength affect DS-MB-UWB system performance significantly. The quantification of how strong the narrowband signal can be given in SIR. The definition of SIR is described in the paragraph following (2.6), and is a representation of the ratio between the signal strength to the narrowband interference strength. Fig.4.4 shows the relationship between SIR and BER performance. In this setup, SNR is set to 20dB. The system occupies  $B=4$  bands, with the  $W_j=10$ MHz narrowband signal constantly placed at the fourth sub-band. The multipath propagation channel is CM1. The Rake receiver selects a total of  $L_c=8$  paths to be combined.

Referring to fig.4.4, as SIR increases, BER performance improves. The improvement however, is not uniform. For  $\Delta b'=0.08$ , the BER improvement is more rapid in the range  $-20\text{dB} \leq \text{SIR} \leq 0\text{dB}$ , whereas for  $\Delta b'=0.8$ , the BER improvement is more rapid in the range  $-20\text{dB} \leq \text{SIR} \leq -10\text{dB}$ . For both, at  $\text{SIR} > 10\text{dB}$ , BER improvement becomes saturated. It is discovered that one of the important factors contributing to achievable BER improvement due to increasing SIR is the level of sub-band power suppression. In other words, the mutual interference able to be reduced by applying low DF mitigation technique is found to be dependent on SIR.

It can also be observed that by applying higher  $\Delta b'$ , better BER performance can be obtained. Moreover, by carefully designing the DS-MB-UWB signal with relevant DF value, further improvement of BER performance can be achieved. In this case, system with  $\delta=0.04$  outperforms those with

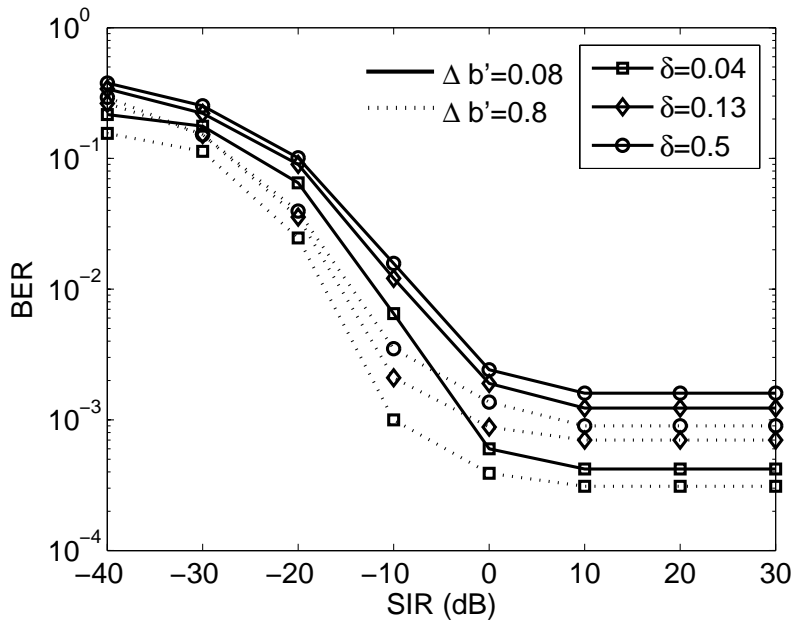


Figure 4.4: BER Performance vs. SIR for DS-MB-UWB System.  $B=4$ ,  $\text{SNR}=20\text{dB}$ ,  $L_c=8$ , CM1.

$\delta=0.13$  and  $0.5$ .

### DS-MB-UWB Performance vs. SNR

Besides SIR, SNR is also an essential system parameter. The definition of SNR can be given in the paragraph following (2.6). In this section, the relationship between SNR and corresponding system performance with varying DF and sub-band power suppression level is investigated. In this setup, SIR,  $L_c$ ,  $W_{sub}$  and  $B$  are set to  $-5\text{dB}$ ,  $8$ ,  $1\text{GHz}$  and  $4$ . The narrowband interference is constantly located at the  $f_{nrb}=6.5\text{GHz}$  with  $W_j=10\text{MHz}$ . The multipath channel is CM1.

As shown in fig.4.5, as SNR increases, BER performance improves. By carefully selecting DF and  $\Delta b'$  values, mutual interference can be mitigated and further BER improvement can be obtained. In this case, by selecting system with higher  $\Delta b'$ , the obtainable BER improvement due to increasing SNR becomes higher. Similarly, with careful design, system with lower DF display better performance. It can be observed that system with  $\delta=0.04$  performs better than those with  $\delta=0.13$  and  $0.5$ .

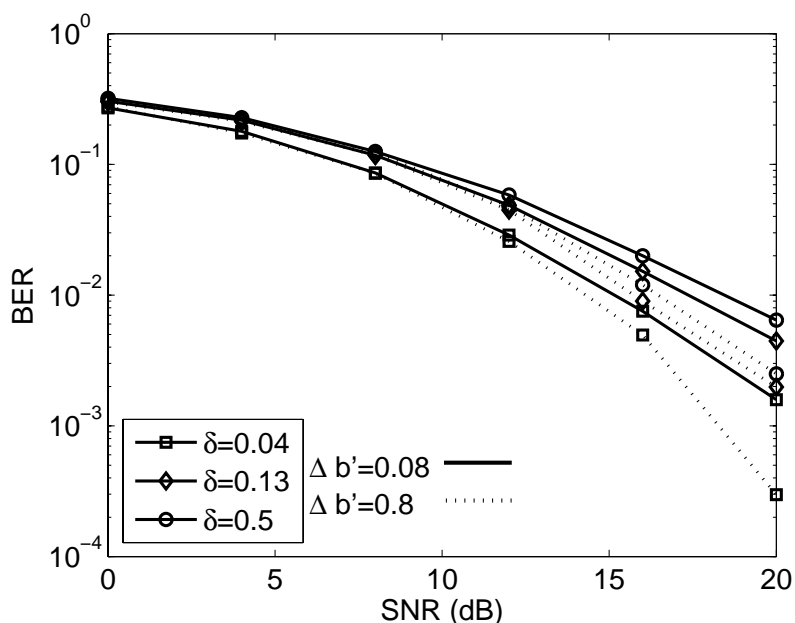


Figure 4.5: BER Performance vs. SNR for DS-MB-UWB System. SIR=-5dB,  $L_c=8$ ,  $B=4$ , CM1.

### DS-MB-UWB Performance vs. Rake Fingers

Rake receivers applied in previous sections select and combine a total of  $L_c=8$  paths. It is also of interest to find out the impact of increasing the total number of  $L_c$ . SNR and SIR are set to be 25dB and -5dB. Other parameters are similar to the previous sections.

In fig.4.6, the relationship between  $L_c$  and BER performance for varying DF and  $\Delta b'$  is presented. As a general observation, as  $L_c$  increases, BER performance improves. This statement is valid until the 'saturating  $L_c$ ' where further increasing  $L_c$  does not further improve BER performance. For signal with lower DF, better performance can be achieved. Also, as sub-band power suppression with higher  $\Delta b'$  is applied to the system, greater mutual interference between UWB system and the coexisting narrowband system can be mitigated to improve BER performance. Additionally, it is found that as  $\Delta b'$  increases, 'saturating  $L_c$ ' increases relatively. This indicates that by suppressing more power in the affected sub-band, more  $L_c$  can be added to obtain BER improvement before reaching the 'saturating  $L_c$ '.

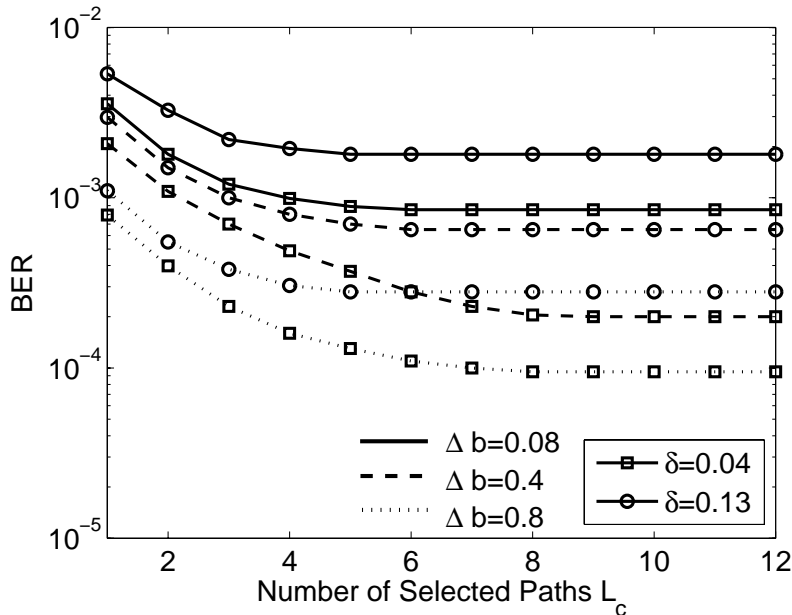


Figure 4.6: BER Performance vs. Selected and Combined Paths for DS-MB-UWB System. SNR=25dB, SIR=-5dB,  $B=4$ , CM1.

### 4.3.2 Performance with Low DF Mitigation

In this section, the performance improvement of UWB system due to interference mitigation employing low DF signaling design is presented. Parallel to UWB performance improvement, UWB interference to coexisting narrowband systems can also be mitigated to enable coexistence in the spectrum band. Besides, SI and MUI can also be mitigated, thus further improving system performance. Both DS-UWB and DS-MB-UWB system are evaluated and discussed. The systems are assumed to operate over multipath and multi-user in the presence of a coexisting narrowband signal.

#### DS-MB-UWB Performance vs. Chip Duty Factor

Fig.4.7 shows how BER performance can be improved by manipulating DF while maintaining system resources such as PG,  $R_b$  and  $W_t$ . In this system setup, SNR and SIR are set to be 25dB and -5dB respectively. The system is designed to occupy  $B=4$  sub-bands, each with  $W_{sub}=1$ GHz so that  $W_t=4$ GHz. At the Rake receiver, a total of  $L_c=8$  best paths are selected and combined. The narrowband interference is assumed to have  $f_{nrb}=6.5$ GHz and  $W_j=10$ MHz. Here, the scenario of a single user environment is considered. Also, in order to design signal with lower DF,  $N_s$  is decreased. The

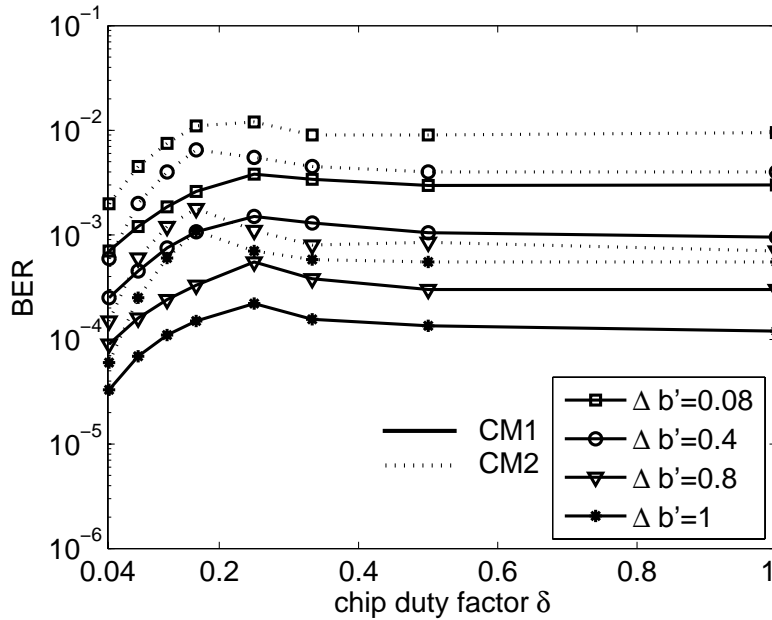


Figure 4.7: BER Performance vs. Chip Duty Factor for DS-MB-UWB System. SNR=25dB, SIR=-5dB,  $B=4$ .

pairs of DF and  $N_s$  can be given in tab.4.2.

Significant improvement can be observed below  $\delta=0.25$ . The improvements take place due to the mitigation of narrowband interference and SI in the propagation channel. As DF decreases, 'collision' per symbol between the UWB signal and the narrowband signal becomes lower, thus contributing to better performance of UWB system. Simultaneously, the potential interference generated by UWB system to the narrowband system can also be reduced drastically. However, it should be noted that as DF decreases, peak power of each pulse becomes higher. Careful system design should be conducted to obtain the optimum peak to average power ratio. Furthermore, the considerations of peak power limit set by regulators for UWB system is also an essential concern in the design of interference mitigation employing low DF signaling.

Besides narrowband interference, another main reason of the BER improvement comes from the mitigation of SI in the multipath channel. As DF decreases, SI is reduced due to the adjacent chips becoming farther apart. The combination of these factors results in the BER performance to improve significantly in the range of  $0.04 \leq \delta \leq 0.25$ .

From the analysis, it can be concluded that in order to utilize low DF signaling as an approach for interference mitigation, a considerable low range

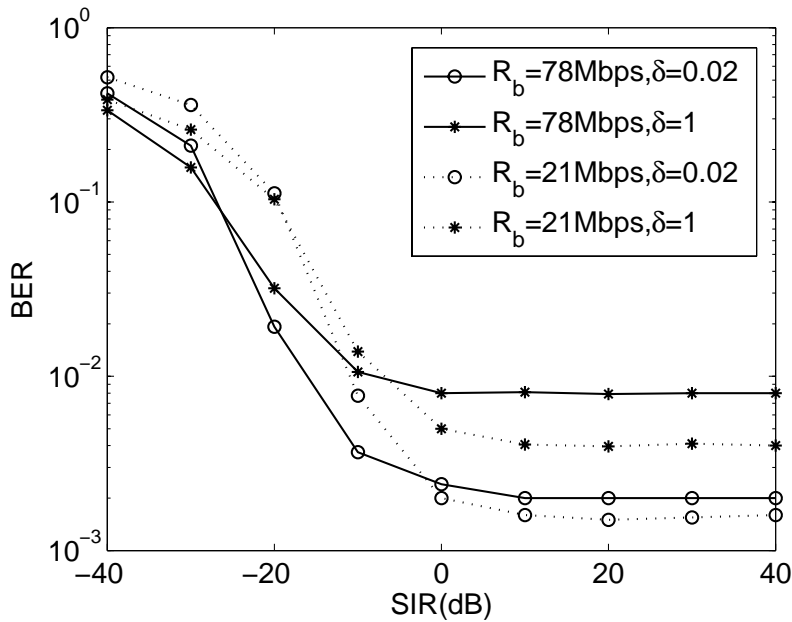


Figure 4.8: BER Performance vs. SIR for DS-UWB System. SNR=16dB,  $L_c=8$ ,  $f_c=6\text{GHz}$ ,  $f_{nrb}=6\text{GHz}$ ,  $W_j=10\text{MHz}$ , CM1.

of DF value is needed before the effect of mitigation can take place. And in the example in fig.4.7,  $\delta < 0.04$  is needed.

### DS-UWB Performance vs. SIR

In this section, DS-UWB system is considered with parameters  $L_c$  and  $f_c$  set to 8 and 6GHz respectively. The coexisting narrowband signal has  $f_{nrb}=6\text{GHz}$  and  $W_j=10\text{MHz}$ . The PG for all systems are constantly 48, as shown in tab.3.3. Here,  $W_t$  considered are 2 and 7.5GHz respectively. The system is simulated over different multipath channel and is constantly affected by a coexisting narrowband signal.

Fig.4.8 shows the relationship between SIR and BER performance corresponding to different DF and  $R_b$ . At very low SIR of less than -20dB, systems with higher DF slightly outperforms those with lower DF. As SIR increases, low DF systems takes over and outperform high DF systems. A crossing point is discovered between systems with high and low DF as SIR increases. And this crossing point differs as  $R_b$  changes. In fig.4.8, crossing point for systems with  $R_b=78$  and 21Mbps take place at SIR=-25 and -20dB respectively. Besides, it is also discovered that employing lower DF signal in system with lower  $R_b$  has more significant BER improvement as compared to that of higher  $R_b$  when SIR increases.

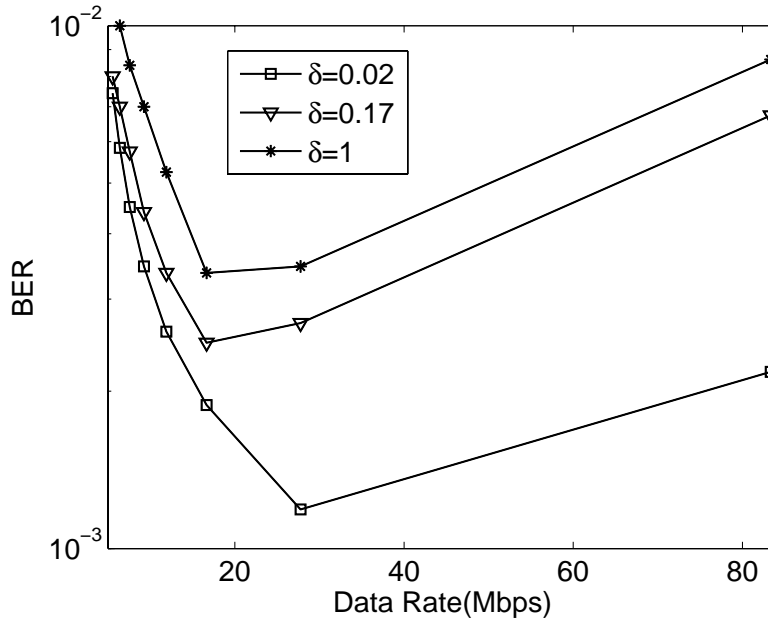


Figure 4.9: BER Performance vs. Data Rate for DS-UWB System. CM1, PG=48, SNR=16dB, SIR=10dB,  $L_c=8$ ,  $f_c=6$ GHz,  $f_{nrb}=6$ GHz,  $W_j=10$ MHz.

At very low SIR, systems with higher DF are able to utilize the advantage of chip randomization due to the employment of more  $N_s$  against the relatively stronger narrowband interference, therefore outperforming systems with lower DF. On the other hand, the advantage of employing low DF can only be noticeable in higher SIR environment, where the signal is able to dominate the relatively weaker narrowband interference, with the total UWB signal energy distributed over the lesser  $N_s$ .

This result suggests that low DF signaling is suitable for interference mitigation only beyond certain level of SIR. At extremely low SIR, systems with higher DF have slight advantage. Therefore, the employment of low DF signal to mitigate interference should be designed with reference to different SIR environments.

### DS-UWB Performance vs. Data Rate

This section presents the relationship between system data rate  $R_b$  and BER performance in systems with varying DF. The related system parameters such as SIR, SNR,  $L_c$  and  $f_c$  are set to 10dB, 16dB and 8 respectively. As for the narrowband signal, the  $f_{nrb}$  and  $W_j$  are 6GHz and 10MHz respectively. The processing gain PG is set to constant 48 for fair comparison.

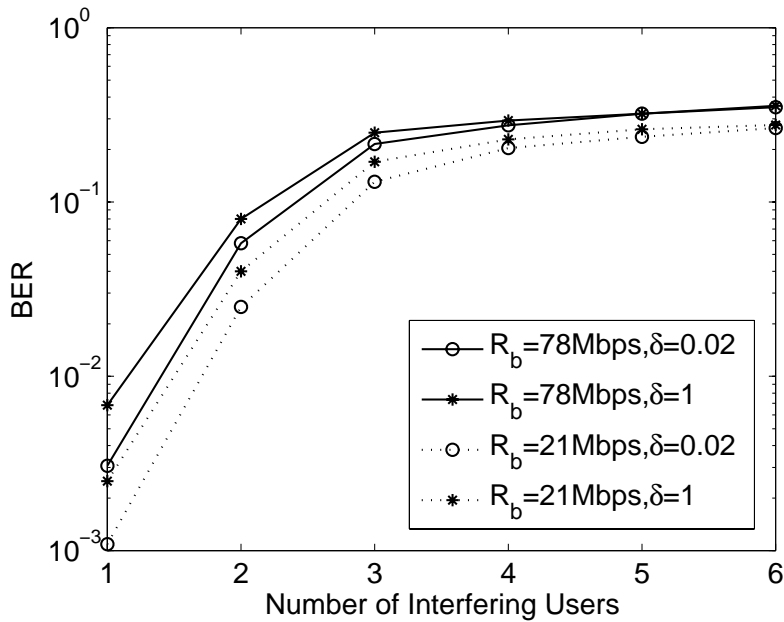


Figure 4.10: BER Performance vs. Number of Users for DS-UWB System. SNR=16dB, SIR=10dB,  $L_c=8$ ,  $f_c=6\text{GHz}$ ,  $f_{nrB}=6\text{GHz}$ ,  $W_j=10\text{MHz}$ , CM1. Signal to Multi-user Interference Ratio is set to unity.

Fig.4.9 shows that for the same PG, systems employing lower DF outperforms those with higher DF in all range of  $R_b$ . It can also be observed that reducing  $R_b$  as a tradeoff parameter does not always improve BER performance. This observation is valid for all  $\delta=1, 0.17$  and  $0.02$  in fig.4.9. As  $R_b$  decreases from 83Mbps to approximately 20Mbps, BER performance improves correspondingly. However, below that level, as  $R_b$  continues to decrease, BER performance on the other hand, degrades. This suggests the existence of an optimum  $R_b$  for DS-UWB systems with varying DF, where the relative best BER performance can be achieved. Additionally, the optimum  $R_b$  for each  $\delta=0.02, 0.17$  and  $1$  are slightly different. The higher the DF is the lower the optimum  $R_b$  becomes. This indicates that if interference mitigation technique with lower DF signaling is applied, the relative best BER performance can actually be achieved at a higher  $R_b$ .

#### DS-UWB Performance vs. Number of Users

The number of simultaneous users sharing the same propagation channel causes MUI. By employing signal with lower DF, MUI can be mitigated. This section presents the simulation results of the performance of DS-UWB system in multi-user environment corresponding to different number of in-

terfering users. The total number of users  $K$  is set to 6. The SNR and SIR of the system are 16dB and 10dB respectively. The narrowband system has  $f_{nrb}=6\text{GHz}$  and  $W_j=10\text{MHz}$ , while  $f_c=6\text{GHz}$ . A total of  $L_c=8$  paths are selected and combined.

Fig.4.10 shows the relationship between number of users  $U$  and BER performance. It is found that as  $U$  increases, BER performance degrades. By employing signal with lower DF, BER improvement can be observed. For system with  $R_b=78\text{Mbps}$ , the BER improvement due to decreasing  $\delta$  from 1 to 0.02 starts at  $U=4$ . As  $R_b$  is decreased to 21Mbps, BER improvement can be observed starting from  $U=5$ .

By applying mitigation technique with lower DF signaling, more MUI can be mitigated. This is because at lower DF, the signal has less pulse per symbol, thus reducing the possibility of ‘collision’ between signals from interfering users and the desired user. Less ‘collision’ results in lower MUI and therefore better BER performance.

#### 4.4 Concluding Remarks

In this chapter, two interference mitigation techniques are proposed for UWB system. These mitigation techniques have a common objective to mitigate interference generated by UWB system to narrowband systems sharing the same or nearby spectrum bands, and simultaneously, to mitigate corresponding narrowband interference. Firstly, the mitigation technique applying power suppression on sub-band of a DS-MB-UWB system is introduced. Then, the mitigation technique employing signaling design with lower chip duty factor is also proposed. The techniques are applied in DS-UWB and DS-MB-UWB systems over multipath and multi-user environment in the presence of a coexisting narrowband signal. The system performance related to the application of the mitigation techniques are then presented and analyzed. The dependence of the mitigation techniques on different system parameter is also investigated.

Future works include practicality of the mitigation techniques in the implementation and circuit design. Besides, the issue of peak power is also an essential parameter to be considered as these mitigation techniques are applied.

The next chapter will discuss the issue of timing error in the UWB signaling design with very short duration. The impact of timing error will be studied considering different system parameters.

## Chapter 5

# Timing Jitter in UWB System

UWB system is able to offer encouraging technical advantages by employing pulses with very short duration. Some of the common advantages are better multipath resolvability, better coexistence capability and robustness to multi-user interference. However, as shorter pulse are employed, the issue of timing error, or widely known as timing jitter, becomes more significantly pronounced in performance degradation. Degradation caused by timing jitter is unavoidable since it is due to circuitry imperfection in the system. Particularly in UWB system, issues involving tolerance against timing jitter are closely related to nano-second order signaling design, and these issues have to be taken into consideration when the system link budget is established.

UWB radios involving pulse design in the order of several nanoseconds have to take into consideration of at least timing jitter in the order to 10ps achievable only by recently reported clock stability [45, 46]. Besides, there are also other factors such as timing tracking and relative velocities between transmitter and receiver which will introduce additional degradation in synchronization [47].

The potential degradation caused by timing jitter in UWB systems has inspired investigations to be conducted to assess its impact. Timing error tolerance of time hopping (TH) UWB impulse radio for both pulse amplitude modulation (PAM) and pulse position modulation (PPM) is investigated in [48] and [49]. The different impact of timing jitter on various modulation techniques such as orthogonal PPM, optimum PPM, binary phase shift keying (BPSK) and on-off keying (OOK) in UWB impulse radio are compared and commented in [47]. The effect of timing jitter on TH spread spectrum signaling scheme is investigated in [50]. The impact of Gaussian distributed timing jitter with both uncorrelated and correlated successive jitter samples on TH-UWB systems are compared in [51]. Performance evaluation

of TH-UWB system in timing jitter environment from the perspective of processing gain can be found in [52]. Performance degradation of TH-UWB system due to timing jitter in multi-user environment is investigated in [53]. It is worth to note that most of the existing literatures are found focusing on conventional TH-UWB impulse radios.

In this chapter, the potential performance degradation due to timing jitter is investigated in different UWB signaling designs. Instead of the more established TH-UWB impulse radio, the less studied direct sequence (DS) UWB signaling is investigated in the presence of timing jitter.

Next, in order to mitigate the impact of timing jitter, mitigation method employing DS-MB-UWB signaling design is proposed. DS-MB-UWB system uses longer pulse to occupy narrower sub-bands, and is therefore able to increase tolerance against degradation of timing jitter. There are existing literatures reporting methods of mitigating the impact of timing jitter in UWB systems by manipulating pulse shapes [54] and different Rake receivers [55], but none with system design employing multiple sub-bands to achieve better system performance in timing jitter environment.

The outline of this chapter is given as below. Firstly, the detailed mechanism of timing jitter in UWB receiver is explained. Then the impact of timing jitter on UWB system relating to various system parameters is presented and discussed. Finally, the timing jitter mitigation signaling design is proposed. The analysis can also be found in the author's publications [56,57]

## 5.1 Timing Jitter

A BPSK DS-UWB system is considered. The transmitted and received signal model are similar to the ones previously developed. Transmitted signal can be given by (2.2), and the received signal over multipath and multi-user can be given by (2.7),

In the receiver, assuming that timing jitter occurs in the reference signal (hereon referred as template signal) used to correlate the received signal due to circuitry imperfection. Thus, modifying (2.10), the correlation process between the received signal  $r(t)$  at the  $l$ -th Rake finger with delay  $\tau_l$  and the template signal  $\psi(t)$  with an instantaneous timing jitter  $\nu_l$ , can be described as:

$$Z_l = \int_0^{T_s} r(t)\psi(t - \tau_l - \nu_l)dt = \sqrt{E_p N_s E_d} \chi_l \alpha(\tau_l + \nu_l) + \eta_l$$

$$l = 0, 1, \dots, L - 1 \quad (5.1)$$

where  $L = T_d/T_p$  is the total resolvable paths. Here, it is assumed that Rake reception with MRC method is applied. Fig.5.1 illustrates how the Rake fingers are positioned in multiple  $T_p$  to capture the signal energy from

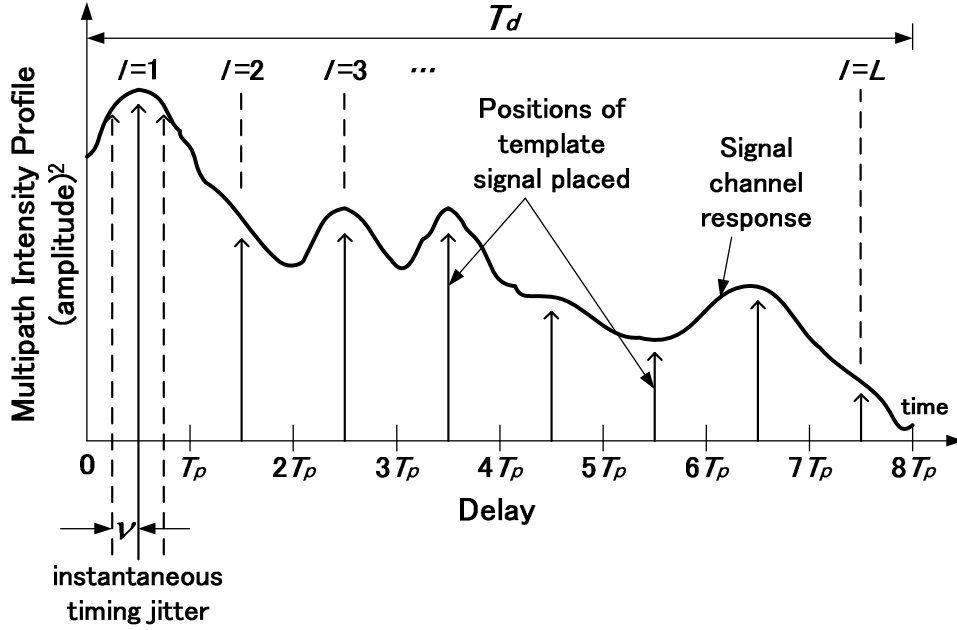


Figure 5.1: Placement of Template Signals by Correlators in the Rake Receiver. Solid line arrows: ideal positions of the template, Dashed line arrows: positions of the template with timing jitter  $\nu$ .

the channel response and how an instantaneous timing jitter  $\nu$  affects the positions. Fig.5.1 can be compared to fig.2.3 where no timing jitter is assumed in the template signals.

Then, by using an SRake receiver to combine  $L_c < L$  number of paths, the decision statistic can be given as:

$$Z = \sqrt{E_p N_s E_d} \sum_{l=0}^{L_c-1} \chi_l \alpha(\tau_l) Z_l = E_p N_s E_d \sum_{l=0}^{L_c-1} \chi_l^2 \alpha(\tau_l) \alpha(\tau_l + \nu_l) + \eta \quad (5.2)$$

Finally, the energy capture (EC) and system performance quantified as BER can be referred to that given in (2.11) and (2.15), respectively.

## 5.2 Simulation Model and Parameters

The system models provided in the previous section are further elaborated by specific numerical examples. This section discusses the setup of the simulation environment and related system parameters for these numerical examples. Firstly, the system parameters of the transceivers and propagation environment are presented. Then the characteristics of the timing jitter existing in the system are discussed.

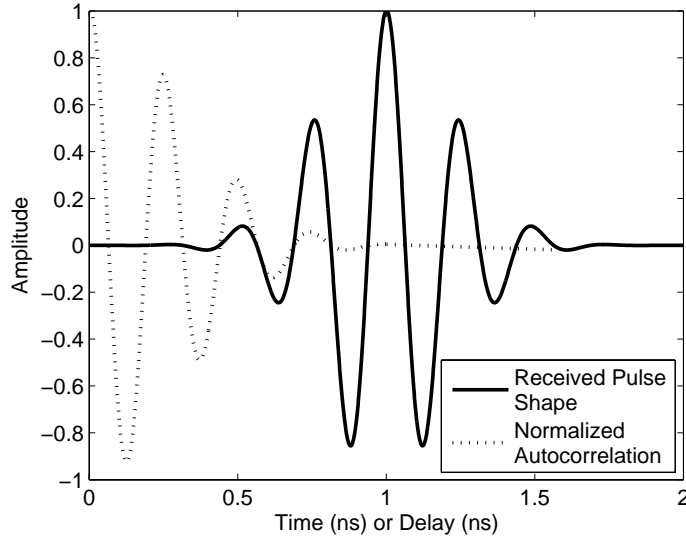


Figure 5.2: Received Modulated Gaussian Pulse and its Normalized Autocorrelation Function.  $T_p=2\text{ns}$ ,  $t_m=0.39T_p$ ,  $f_c=4\text{GHz}$ .

### 5.2.1 System Parameters

The transmitted DS-UWB pulse waveform  $p(t)$  is the modulated Gaussian pulse as given in (2.17). Fig.5.2 illustrates the received modulated Gaussian pulse without loss or fading and the correlator output due to delay or timing jitter of the template signal. Fig.5.2 suggests that delay or timing jitter decreases the correlator output and thus decreases the amount of EC. Additionally, it is worth to note that the autocorrelation function depends greatly on the pulse waveform, center frequency and pulse duration.

The UWB system is designed to transmit signal over indoor multipath and multi-user environment. At the receiver end, timing jitter is assumed to be present in the template signal generator. Then, corresponding to various system parameters such as SNR, Rake fingers, chip length, number of users and so on, system performance is determined through computer simulations. The summary of the simulation parameters are as shown in tab.5.1.

### 5.2.2 Timing Jitter Model

The receiver described in (5.1) shows that the timing jitter present at the template signal generator is an instantaneous value  $\nu$ . In the computer simulation, timing jitter with a statistical distribution is modeled for a more realistic investigation. Here, the timing jitter is assumed to have a Gaussian distribution. In most electrical circuits, thermal noise that causes timing

Table 5.1: Simulation Parameters for DS-UWB System in the Presence of Timing Jitter.

Parameters	
pulse duration $T_p$	0.267 to 4ns
chip length $N_s$	1 to 50
SNR	0 to 30dB
Rake fingers $L_c$	1 to 20
Rake combining method	MRC
multipath channel model	IEEE 802.15.3a CM1, CM2, CM3, CM4
system bandwidth $W_t$	0.5 to 7.5GHz
chip duty $\delta$	0.2 to 1
pulse center frequency $f_c$	4 to 10GHz
number of simultaneous users $U$	1 to 30
data modulation	BPSK
pulse waveform	modulated Gaussian

error is Gaussian distributed. And if there are several uncorrelated composite effects with different distributions taking place simultaneously, these effects will approach Gaussian distribution, according to the central limit theorem [58, 59].

The Gaussian probability density function (PDF) can be given as:

$$G(\nu) = \frac{1}{\sigma\sqrt{2\pi}} \exp\left(-\frac{\nu^2}{2\sigma^2}\right) \quad (5.3)$$

where  $\nu$  is the instantaneous timing jitter value,  $\sigma$  is the standard deviation of the timing jitter distribution,  $\sigma$  is defined as the root mean square jitter (RMSJ) and is expressed in nanoseconds or picoseconds in the following sections. The term ‘timing jitter’ applied in the following discussions are referred to RMSJ, if not specified otherwise.

### 5.3 Performance in the Presence of Timing Jitter

This section presents the impact of timing jitter on UWB system performance corresponding to different system parameters. The signaling design for UWB system is DS spreading with various pulse duration and chip duty factor. The DS-UWB performance in multipath environment with single user is firstly discussed, followed by multi-user environment.

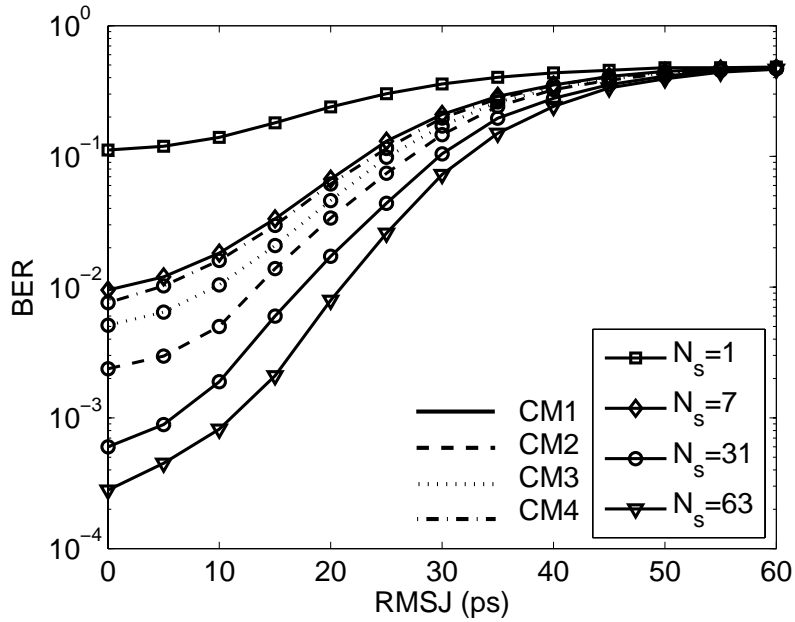


Figure 5.3: BER Performance vs. Root Mean Square Jitter over Different Multipath Channels for DS-UWB System. SNR=20dB,  $T_p=2$ ns,  $f_c=4$ GHz,  $L_c=8$ ,  $\delta=1$ , CM1-4.

### 5.3.1 Performance in Multipath Channel

#### DS-UWB Performance vs. RMSJ

Fig.5.3 presents the relationship between BER performance and RMSJ with varying chip length  $N_s$  for DS-UWB systems in different indoor multipath channel models. System parameters such as SNR,  $L_c$ ,  $f_c$  and  $T_p$  are set to 20dB, 8, 4GHz and 2ns respectively. Multipath CM1 to CM4 are considered over single user environment.

In fig.5.3, a general observation is that as RMSJ increases, all systems display performance degradation regardless of  $N_s$  and channel models. It is found that systems with higher  $N_s$  give better BER performance, especially at lower values of RMSJ (from 0 to 10ps). Without the presence of timing jitter (RMSJ=0ps), BER performance for systems with  $N_s=1$  and 7 are  $10^{-1}$  and  $10^{-2}$  respectively, whereas systems with  $N_s=31$  and 63 have better BER of below  $10^{-3}$ . Next, as RMSJ increases towards 20ps, the difference in BER performance for various  $N_s$  becomes smaller. Furthermore, as RMSJ increases beyond 50ps, most systems performance approach to BER of  $10^{-0.5}$ .

Next, BER performance for systems with  $N_s=31$  and varying RMSJ are

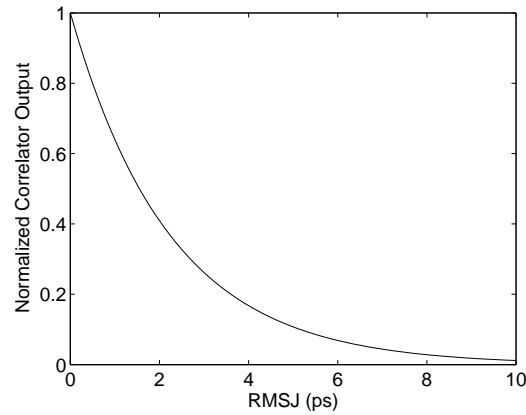


Figure 5.4: Simplified Relationship between the Average Value of Normalized Correlator Output and Timing Jitter (AWGN and channel fading neglected).  $T_p=2\text{ns}$  and  $f_c=4\text{GHz}$ .

also analyzed in different channel models. Results for CM1 and CM2 show the different impacts of LOS and NLOS receptions in jitter environment, whereas CM3 provides fading analysis due to distance and CM4 outlines the effects of an extreme condition of NLOS. From fig.5.3, it is observed that the pattern of BER performance degradation (the curvature of the graphs) due to timing jitter is similar for all channel models. Without the presence of timing jitter, it is found that the difference between CM1 and CM2 is greater as compared to CM2 and CM3. Thus it can be said that the effect of NLOS is more significant as compared to the effects of distance. As RMSJ increases to 20ps, the difference among the systems with different channel models becomes less obvious.

Fig.5.4 can be used to explain the effects of timing jitter on system performance. As RMSJ increases, the average value of the correlator output decreases due to mistiming of the template signal placement in the correlation process (refer fig.5.1). Referring to fig.5.4, the quantitative relationship between timing jitter (RMSJ) and the average value of correlator output can be identified. Neglecting AWGN and channel fading, correlator output of 1 (100% energy capture) can be obtained if not timing jitter is present. However, as RMSJ increases, the correlator output decreases considerably, causing performance degradation to take place.

### DS-UWB Performance vs. Chip Length

Fig.5.3 has shown BER performance for DS-UWB systems with  $N_s=1, 7, 31, 63$  corresponding varying RMSJ and found that the more number of  $N_s$  used, the better the BER performance becomes. Since employment of

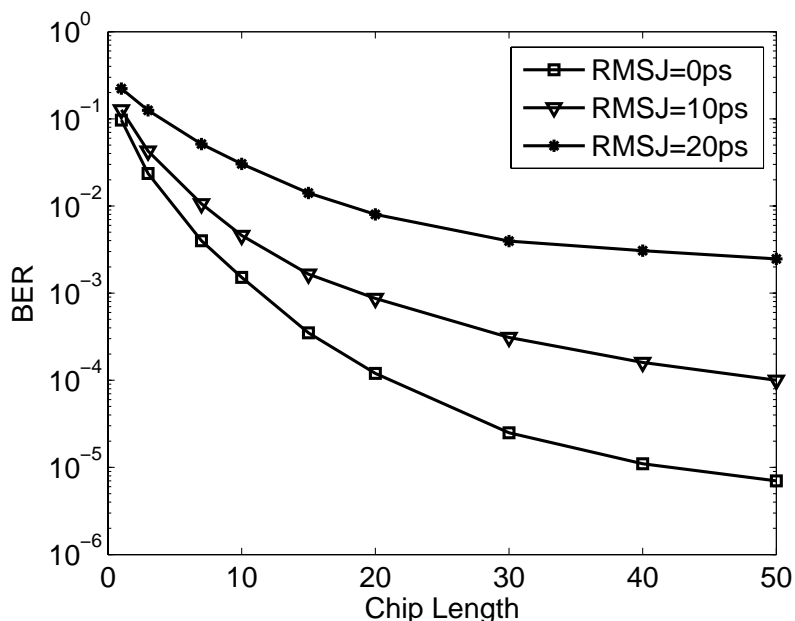


Figure 5.5: BER Performance vs. Chip Length for DS-UWB System. SNR=25dB,  $T_p=2$ ns,  $f_c=4$ GHz,  $L_c=8$ ,  $\delta=1$ , CM1.

spreading chips is the main design option applied in DS signaling scheme, in this section, a more overall picture of the effects of increasing  $N_s$  is presented. Fig.5.5 presents the BER performance versus varying  $N_s$  for DS-UWB system. At  $N_s=1$ , the difference in BER performance for systems in RMSJ=0, 10 and 20ps are not significant, all at BER of approximately  $10^{-1}$ . However, as  $N_s$  increases, the difference becomes greater. At  $N_s=50$ , the BER performance for systems in the presence of RMSJ=0,10 and 20ps are  $10^{-5}$ ,  $10^{-4}$  and  $2 * 10^{-3}$  respectively.

As  $N_s$  increases, longer DS spreading code is employed and thus increases chip randomization between adjacent received symbols. As a result, the SI between adjacent symbols decreases due to increasing chip orthogonality, and BER performance improves. In a jitter-free environment (RMSJ=0ps), it is observed that BER performance improves significantly particularly from  $N_s=1$  to 40, after where BER improvement slows down and saturates despite continuously increasing  $N_s$ . This can be defined as the ‘saturating  $N_s$ ’. On the other hand, in the presence of timing jitter, the mistiming of template signal causes the average correlator output to decrease and generates more error in the detection process, therefore degrading BER performance severely. Additionally, timing jitter also causes the ‘saturating  $N_s$ ’ to be observed at lower value. For example, with RMSJ=20ps in the system, sig-

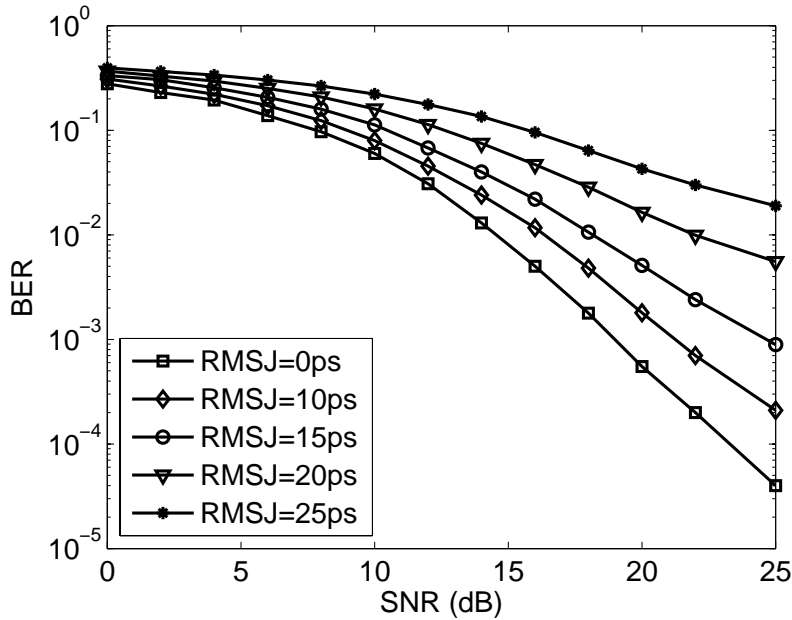


Figure 5.6: BER Performance vs. SNR for DS-UWB System.  $N_s=31$ ,  $T_p=2\text{ns}$ ,  $\delta=1$ ,  $f_c=4\text{GHz}$ ,  $L_c=8$ , CM1.

nificant BER improvement can only be observed up to  $N_s=30$  (as compared to  $N_s=40$  in RMSJ=0ps). It is well known that increasing number of DS chips to gain better performance is an important system resource in DS-UWB systems. But the presence of timing jitter has clearly compromised the effectiveness of this resource.

### DS-UWB Performance vs. SNR

Besides manipulating number of  $N_s$  in DS-UWB signaling design, another option for improving BER performance is by transmitting signals with higher SNR. Fig.5.6 presents the relationship between BER performance and transmitted signal with different SNR in the presence of timing jitter. At system SNR lower than 10dB, the BER performance difference among systems with various RMSJ is not obvious. As SNR increases beyond 10dB, systems with higher RMSJ have worse BER performance. Systems with higher RMSJ require higher SNR to reach the same BER level as systems with lower SNR. As an example, for systems with RMSJ=0, 10 and 15ps, the SNR needed to achieve BER of  $10^{-3}$  are approximately 19, 21 and 25dB. It is also observed that for systems with higher RMSJ, BER improvement due to increasing SNR also becomes less efficient. For example, as SNR increases from 20dB to 25dB, at RMSJ=10ps, BER improvement is  $2 \times 10^{-3} / 2 \times 10^{-4} = 10$  times,

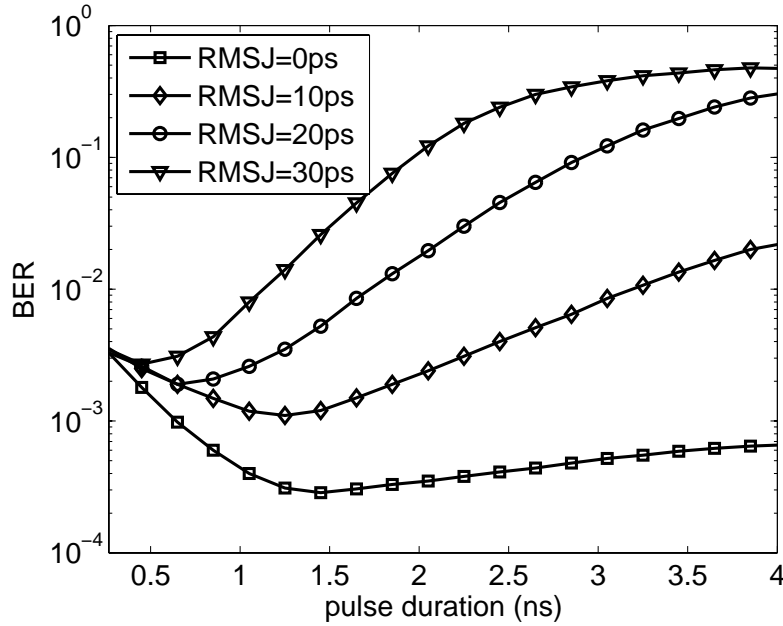


Figure 5.7: BER Performance vs. Pulse Duration for DS-UWB System. SNR=25dB,  $N_s=15$ ,  $\delta=1$ ,  $f_c=4\text{GHz}$ ,  $L_c=8$ , CM1.

whereas at RMSJ=25ps, BER improvement is only  $4 * 10^{-2} / 2 * 10^{-2} = 2$  times.

### DS-UWB Performance vs. Pulse Duration

Fig.5.7 shows the effects of employing different pulse duration  $T_p$  in DS-UWB system in the presence of timing jitter. An SRake receiver that selects and combines  $L_c=8$  best paths from a total of  $L$  resolvable paths is employed. SNR and  $N_s$  are set to 25dB and 15 respectively.

For a jitter-free environment (RMSJ=0ps) shown in fig.5.7, as  $T_p$  increases from 0.267ns to 1.5ns, BER performance improves. The reason is that as  $T_p$  becomes longer,  $L = T_d/T_p$  decreases. Then, by selecting and combining a fixed value of  $L_c=8$  paths from the decreasing  $L$ , more fractional energy can be captured in each path. This factor contributes to the BER improvement from  $T_p=0.267$  to 1.5ns. However, if  $T_p$  continues to increase beyond 1.5ns, BER performance on the other hand, degrades. This is because beyond  $T_p=1.5\text{ns}$ , the received multipath profiles become longer and start to overlap each other (paths becoming less isolated), resulting in amplitude fluctuation (channel fading) [20,34,60,61]. Fig.5.8 presents a simplified illustration on how longer pulses result in more overlapped paths (fig.5.8 bottom) as compared to shorter pulse with more isolated paths (fig.5.8 top).

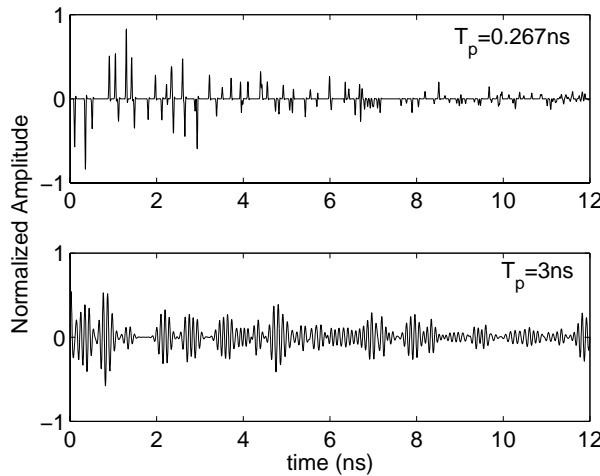


Figure 5.8: Truncated Noiseless Channel Response over CM1 for Transmitted Unit Energy Pulse Duration 0.267ns (top) and 3ns (bottom).

The longer  $T_p$  becomes, the more paths overlap with each other, causing more channel fading, thus degrading BER performance. The emergence of these two contrary factors causes the existence of an optimum value of  $T_p=1.5\text{ns}$  as observed in fig.5.7 at  $\text{BER}=2.5 \times 10^{-4}$ . The optimum pulse duration  $T_{po}$  is defined as the pulse duration that provides minimum achievable BER at a specified SNR.

With timing jitter present in the system, it is found that the corresponding  $T_{po}$  becomes lower. Also, the achievable BER performance with each  $T_{po}$  degrades as RMSJ increases. For example, at RMSJ=10, 20 and 30ps,  $T_{po}$  are found to be 1.25, 0.7 and 0.5ns at  $\text{BER}=1 \times 10^{-3}$ ,  $2 \times 10^{-3}$  and  $3 \times 10^{-3}$  respectively. From the discussions given above, it can be shown that as  $T_p$  increases from 0.267ns, more fractional energy can be captured. However, the presence of timing jitter limits the increase in EC due to longer  $T_p$  with the mistiming of template signal. This phenomenon becomes more dominant as RMSJ increases and forces the opposite factor of overlapped paths degradation to take over at lower  $T_p$ . In other words, timing jitter can be seen as ‘helping’ the effects of channel fading and result in  $T_{po}$  to occur at a lower  $T_p$ . Increasing spreading bandwidth  $W_t$  by reducing  $T_p$  is one of the main resource in UWB system to increase data rate and improve performance, timing jitter is found to compromise this system resource.

### DS-UWB Performance vs. Chip Duty Factor

In DS-UWB systems, chip duty factor (DF)  $\delta$  is normally set to less than unity to occupy a wide  $W_t$ . Fig.5.9 presents BER performance corresponding

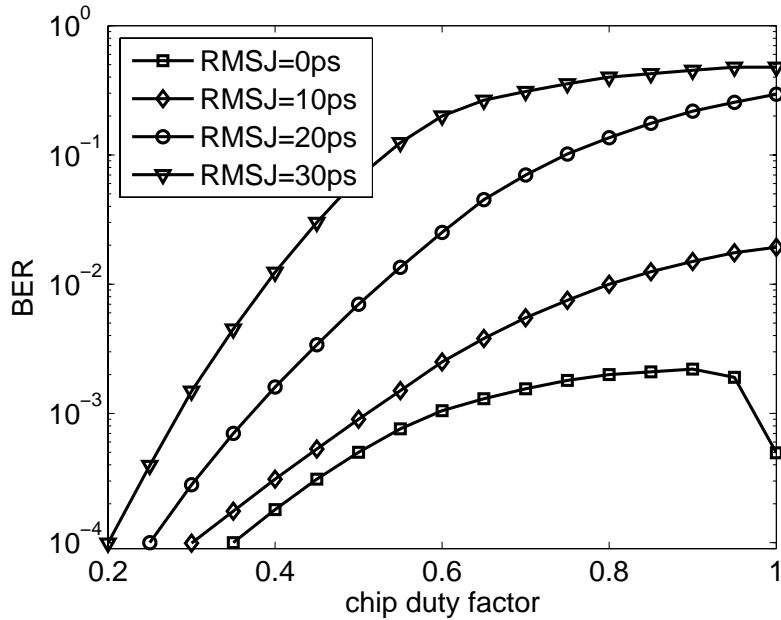


Figure 5.9: BER Performance vs. Chip Duty Factor for DS-UWB System. SNR=25dB,  $N_s=15$ ,  $T_c=4\text{ns}$ ,  $f_c=4\text{GHz}$ ,  $L_c=8$ , CM1.

to varying DF in the presence of timing jitter. Chip duration  $T_c$  is set to 4ns and  $T_p$  is decreased to obtain lower DF.

Referring to fig.5.9, without timing jitter, BER performance for  $\delta < 0.5$  is better than BER at  $\delta=1$ . The worst BER performance takes place in  $0.5 < \delta < 1$ . This is due to partial correlation products of adjacent pulses besides the desired pulse. Detailed explanation has been given following fig.3.6.

With timing jitter present in the system, the idea of decreasing DF to obtain better BER performance is still relevant, but BER performance is degraded in an overall manner. For example, at  $\delta=0.4$ , an RMSJ of 10ps causes BER performance to achieve only  $3 \times 10^{-4}$  as compared to  $2 \times 10^{-4}$  without timing jitter. And BER performance for systems with RMSJ=20 and 30ps are  $2 \times 10^{-3}$  and  $1 \times 10^{-2}$  respectively at  $\delta=0.4$ .

Note that manipulating DF produces an advantage towards timing jitter. From fig.5.9, for different RMSJ, the BER performance difference in  $\delta < 0.3$  becomes less obvious as compared to higher DF. In other words, BER performance for systems with high RMSJ can be improved effectively by decreasing DF. The reason is that as DF decreases, the increasing resolvable path and decreasing channel fading due to shorter pulse is more dominant over the mistiming of the template pulse.

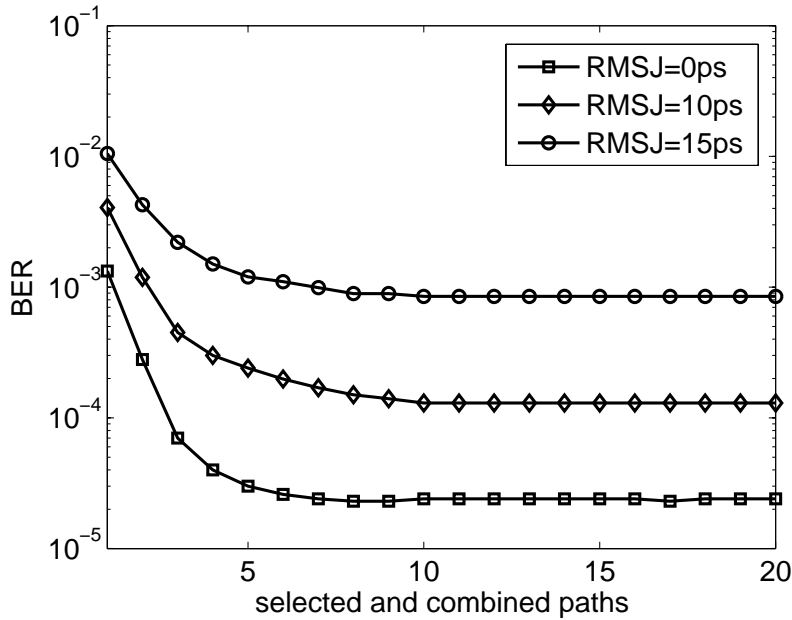


Figure 5.10: BER Performance vs. Combined and Selected Paths for DS-UWB System. SNR=25dB,  $N_s=31$ ,  $T_p=2\text{ns}$ ,  $\delta=1$ ,  $f_c=4\text{GHz}$ , CM1.

### DS-UWB Performance vs. Rake Fingers

Fig.5.10 presents the BER performance for DS-UWB system with varying SRake combined paths  $L_c$  in the presence of timing jitter. Without timing jitter, as  $L_c$  increases from 1 to 8, improvement in BER performance from  $1 \times 10^{-3}$  to  $2 \times 10^{-5}$  can be observed. Beyond  $L_c=8$ , further increasing  $L_c$  saturates and does not further improve BER performance. However, with the presence of timing jitter, the capability of improving BER performance by increasing  $L_c$  is compromised. For RMSJ=15ps, BER saturates at  $1 \times 10^{-3}$  with  $L_c=4$ . In other words, timing jitter causes the ‘saturating  $L_c$ ’ to become lower and the corresponding BER to become worse. Thus, the design flexibility provided by SRake receiver to achieve better BER by increasing  $L_c$  is limited as RMSJ increases.

### DS-UWB Performance vs. Pulse Center Frequency

Conventional impulse radio uses baseband pulses for transmitting signals. However, in order to ensure practicality in high speed communication and to fully utilize the UWB bandwidth, it is essential to modulate the system to a higher center frequency  $f_c$ . Fig.5.11 shows the impact of using different  $f_c$  on BER performance in the presence of timing jitter. Without timing jitter

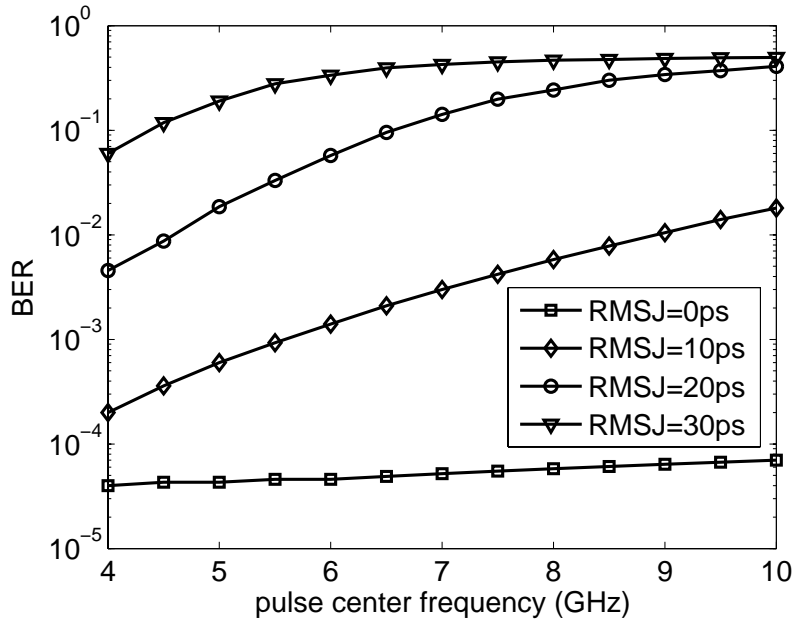


Figure 5.11: BER Performance vs. Center Frequency for DS-UWB System. SNR=25dB,  $N_s=31$ ,  $T_p=2\text{ns}$ ,  $\delta=1$ ,  $L_c=8$ , CM1.

(RMSJ=0ps), increasing  $f_c$  in the transmitted pulse does not show significant changes in BER, that is constantly around  $4 \times 10^{-5}$ . However, as RMSJ increases, BER degradation corresponding to increasing  $f_c$  becomes more obvious. At RMSJ=10ps, BER at  $f_c=4\text{GHz}$  is  $2 \times 10^{-4}$ , but it degrades to  $2 \times 10^{-2}$  at  $f_c=10\text{GHz}$ . It is also found that at higher RMSJ, the BER degradation is more rapid at lower range of  $f_c$ . For example, at RMSJ=20ps, BER saturates towards  $10^{-0.5}$  at  $f_c=9\text{GHz}$  but at RMSJ=30ps, BER saturates towards  $10^{-0.5}$  starting from as low as  $f_c=6\text{GHz}$ .

These observations can be explained by using fig.5.2. As  $f_c$  becomes higher, the autocorrelation function drops more rapidly as delay or timing jitter takes place. In other words, for higher  $f_c$ , a shorter timing jitter is required to cause more severe degradation in the correlator output due to the more rapidly fluctuating autocorrelation function.

### 5.3.2 Performance in Multi-user Channel

The previous section discusses the impact of timing jitter on BER performance in accordance to various system parameters in single user environment. As number of interference user  $U$  increases, the system performance changes considerably. This section presents the analysis of such conditions. In this section,  $U$  refers to interfering users other than the desired user.

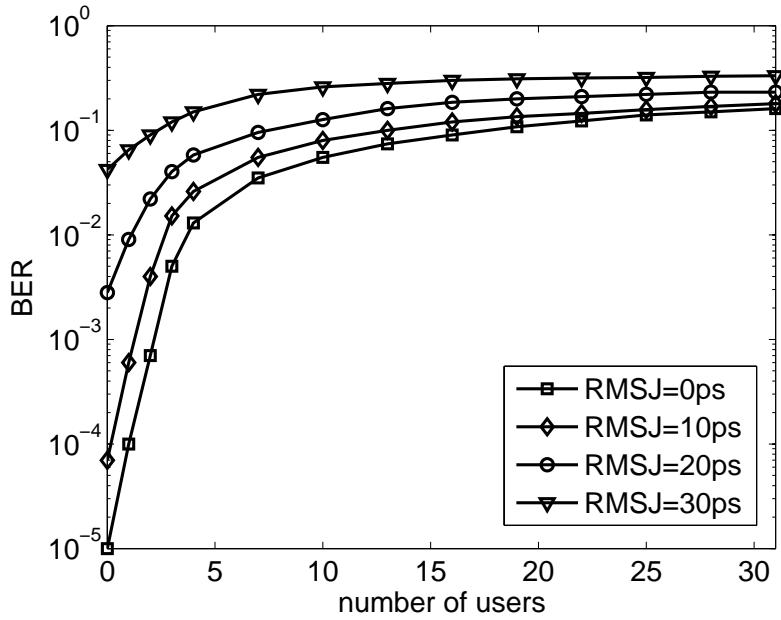


Figure 5.12: BER Performance vs. Number of Interfering Users for DS-UWB System. SNR=30dB,  $N_s=31$ ,  $T_p=2\text{ns}$ ,  $\delta=1$ ,  $L_c=8$ ,  $f_c=4\text{GHz}$ , CM1.

### DS-UWB Performance vs. Number of Users

Fig.5.12 presents the relationship between BER performance and number of interfering users  $U$  supported in the system. SNR and  $N_s$  are set to 30dB and 31. A total of  $L_c=8$  paths are combined from multipath CM1.

It is shown that without timing jitter (RMSJ=0ps), as  $U$  increases, BER performance degrades. For example, at  $U=0$  (single user environment), BER is  $10^{-5}$  whereas at  $U=5$  BER degrades to  $2 \times 10^{-2}$ . Furthermore, if timing jitter is present in the system, more degradation is observed. An environment with  $U=5$  and RMSJ=20ps gives BER as high as  $6 \times 10^{-2}$ , as compared to  $2 \times 10^{-2}$  without jitter. Besides, it is also observed that BER degradation is especially rapid at low number of users ( $U \leq 5$ ) than higher number of users. For RMSJ=10ps, single user environment gives BER of  $8 \times 10^{-5}$  and as  $U$  increases to 5, BER is  $4 \times 10^{-2}$ , around 500 fold of degradation. As  $U$  continues to increase from 5 to 30, BER degrades to  $2 \times 10^{-1}$ , which is only 5 fold.

### DS-UWB Performance vs. RMSJ in Different Multipath Channels

In fig.5.13, the effect of varying RMSJ on DS-UWB system over multi-user and various multipath channels is presented. System SNR,  $T_p$  and  $L_c$  are

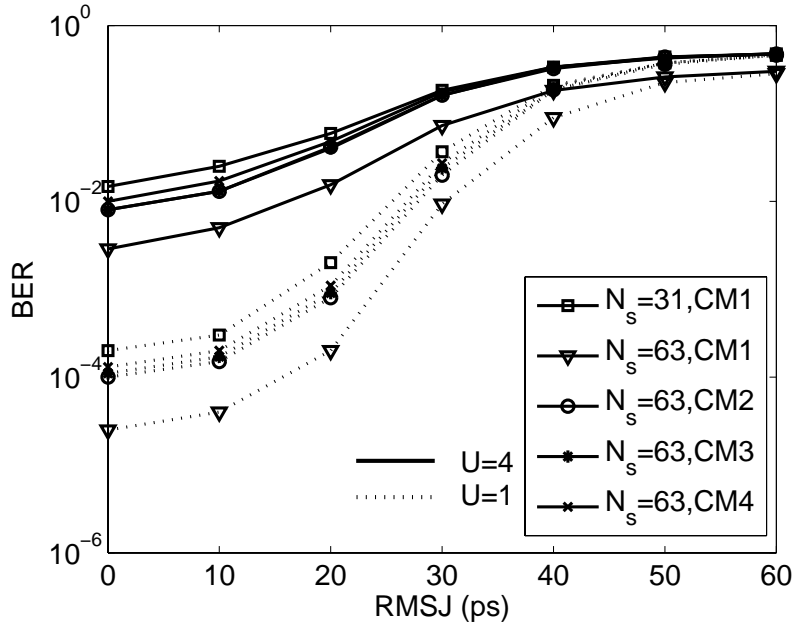


Figure 5.13: BER Performance vs. RMSJ in Multi-user and Multipath Channels for DS-UWB System. SNR=30dB,  $T_p=2$ ns,  $\delta=1$ ,  $f_c=4$ GHz,  $L_c=8$ , CM1-4.

set to 30dB, 2ns and 8 respectively.

Firstly, it is found that increasing  $N_s$  is effective in improving BER performance even in multi-user environment. The reason is that as  $N_s$  increases, more number of chips are used to spread the symbols, thus increasing the randomization not only among adjacent chips, but also among simultaneous users sharing the same propagation channel.

On the other hand, timing jitter is found to degrade differently, BER performance for systems with different  $U$ . For example, BER performance for  $U=1$  is found to be significantly better than BER for  $U=4$  at RMSJ below 30ps. However, as RMSJ increases from 0 to 30ps, performance for system with  $U=1$  degrades more rapidly as compared to that with  $U=4$ . This observation indicates that with RMSJ reaching a certain value (in this particular analysis, 30ps), timing jitter becomes the dominant factor for BER performance degradation. Furthermore, increasing  $N_s$  to achieve better BER performance is also found to be less effective at higher RMSJ.

Propagation of DS-UWB signal over multi-user environment in the presence of timing jitter shows a rather different scenario from that in single user environment. In multipath environment, the main observation is that different channel models representing different physical conditions are found to have less significant effects on BER performance. Referring to fig.5.13,

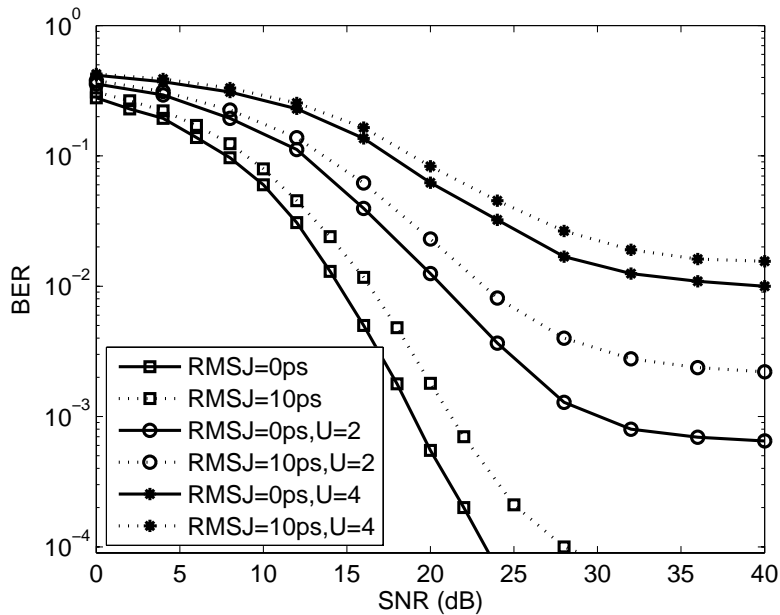


Figure 5.14: BER Performance vs. SNR in Multi-user Environment for DS-UWB System.  $N_s=31$ ,  $T_p=2\text{ns}$ ,  $\delta=1$ ,  $L_c=8$ ,  $f_c=4\text{GHz}$ , CM1.

BER performance difference is not distinguishable in CM2, CM3 and CM4. Meanwhile, CM1 has the relative best performance. In other words, the effects of LOS and NLOS are the main factors determining BER performance in the presence of timing jitter.

### DS-UWB Performance vs. SNR

Fig.5.14 presents BER performance corresponding to SNR for DS-UWB over timing jitter and multi-user environment. System parameters such as  $N_s$ ,  $T_p$  and  $L_c$  are set to 31, 2ns and 8 respectively.

The results show BER performance for  $U=0$ , 2 and 4. Increasing SNR to achieve better BER performance for single user environment has been concluded in the earlier section. However, in multi-user environment, beyond a certain value of SNR, BER performance saturates despite continuously increasing SNR. This is defined as the ‘saturating SNR’. In fig.5.14, the ‘saturating SNR’ for systems with  $U=2$  and 4 are approximately 30dB. Without the presence of timing jitter (RMSJ=0ps), BER at ‘saturating SNR’ for systems with  $U=2$  and 4 are  $7 \times 10^{-4}$  and  $10^{-2}$ , respectively. And with the presence of timing jitter, the ‘saturating SNR’ remains similar but the corresponding BER performance further degrades. For RMSJ=10ps, the corresponding BER performance for systems with  $U=2$  and 4 become

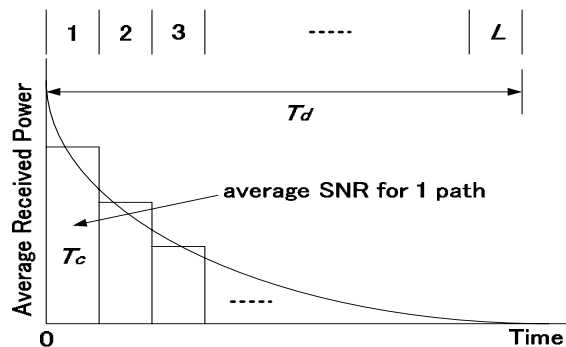


Figure 5.15: Multipath Channel with Exponentially Decaying PDP.

$2 * 10^{-3}$  and  $1.8 * 10^{-2}$ , respectively. In other words, the presence of timing jitter compromises the improvement of BER performance due to increasing SNR in multi-user environment, especially in higher range of SNR.

#### 5.4 Timing Jitter Mitigation Technique Employing Multiband UWB Signaling Design

Up to this section, the impact of timing jitter is evaluated from various aspects, and it can be commented that considerable performance degradation is observed when timing jitter is present in UWB system. In this section, by employing multiband UWB signaling, the impact of timing jitter is found to be reduced. The attempt to develop mitigation technique employing DS-MB-UWB system with multiple narrower sub-bands (thus longer-duration pulses) should display encouraging results. The previous section shows that signal with shorter pulse duration is subjected to more severe timing jitter degradation. Therefore, designing DS-MB-UWB signaling provides potentials to mitigate performance degradation due to timing jitter.

In this section, both DS and DS-MB UWB systems are designed over multipath channel with Rayleigh distributed fading. The signal models can be referred to (2.2) and (2.1).

Then, the channel model can be described as the pattern of how the energy in the received signal is distributed along the multipaths. Firstly, the received signal amplitudes at a certain path are assumed to follow the Rayleigh fading distribution. The mean value of these faded signals give the average energy present at that particular path. Here, the distribution pattern of average energy along the multipath profile is defined by exponentially decaying power delay profile (PDP). As shown in fig.5.15, for an exponentially decaying PDP, the first path has the largest portion of average SNR, and for the following paths the SNR decreases in an exponential

manner.

The average SNR for each path can be given by:

$$\Psi_l = \Gamma \left[ \frac{1 - \exp(-C/L)}{1 - \exp(-C)} \right] e^{-C \left[ \frac{l-1}{L} \right]}$$

$$C > 0, l = 1, 2, \dots, L \quad (5.4)$$

where  $\Gamma = E_s/N_0$  is the total SNR with  $E_s$  as the symbol energy,  $C$  denotes the representation of the decaying rate of the average path SNR. At different values of  $C$ , the energy distribution pattern versus time will be different, but the total amount of energy in the channel response remains the same. For larger  $C$  values, most energy are concentrated at the earlier period of time and decaying process takes place more rapidly.

Next, the DS-MB-UWB pulse autocorrelation function in the presence of a Gaussian distributed timing jitter having a standard deviation  $\sigma$  can be described as:

$$G(\sigma) = \left( \frac{1}{\sigma\sqrt{2}} \right) \left( \frac{1}{\sqrt{\frac{\pi}{t_m^2} + \frac{1}{2\sigma^2}}} \right) \exp \left( \frac{-\pi^2 E[f_m]^2}{\sqrt{\frac{\pi}{t_m^2} + \frac{1}{2\sigma^2}}} \right)$$

$$m = 1, 2, 3, \dots, B \quad (5.5)$$

where  $t_m$  is the pulse width constant and  $E[.]$  denotes the expected value. By changing  $f_m$  to a constant center frequency  $f_c$ , (5.5) can be modified to represent a DS-UWB signal autocorrelation.

The average energy able to be capture at the  $l$ -th path can be given by:

$$\beta_l = E_s G(\sigma)^2 \left[ \frac{1 - \exp(-C/L)}{1 - \exp(-C)} \right] e^{-C \left( \frac{l-1}{L} \right)}$$

$$C > 0, l = 1, 2, \dots, L \quad (5.6)$$

Finally the symbol error rate (SER) can be described as [61]:

$$SER_{SRake} = \frac{1}{\pi} \int_0^\Theta \prod_{l=1}^{L_c} \left[ \frac{\sin^2(\theta)}{\lambda_{MPSK} \Psi_l G(\sigma)^2 + \sin^2(\theta)} \right]$$

$$\cdot \prod_{l=L_c+1}^L \left[ \frac{\sin^2(\theta)}{\Psi_{MPSK} \Psi_l G(\sigma)^2 \frac{L_c}{L} + \sin^2(\theta)} \right] d\theta \quad (5.7)$$

where  $\Psi_l$  is the average SNR in the  $l$ -th path,  $L_c$  is the number of selected and combined paths out of the  $L$  number of total resolvable paths,  $\lambda_{MPSK} = \sin^2(\pi/M)$ ,  $\Theta = \pi(M-1)/M$  and  $M$  is the  $M$ -ary signaling level.

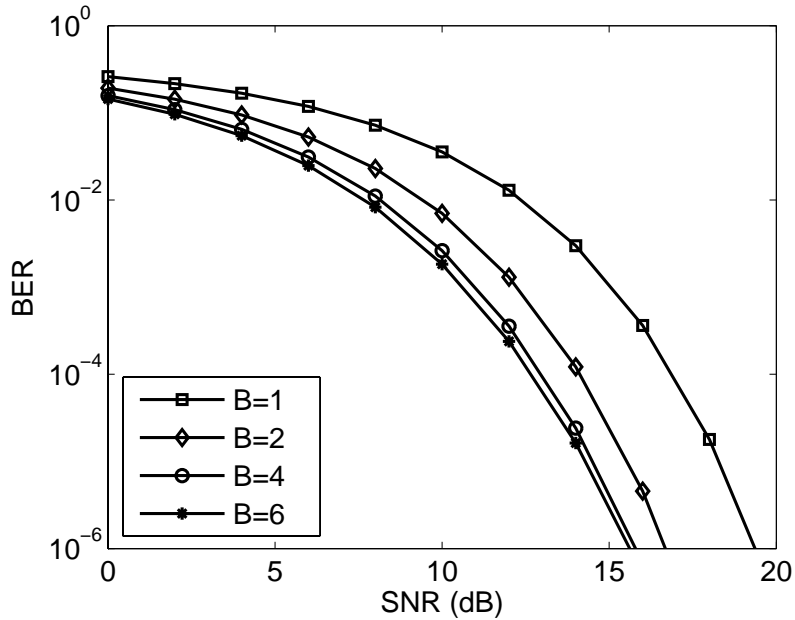


Figure 5.16: BER Performance vs. SNR for Different UWB Signaling Design.  $L_c = 4$ ,  $W_t = 6\text{GHz}$ ,  $\text{NRMSJ} = 0.01\%$ ,  $T_d = 200\text{ns}$ , Exponential Decaying PDP,  $C = 10$ .

In this section, numerical examples are provided to show that timing jitter can be mitigated by employing DS-MB-UWB signaling schemes. Here, note that SER can be understood as BER since BPSK is used. Also, timing jitter is referred as normalized RMSJ (NRMSJ). NRMSJ is the ratio of RMSJ to pulse duration and is expressed in percentage. The higher the NRMSJ, the more severe the mistiming becomes.

Fig.5.16 presents the mitigation capability of DS-MB-UWB signaling as compared to DS-UWB signaling. The total bandwidth  $W_t$  for all systems are 6GHz,  $L_c = 4$  and maximum delay spread  $T_d = 200\text{ns}$ .  $\text{NRMSJ} = 0.01\%$  is considered to present in the systems. The multipath channel follow an exponential decaying PDP with  $C = 10$ .

Fig.5.16 shows that DS-MB-UWB system generally outperforms DS-UWB system. Additionally, it is observed that DS-MB-UWB system employing more number of bands performs better. Note that increasing  $B$  does not improve BER performance proportionately. For example, the BER improvement from  $B = 1$  to 2 bands is higher compared to  $B = 2$  to 4 bands.

The behavior of BER performance can be explained from the perspective of energy capture. Fig.5.17 compares the achievable captured energy by DS-UWB and DS-MB-UWB systems with different number of sub-bands  $B$  and

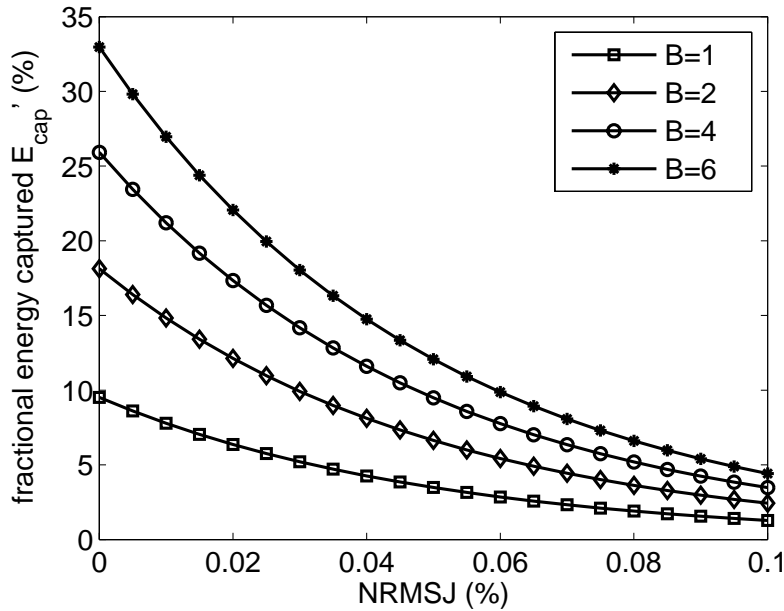


Figure 5.17: Energy Capture vs. Normalized RMSJ for Different UWB Signaling Design.  $L_c = 4$ ,  $W_t=6\text{GHz}$ ,  $T_d=200\text{ns}$ , Exponential Decaying PDP,  $C=10$ .

varying NRMSJ. It can be shown that DS-MB-UWB is able to capture more energy than DS-UWB systems at all value of NRMSJ. Furthermore, the higher  $B$  becomes, the more energy can be captured. The reason is, as more sub-bands are employed, longer pulses are used. When NRMSJ increases, the captured energy generally decreases. However, the observation that DS-MB-UWB with higher  $B$  captures more energy still holds, despite increasing NRMSJ. By employing more sub-bands, DS-MB-UWB system is able to capture more fractional energy, and thus have better BER performance.

This section suggests that mitigation technique can be developed by employing multiband signaling design. Corresponding different system parameters such as  $B$  and SNR, tolerance against timing jitter is found to vary significantly. Careful design has to be conducted to optimize BER performance.

## 5.5 Concluding Remarks

In this chapter, the issue of timing jitter due to circuitry imperfection of the template signal generator in UWB receiver is presented. The impact of timing jitter on UWB system with DS signaling is investigated and miti-

gated. Firstly, the mechanism of timing jitter in the correlation process and how degradation takes place is presented and discussed. Next, the various impact of timing jitter on performance of DS-UWB system corresponding to parameters such as root mean square jitter, chip length, SNR, pulse duration, chip duty factor, pulse center frequency, Rake fingers and number of interfering users are discussed in detail. Finally, by employing DS-MB-UWB signaling, mitigation technique against timing jitter is proposed, and the results are shown. Timing jitter is an unavoidable mistiming in all digital communication systems, and the degradation is furthermore pronounced in UWB systems employing very short pulses. Therefore, the signaling design of UWB system has to seriously take into consideration the issue of timing jitter, so that the additional loss in the link budget can be effectively estimated.

Future works can be focused on other approaches to mitigate the degradation caused by timing jitter in UWB systems. Some suggested methods are employment of robust pulse waveforms, employment of preambles in the receiver and so on. Combinational techniques in DS-MB-UWB system can also be considered.

# Chapter 6

## Conclusion

### 6.1 Summary

This thesis has addressed the significance of signaling design in UWB communication systems. UWB signal with various design options are evaluated for the purposes of performance improvement and interference mitigation. Additionally, potential threats to system performance such as timing jitter has also been investigated. The main contribution of this thesis is to widen the dimension of UWB system design from the perspective of signaling manipulation.

Firstly, the behavior of UWB signal with low chip duty factor (DF) is investigated and presented. It is found that in multipath environment, the employment of low DF signal enables more efficient energy capture, and thus better system performance. However, decreasing DF does not always result in performance improvement. Instead, optimum DF value is found to exist. In multi-user environment, low DF signal is more robust to multi-user interference due to the reduction of collision between signals from simultaneous users. Furthermore, by overlapping sub-bands in multiband UWB system through low DF signaling design, performance improvement can be observed. Various advantages can be obtained from manipulation of DF in UWB signaling design.

Secondly, mitigation technologies are developed for UWB system by manipulating parameters in signaling design. By suppressing sub-band power in multiband system, it is shown that UWB interference towards coexisting narrowband system can be reduced, and at the same time, narrowband interference towards UWB system can also be decreased. Additionally, by employing low DF UWB signals, while mitigating UWB interference towards narrowband systems, performance improvement can also be observed in UWB systems. In other words, the development of mitigation techniques are shown to be mutually beneficial to both UWB system and coexisting wireless services.

Thirdly, the impact of timing jitter on UWB performance is evaluated and reported. As timing jitter increases, system performance generally becomes degraded. Timing jitter is also found to compromise performance improvement achievable by increasing inputs of system resources, such as spreading code length, SNR and Rake fingers. In multipath environment, timing jitter can be viewed as 'helping' channel fading in degrading UWB performance. In multi-user channel, timing jitter limits the total supportable number of users. It is essential for the impact of timing jitter to be understood so that relevant approaches can be taken to reduce degradation caused in system performance. As a mitigation technique to reduce the effect of timing jitter, signaling design employing multiple narrower sub-bands is applied and the mitigation capability is shown with specific numerical examples.

Lastly, it is concluded that by manipulating signaling design in UWB systems, optimum performance can be obtained. More efforts should be dedicated into investigating the potentials of signaling design to further accelerate UWB performance and throughput.

## 6.2 Future Works

There remain several potential prospects for UWB signaling design. The employment of low DF signal produces pulses with higher peak power. Peak power is an interesting topic in UWB communications and its relationship with system performance should be investigated further. The development of a common mitigation technology that serves multi-purposes of simultaneously mitigating interference due to multipath, multiple access, coexisting narrowband signal and timing jitter, should be of great interest to the UWB community.

# Bibliography

- [1] M. Ghavami, L.B. Michael, and R. Kohno, *Ultra wideband: Signals and systems in communication engineering*, John Wiley and Sons Ltd., West Sussex, 2004.
- [2] J.D. Taylor, editor, *Ultra Wideband Radar Technology*, CRC Press 2001.
- [3] G.F. Ross, Transmission and reception system for generating and receiving base-band duration pulse signals without distortion for short base-band pulse communication system. *U.S Patent 3,728,632*, April 1973.
- [4] Time Domain, <http://www.timedomain.com>.
- [5] XtremeSpectrum, <http://www.xtremespectrum.com>.
- [6] Federal Communications Commission, *First Report and Order, Revision of Part No. 15*, April 2002.
- [7] Ministry of Internal Affairs and Communications of Japan (MIC), *Summary of Progress on UWB Technical Study in Japan*, Sept. 2005.
- [8] Electronic Communications Committee (ECC), *Report of the ECC Decision in the 16th Meeting of ECC*, Oct. 2006.
- [9] M.Z. Win, and R.A. Scholtz, "Impulse radio: How it works," *IEEE Communications Letters*, vol. 2, issue 2, pp. 36-38, Feb. 1998.
- [10] M.Z. Win, and R.A. Scholtz, "Ultra-wide bandwidth time-hopping spread-spectrum impulse radio for wireless multiple-access communications," *IEEE Transactions on Communications*, vol. 48, no. 4, pp. 679-691. April 2000.
- [11] B. Hu, and N.C. Beaulieu, "Accurate evaluation of multiple-access performance in TH-PPM and TH-BPSK UWB systems," *IEEE Transactions on Communications*, vol. 52, issue 10, pp. 1758-1766, Oct. 2004.

- [12] M.L. Welborn, "System considerations for ultra-wideband wireless networks," *IEEE Radio and Wireless Conference 2001 (RAWCON 2001)*, pp. 5-8, Aug. 2001.
- [13] R.L. Peterson, R.E. Ziemer, and D.E. Borth, *Introduction to Spread Spectrum Communications*, Prentice Hall Inc., New Jersey, 1995.
- [14] P. Runkle, J. McCorkle, T. Miller, and M. Welborn, "DS-CDMA: The modulation technology of choice for UWB communications," *IEEE Conference on Ultra Wideband Systems and Technologies 2002*, pp. 364-368, Nov. 2003.
- [15] M. Welborn, T. Miller, J. Lynch, and J. McCorkle, "Multi-user perspectives in UWB communication networks," *IEEE Conference on Ultra Wideband Systems and Technologies 2002*, pp. 271-275, May 2002.
- [16] B.M. Sadler, and A. Swami, "On the performance of UWB and DS-spread spectrum communication systems," *IEEE Conference on Ultra Wideband Systems and Technologies 2002*, pp. 289-292, May 2002.
- [17] J.R. Foerster, "The performance of a direct-sequence spread ultra wideband system in the presence of multipath, narrowband interference, and multiuser interference," *IEEE Conference on Ultra Wideband Systems and Technologies 2002*, pp. 87-91, May 2002.
- [18] C.R. Nassar, F. Zhu, and Z. Wu, "Direct sequence spreading UWB systems: frequency domain processing for enhanced performance and throughput," *IEEE International Conference on Communications 2003 (ICC 2003)*, vol. 3, pp. 2180-2186, May 2003.
- [19] J.G Proakis, *Digital Communications, 4th Edition*, McGraw Hill, New York, 2001.
- [20] M.Z. Win, and R.A. Scholtz, "On the energy capture of ultrawide bandwidth signals in dense multipath environments," *IEEE Communications Letters*, vol. 2, no. 9, pp. 245-247, Sept. 1998.
- [21] M.Z. Win, and R.A. Scholtz, "Characterization of ultra-wide bandwidth wireless indoor channels: A communication-theoretic view," *IEEE Journal on Selected Areas in Communications*, vol. 20, no. 9, pp. 1613-1627, Dec. 2002.
- [22] J. Foerster, "Channel modeling sub-committee final report," IEEE P802.15-02/368r5-SG3a, Dec. 2002.
- [23] A.F. Molisch, J.R. Foerster, and M. Pedergrass, "Channel models for ultrawideband personal area networks," *IEEE Wireless Communications*, vol. 10, no. 6, pp. 14-21, Dec. 2003.

- [24] A.A.M. Saleh, and A. Valenzuela, "A statistical model for indoor multipath propagation," *IEEE Journal on Selected Areas in Communications*, vol. SAC-5, no. 2, pp. 128-137, Feb. 1987.
- [25] M.A. Rahman, S. Sasaki, J. Zhou, S. Muramatsu and H. Kikuchi, "Impact of chip duty-factor in DS-UWB communications: Some implications of regulatory emission constraints," *Proceedings of the 7th International Symposium on WPMC 2004*, Italy, Sept. 2004.
- [26] M.Z. Win, and R.A. Scholtz, "On the robustness of ultra-wide bandwidth signals in dense multipath environments," *IEEE Communications Letters*, vol. 2, no. 2, pp. 51-53, Feb. 1998.
- [27] D. Cassioli, M.Z. Win, and A.F. Molisch, "The ultra-wide bandwidth indoor channel: From statistical model to simulations," *IEEE Journal on Selected Areas in Communications*, vol. 20, no. 6, pp. 1247-1257, August 2002.
- [28] L. Yang, and G.B. Giannakis, "A general model and SINR analysis of low duty-cycle UWB access through multipath with narrowband interference and Rake reception," *IEEE Transactions on Wireless Communications*, vol. 4, no. 4, July 2005.
- [29] M.G. Shayesteh, and M. Nasiri-Kenari, "A new TH/DS-CDMA scheme for UWB communication systems and its performance analysis," *IEEE Radio and Wireless Symposium 2006*, pp.147-150, Jan. 2006.
- [30] V. S. Somayazulu, "Multiple access performance in UWB systems using time hopping vs. direct sequence spreading," *IEEE Wireless Communications and Networking Conference (WCNC) 2002*, no. 1, pp. 446-449, March 2002.
- [31] L. Piazzo, and F. Ameli, "Performance analysis for impulse radio and direct-sequence impulse radio in narrowband interference," *IEEE Transactions on Communications*, Vol. 53, Issue 9, pp. 1571-1580. Sept. 2005.
- [32] C.S. Sum, S. Sasaki, and H. Kikuchi, "Impact of Chip Duty Factor in DS-UWB Systems over Indoor Multipath Environment," *IEICE Transactions on Fundamentals*, Vol. E89-A, No. 11, pp. 3152-3156, Nov. 2006.
- [33] C.S. Sum, S. Sasaki, and H. Kikuchi, "The Impact of Chip Duty Factor on DS-UWB System Over Multipath Environment in the Presence of Narrowband Interference," *International Conference on Ultra-Wideband (ICUWB) 2006*, Massachusetts, USA, pp. 423-428, Sept. 2006.

- [34] M.A. Rahman, S. Sasaki, J. Zhou, and H. Kikuchi, "On Rake reception of ultra wideband signals over multipath channels from energy capture perspective," *IEICE Transaction on Fundamentals (Special Section on Ultra Wideband Systems)*, vol. E88-A, no. 9, pp. 2339-2349, Sep. 2005.
- [35] L. Zhao, and A.M. Haimovich, "Performance of ultra-wideband communications in the presence of interference," *IEEE Journal on Selected Areas in Communications*, vol. 20, no. 9, pp. 1684-1691, Dec. 2002.
- [36] D.K. Borah, R. Jana, and A. Stamoulis, "Performance evaluation of IEEE 802.11a wireless LANs in the presence of ultra-wideband interference," *IEEE Wireless Communications and Networking Conference (WCNC 2003)*, no. 1, pp. 83-87, Mar 2003.
- [37] M. Hamalainen, V. Hovinen, R. Tesi, Jari H. J. Inatti, and M. Latva-aho, "On the UWB system coexistence with GSM900, UMTS/WCDMA, and GPS," *IEEE Journal on Selected Areas in Communications*, vol. 20, no. 9, pp. 1712-1721, Dec. 2002.
- [38] J. Bellorado, S. S. Ghassemzadeh, L. J. Greenstein, T. Sveinsson and V. Tarokh, "Coexistence of ultra-wideband systems with IEEE-802.11a wireless LANs," *IEEE Global Telecommunications Conference (GLOBECOM 2003)*, no. 1, pp. 410-414, Dec 2003.
- [39] Wisair Ltd., "Detect and avoid technology: For UWB Spectrum Issue," Sept 2005. URL: <http://www.wisair.com/technology/detect-avoid>.
- [40] J. Romme, K. Witrisal, "Transmitted-reference UWB systems using weighted autocorrelation receivers," *IEEE Transactions on Microwave Theory and Techniques*, vol. 54, issue 4, part 2, pp. 1754-1761, June 2006.
- [41] F. Ramirez-Mireles, "On the performance of ultra-wide-band signals in Gaussian noise and dense multipath," *IEEE Transactions on Vehicular Technology*, vol. 50, issue 1, pp. 244-249, Jan. 2001.
- [42] J. Zhang, R.A. Kennedy, T.D. Abhayapala, "Performance and parameter optimization of UWB Rake reception with interchip interference," *IEEE International Conference on Communications (ICC 2005)*, no. 1, pp. 2830-2834, May 2005.
- [43] B. Hu, N.C. Beaulieu, "Accurate performance evaluation of time-hopping and direct-sequence UWB systems in multi-user interference," *IEEE Transactions on Communications*, vol. 53, no. 6, pp. 1053-1062, Jun 2005.

- [44] G. Durisi, S. Benedetto, "Performance evaluation of TH-PPM UWB systems in the presence of multiuser interference," *IEEE Communications Letters*, vol. 7, no. 5, pp. 224-226, May 2003.
- [45] D. Kelly, S. Reinhardt, R. Stanley, and M. Einhorn, "PulseOn second generation timing chip: enabling UWB through precise timing," *IEEE Conference on Ultra Wideband Systems and Technologies 2002*, pp. 117-121, May 2002.
- [46] D. Rowe, B. Pollack, J. Puller, W. Chon, P. Jett, J. Fullerton and L. Larson, "A Si/SiGe HBT timing generator IC for high-bandwidth impulse radio applications," *IEEE Proceedings on MILCOM 1999*, Oct. 1999.
- [47] I. Guvenc, and H. Arslan, "Performance evaluation of UWB systems in the presence of timing jitter," *IEEE Conference on Ultra Wideband Systems and Technologies 2003*, pp. 136-141, Nov. 2003.
- [48] Z. Tian, and G.B. Giannakis, "BER sensitivity to mistiming in ultra-wideband impulse radios - Part I: nonrandom channels," *IEEE Transaction on Signal Processing*, vol. 53, issue 4, pp. 1550-1560, Apr 2005.
- [49] Z. Tian, and G.B. Giannakis, "BER sensitivity to mistiming in ultra-wideband impulse radios - Part II: fading channels," *IEEE Transaction on Signal Processing*, vol. 53, issue 5, pp. 1897-1907, May 2005.
- [50] M.Z. Win, "A unified spectral analysis of generalized time-hopping spread-spectrum signals in the presence of timing jitter" *IEEE Journal on Selected Areas in Communications*, vol. 20, no. 9, December 2002 pp. 1664-1676.
- [51] B.H. Poh, C.C. Ko, W. Zhi, "BER performance of pulsed UWB system in the presence of colored timing jitter," *International Workshop on Joint UWBST & IWUWBS 2004*, pp. 293-297, May 2004.
- [52] S. Gezici, A.F. Molisch, H.V. Poor, and H. Kobayashi, "The trade-off between processing gains of impulse radio systems in the presence of timing jitter," *IEEE International Conference on Communications 2004*, vol. 6, pp. 3596-3600, June 2004.
- [53] W.M. Lovelace, J.K. Townsend, "The effects of timing jitter and tracking on the performance of impulse radio," *IEEE Journal on Selected Areas in Communications*, vol. 20, pp. 1646-1651, Dec. 2002.
- [54] G.T.F. Abreu, R. Kohno, "Design of jitter-robust orthogonal pulses for UWB systems," *IEEE Global Telecommunications Conference (GLOBECOM) 2003*, vol. 22, no. 1, pp. 739-743, Dec 2003.

- [55] Y. Yin, J.P. Fonseka, I. Korn, "Sensitivity to timing errors in EGC and MRC techniques," *IEEE Transactions on Communications*, vol. 51, no. 4, pp. 530-534, Apr 2003.
- [56] C.S. Sum, S. Sasaki, H. Kikuchi, "Impact of Timing Jitter on DS-UWB and Hybrid DS-Multiband UWB Systems with Rake Reception over Multipath Environment," *IEICE Transactions on Fundamentals*, vol. E89-A, no. 6, pp. 1657-1667, June 2006.
- [57] C.S. Sum, M.A. Rahman, S. Sasaki, J. Zhou and H. Kikuchi "Impact of Timing Jitter on Rake Reception DS-UWB Signal over AWGN and Multipath Environment," *IEEE WirelessCom 2005*, vol. 2, pp. 1225-1230, June 2005.
- [58] Tektronix Jitter and Timing Analysis Reference Guide, "Understanding and characterizing timing jitter," URL: [www.tektronix.com](http://www.tektronix.com).
- [59] A. Papoulis, S. U. Pillai, *Probability, Random Variables and Stochastic Processes, 4th Edition*, McGraw Hill, New York, 2002.
- [60] M.Z. Win, and Z.A. Kostic, "Impact of spreading bandwidth on Rake reception in dense multipath channels," *IEEE Journal on Selected Areas in Commununications*, vol. 17, no. 10, pp.1794-1806, Oct. 1999.
- [61] M.Z. Win, G. Chrisikos, and N.R. Sollenberger, "Performance of Rake reception in dense multipath channels: Implications of spreading bandwidth and selection diversity order," *IEEE Journal on Selected Areas in Commununications*, vol. 18, no. 8, pp. 1516-1525, Aug. 2000.





# Publication List

## Academic Papers

### Journals

1. C. S. Sum, S. Sasaki, H. Kikuchi: “**Impact of Timing Jitter on DS-UWB and Hybrid DS-Multiband UWB Systems with Rake Reception over Multipath Environment,**” *IEICE Trans. on Fundamentals*, Vol. E89-A, No. 6, pp. 1657-1667, June 2006.
2. C. S. Sum, S. Sasaki, H. Kikuchi: “**Impact of Chip Duty Factor in DS-UWB Systems over Indoor Multipath Environment,**” *IEICE Trans. on Fundamentals*, Vol. E89-A, No. 11, pp. 3152-3156, Nov. 2006.

### International Conferences

1. C. S. Sum, S. Sasaki, H. Kikuchi: “**The Impact of Chip Duty Factor on DS-UWB System Over Multipath Environment in the Presence of Narrowband Interference,**” *Intl. Conf. on Ultra-Wideband (ICUWB) 2006*, Massachusetts, USA, pp. 423-428, Sept. 2006.
2. C. S. Sum, M. A. Rahman, S. Sasaki, J. Zhou and H. Kikuchi: “**Impact of Timing Jitter on Rake Reception DS-UWB Signal over AWGN and Multipath Environment,**” *IEEE WirelessCom 2005, Hawaii*, vol. 2, pp. 1225-1230, June 2005.
3. C. S. Sum, S. Sasaki, T. Kusama H. Kikuchi: “**Simple Performance Analysis of M-ary PSK DS-UWB Signal with the Presence of Timing Jitter,**” *Intl. Symposium on Ultra-Wideband Technology (IWUWBT) 2005*, YRP, Japan, pp.159-163, Dec. 2005.
4. C. S. Sum, S. Sasaki, H. Kikuchi: “**On Interference Mitigation of DS-Multiband-UWB System over Indoor Multipath Environment,**” *Intl. Symp. on Information Theory and Its Applications (ISITA) 2006*, Seoul, Korea, pp. 323-326, Oct. 2006.

5. C. S. Sum, S. Sasaki, H. Kikuchi: **“On Frequency Agility of DS-Multiband-UWB System In Interference Mitigation,”** *Proc. ITC-CSCC 2006*, Chiangmai, Thailand, vol. 1, pp. 125-128, July 2006.
6. C. S. Sum, S. Sasaki, H. Kikuchi: **“Impact of Timing Jitter on Carrier-Based DS-UWB Communications over AWGN Multipath Channel,”** *Malaysia Intl. Conf. on Communications (MICC) 2005*, Kuala Lumpur, Malaysia, vol. 2, pp. 6, Nov. 2005.
7. C. S. Sum, S. Sasaki, H. Kikuchi: **“Performance Analysis of DS-UWB Communication with Presence of Timing Jitter,”** *Proc. ITC-CSCC 2005*, Jeju, Korea, pp. 245-246, July 2005.
8. Y. S. Song, S. Sasaki, C. S. Sum, H. Kikuchi: **“Impact of Narrowband Interference for DS-multiband-UWB Wireless Communications,”** *Intl. Symp. on Information Theory and Its Applications (ISITA) 2006*, Seoul, Korea, pp. 319-322, Oct. 2006.

#### National Conferences

1. C. S. Sum, S. Sasaki, H. Kikuchi: **“Impact of Chip Duty Factor on DS, TH and DS-TH UWB Systems over Multipath and Multi-user Environment,”** *The 29th Symposium on Information Theory and its Application (SITA2006)*, vol. 1, pp. 423-426, Nov. 2006.
2. C. S. Sum, S. Sasaki, H. Kikuchi: **“Impact of Chip Duty Factor in TH-UWB and DS-TH-UWB Systems over Indoor Multipath Environment,”** *IEICE General Conf. 2006*, Kokushikan University, A-5-15, pp. 4, March 2006.
3. C. S. Sum, M. A. Rahman, S. Sasaki, Y. Kawashima, J. Zhou and H. Kikuchi: **“The Effects of Timing Jitter on Rake Reception of DS-UWB Signal over Multipath Environment,”** *IEICE General Conf. 2005, Osaka University*, A-5-12, pp. 128, March 2005.
4. C. S. Sum, M. A. Rahman, S. Sasaki, Y. Kawashima, J. Zhou and H. Kikuchi: **“The Effects of Timing Jitter on Rake Reception of DS-UWB Signal over AWGN and Multipath Environment,”** *IEICE Technical Report*, vol. 104, no. 672, WBS2004-89, pp. 195-200, March 2005.
5. C. S. Sum, S. Sasaki, J. Zhou, and H. Kikuchi: **“Multiple Access Performance of Hybrid DS-Multiband-UWB System,”** *IEICE Wideband System Technical Meeting*, Sendai, WBS2004-41, pp.19-24, Oct 2004.

6. Y. S. Song, S. Sasaki, C. S. Sum, H. Kikuchi: “**Impact of Narrowband Interference for DS-multiband-UWB Wireless System,**” *IEICE General Conf. 2006*, Kokushikan University, A-5-6, pp. 120, March 2006. (in Japanese)
7. Y. S. Song, S. Sasaki, C. S. Sum, T. Kusama, H. Kikuchi: “**Study on DS-Multiband-UWB System in the Presence of Narrowband Interference,**” *IEICE Section Conf. 2005*, Nagaoka University of Technology, 3C-2, Oct. 2005. (in Japanese)